MULTIMODAL BIOMETRIC RECOGNITION USING
BIO-INSPIRED OPTIMIZATION AND FUZZY FUSION

BY

GALAL MUNASSAR BIN MAKHASHEN

A Thesis Presented to the

DEANSHIP OF GRADUATE STUDIES

KING FAHD UNIVERSITY OF PETROLEUM & MINERALS

DHAHRAN, SAUDI ARABIA

In Partial Fulfillment of the
Requirements for the Degree of

MASTER OF SCIENCE
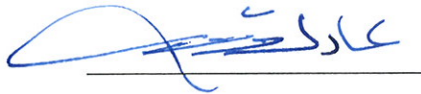
In

COMPUTER SCIENCE

April 2013

KING FAHD UNIVERSITY OF PETROLEUM & MINERALS

DHAHRAN 31261, SAUDI ARABIA

DEANSHIP OF GRADUATE STUDIES

This thesis, written by **Galal Munassar Bin Makhashen** under the direction of his thesis

advisor and approved by his thesis committee, has been presented to and accepted by the

Dean of Graduate Studies, in partial fulfillment of the requirements for the degree of

MASTER OF SCIENCE IN COMPUTER SCIENCE.

Sayed 1/4/2013

Dr. El-Sayed M. El-Alfy
(Advisor)

Dr. Zubair A. Baig
(Member)

Dr. Sajjad Mahmood
(Member)

Dr. Adel F. Ahmed
Department Chairman

Dr. Salam A. Zummo
Dean of Graduate Studies

7/4/13

Date

Dedication

This Thesis is dedicated to my parents, wife and lovely daughter

ACKNOWLEDGMENT

TABLE OF CONTENTS

LIST OF TABLES

LIST OF FIGURES

LIST OF ABBREVIATIONS

2D-DWT	Two-Dimensional Discrete Wavelet Transform
Acc	Accuracy
AUC	Area Under the Curve
DB	Database
DCT	Discrete Cosine Transform
EER	Equal Error Rate
FAR	False Accept Rate
FRR	False Reject Rate
FS	Feature Selection
GAR	Genuine Accept Rate ($1 - \text{FRR}$)
GMM	Gaussian Mixture Model
ICA	Independent Component Analysis
KFDA	Kernel Fisher Discriminant Analysis
K-NN	K-Nearest Neighbor
LDA	Linear Discriminant Analysis
MACE	Minimum Average Correlation Energy
MTR	Minimum Total Error
NIR	Near Infra-Red
PCA	Principal Component Analysis
POC	Phase-Only-Correlation
PSO	Particle Swarm Optimization
RBFNN	Radial-Basis Function Neural Network
ROC	Receiver Operating Characteristic
ROI	Region Of Interest
SIFT	Scale-Invariant Feature Transform
SVM	Support Vector Machine
WTA	Winner-Takes-All

THESIS ABSTRACT

NAME: Galal Munassar Abdullah Bin Makhashen

TITLE: Multimodal Biometric Recognition Using Bio-Inspired Optimization and Fuzzy
Fusion

MAJOR FIELD: COMPUTER SCIENCE

DATE OF DEGREE: April 2013

Multimodal biometric recognition systems are an emerging field of research. Basically, this technology has been recommended to mitigate the limitations of the unimodal biometric systems with more enhanced performance. However, due to the increased dimensionality of the feature space, more innovative techniques are still required to tackle the curse of dimensionality problem. One of the promising fields that has not been intensively investigated is the application of bio-inspired optimization with fuzzy fusion for such systems. Also, not all combinations of different biometrics have been studied yet.

In this thesis, we proposed a novel multimodal biometric system based on particle swarm optimization and fuzzy fusion that can be adopted in different applications with moderate to high security requirements. We evaluated various forms of unimodal and multimodal face, iris, and hand biometrics. We have conducted intensive experimental work to study and compare the performance of the proposed system under different settings. For multimodal systems, six different combinations have been investigated and evaluated for verification and identification modes.

ملخص الرسالة

الاسم: جلال منصّر عبدالله بن مخاشن

عنوان الرسالة: القياس الحيوي متعدد الأنماط باستخدام الدمج الضبابي والأمثلة المستوحاة من الكائنات الحية

تاريخ التخرج: جمادى الأولى 1434

إن أنظمة تكنولوجيا التعرف على الأشخاص من خلال دمج مجموعة من القياسات الحيوية آخذة في التطور باستمرار. وتأتي أهمية تلك الأنظمة لقدرتها على التغلب على مجموعة من نقاط الضعف المحتملة في أنظمة التعرف أُحادية المصدر (ذات قياس حيوي وحيد)، بالإضافة إلى تحسينها للأداء العام لتلك الأنظمة. وبغض النظر عن حجم البحث العلمي في هذا المجال إلا أن تبني طرق التحسين المستوحاة من الكائنات الحية وطرق الدمج الضبابي لم يتم دراستها وتقييمها بشكل مكثّف لمعرفة أدائها مقارنةً بطرق الدمج الإحصائية الأخرى. لذلك تقترح هذه الدراسة نظاماً متعدد الأنماط الحيوية يعتمد على أمثلة سرب الجزيئات والدمج الضبابي. ويستخدم هذا النظام سمات مستخرجة من الوجة وقزحية العين وراحة اليد بالإضافة إلى القياسات الهندسية لليد. وقد أجرينا عدة تجارب لتقييم أداء هذا النظام المقترح ومقارنته مع طرق أخرى في حالات مختلفة، وأظهرت النتائج تحسناً ملحوظاً في حالات كثيرة للنظام المقترح. ويمكن استخدام النظام المقترح في كثير من التطبيقات ذات المستوى الأمني المتوسط أو العالي.

CHAPTER 1

INTRODUCTION

Personal recognition is an important and challenging task in many applications. Examples of these applications are banking transactions, access control to physical locations or devices (laptops and smart phones), personal screening at international borders, etc. There are various authentication techniques that may fall into three main categories: knowledge (e.g., passwords and PINs), possession (e.g., keys and cards) and biometric based authentication. The first two categories are traditionally used to authorize users for accessing information and services. Although these two categories are commonly used, they suffer from several limitations [1]. For instance, passwords may be forgotten due to the increased intricacy, or exposed because of being easy to guess. Moreover, smart cards, keys or passports may be stolen or lost. In addition, both categories might be susceptible to various attacks that forge an identity. Besides that, these techniques are not used for recognition (identification) purposes. Alternatively, biometric-based technology can overcome the weakness of these traditional techniques. It can be used in authentication (verification) or recognition (identification) modes. Furthermore, it neither needs memorization nor being easily forged or shared. Besides that, it is one of the most recent attractive solutions that have been commercialized.

There are two general methodologies for biometric system designs: unimodal and multimodal. In unimodal, the biometric system utilizes only one biometric trait to recognize a person. On the other hand, multiple biometric traits are used in the multimodal biometric system. Thus, it can resemble the human recognition perceptual system which is capable of identifying persons based on a variety of their biometric traits.

1.1   Problem Statement & Motivation

A unimodal biometric technology may suffer from many issues such as noisy data, limited discrimination information, vulnerability to spoof attacks, and/or increased intra-class variability [1]. To cope with such issues, several approaches have been proposed for combining information at different levels from multiple biometrics. The aim of our work is to develop a multimodal biometric system based on the fusion of face, iris and hand biometric traits using bio-inspired optimization and fuzzy integral fusion techniques. We choose this combination for various reasons. These traits collectively can have better properties in terms of availability, uniqueness, robustness, acceptability, and circumvention. Furthermore, each biometric has various modalities, e.g., hand biometric includes hand geometry, palmprint, fingerprint and vein patterns. But in our study we will focus only on hand geometry and palmprint in addition to face and iris. Finally, some of these traits can be acquired using a single inexpensive sensor. The adoption of bio-inspired optimization and fuzzy fusion can reduce the dimensionality of the feature space and handle uncertainties in various biometrics, which consequently can lead to enhanced overall system performance.

1.2   Main Objectives & Methodology

The main objectives of this thesis work are as follow:

a) Investigate and benchmark different biometric fusion techniques for face, iris and hand biometrics.

b) Design a novel multimodal biometric system using bio-inspired optimization and fuzzy fusion.

c) Evaluate and compare the performance of the proposed system, and identify factors that can affect the accuracy of the fusion techniques.

To achieve the above objectives, we reviewed the state-of-the-art techniques on biometric systems including single and multimodal designs using a variety of fusion techniques for verification and identification modes. We focused on face, iris, and hand shape biometrics. After thorough investigation of the single biometric systems using some benchmarking datasets, we studied the performance of traditional fusion techniques such as the sum rule, product rule and maximum rule. Inspired by the success of fuzzy integral and particle swarm optimization (PSO), we developed a novel multimodal biometric framework that can combine two to three biometric traits. This framework is validated and compared with other considered systems in terms of different measures such as recognition Accuracy (Acc), False Rejection Rate (FRR), False Acceptance Rate (FAR), Receiver Operating Characteristic (ROC) curve, and area under the ROC curve (AUC). Figure 1 provides a high-level overview for our research work.

1.3   Organization of the Thesis

This thesis is divided into six chapters. Following this introduction chapter, Chapter 2 presents background information on biometric authentication and recognition as well as the common evaluation measures used in these systems. Chapter 3 briefly surveys the related work. Chapter 4 describes the proposed biometric system components. Chapter 5 discusses the conducted experimental work on unimodal and multimodal biometric systems. Chapter 6 is a closing remark of this thesis and pinpoints some directions for future research work.
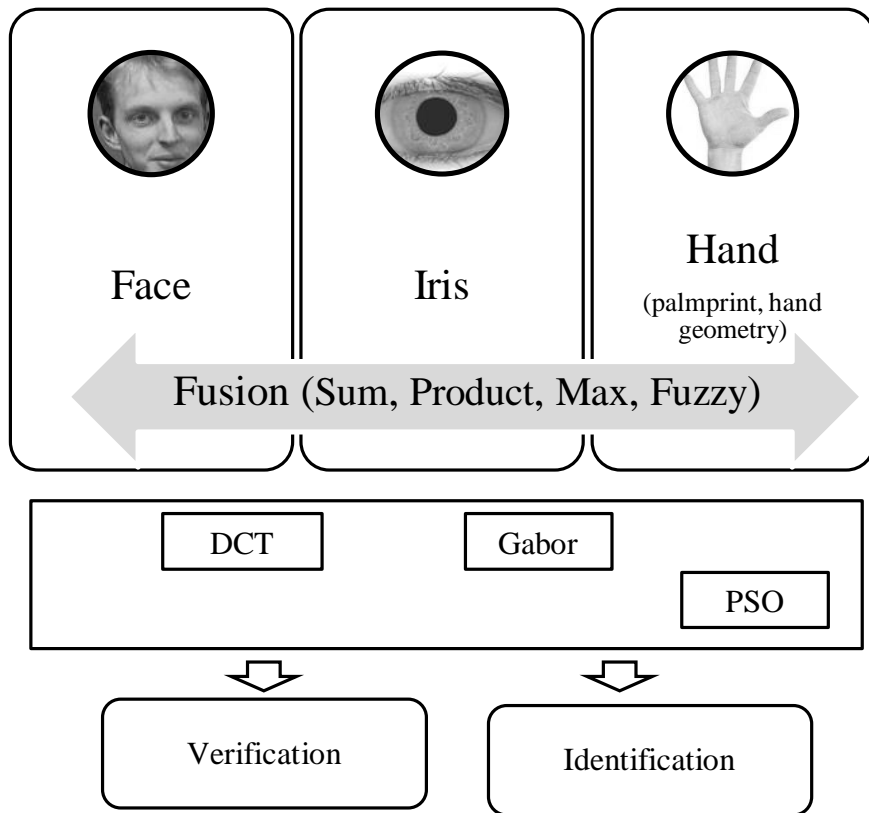
Figure 1 Overview of our research work

CHAPTER 2

BACKGROUND AND PRELIMINARIES

Nowadays, biometric technology has been widely used in many security applications for personal identification or authentication based on some traits of the human body such as face, iris and fingerprint. In this chapter, we provide some background and briefly discuss elementary information about the biometric systems. We will describe the main components of a biometric system, operation modes and evaluation criteria. Then, we will focus on the multibiometric systems and describe the various information sources and fusion techniques.

2.1   Biometric System Components

Essentially, a biometric technology is a pattern recognition system with a backend database that stores biometric information of previously enrolled users. Figure 2 illustrates the main components of a biometric system, which are as follow [3]:

a) Biometric sensors: These are readers or scanners (such as camera or microphones) used to acquire biometric representations (e.g., images or waves). They produce raw data that will need further processing.

b) Pre-processing component: This component can involve different signal and image processing techniques to enhance the quality of the raw data captured by various sensors, e.g., noise filtering, smoothing, normalization, masking and segmentation of regions of interest (ROI).

c) Feature extraction and selection components: Raw data can have a lot of information but the dimensionality is too high. Hence, it is required to represent each sample with the most relevant information for the recognition process and these are the roles of the feature extraction and selection components.

d) Database component: During the enrollment phase, a group of potential users of the system has to register extracted feature vectors for their biometric traits with their Personal Identification Numbers (PINs). The combination of the feature vector and the corresponding PIN is known as a biometric template. This information is saved into a central database (and it is also possible to save it on smart cards or machine readable documents).

e) Matching and decision-making components: This component is required for the identification or authentication operation. A feature vector is extracted from the biometric trait of the user to be identified or authenticated in a similar way to what has occurred during the enrollment phase. Then, it will be matched with the pre-stored templates (for identification) or the template associated with the claimed PIN (for authentication). This comparison results in a matching score which could measure how similar (similarity score) or how far (distance measure) two feature vectors are. This matching score will be compared with a threshold value and a final decision will be made.
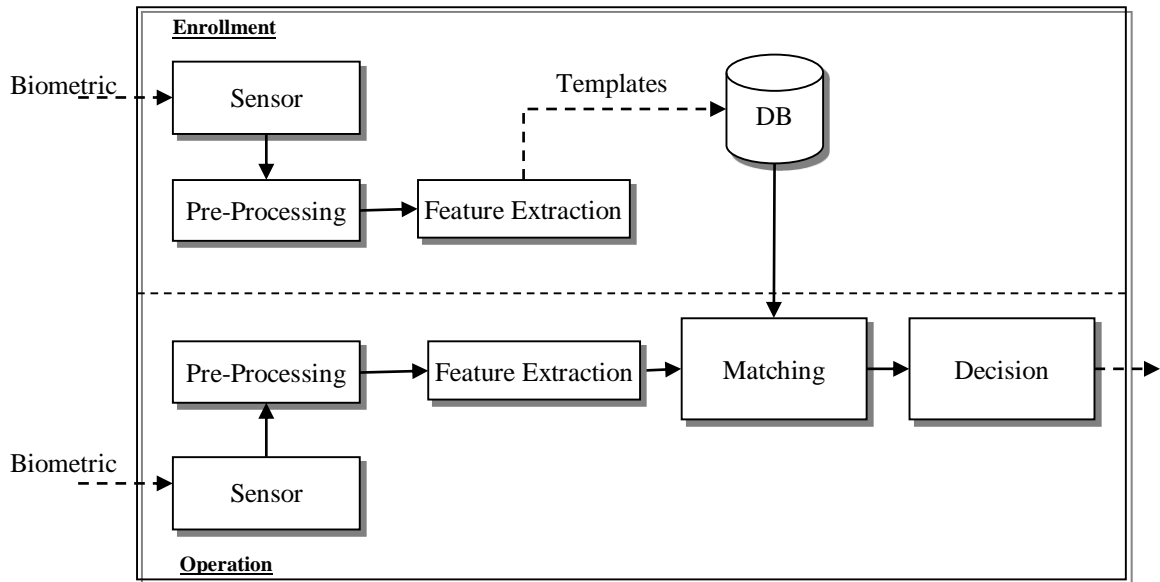
Figure 2 Overview of a biometric recognition system

2.2 Operation Modes

The biometric technology is adopted in many applications either for personal recognition (identification) or authentication (verification). For instance, in forensic applications, it can be used for determining the parenthood of a child or the identity of a suspected criminal, i.e., identification mode. On the other hand, in access control to special premises and banking transactions, the system is required to verify the claimed identity of a user before granting him access or approving his transaction. In the following subsections, we describe in details the differences between these operation modes.

2.2.1 Verification Mode

In this mode, the system authenticates a user by comparing his biometric features (newly acquired) with the feature vector associated with the claimed PIN which was pre-registered in the system database. The typical scenario that the system follows is explained next. First, the user has to claim an identity (i.e., gives a PIN). Then, the system captures the user's biometric trait and extracts the necessary representation. After

7

that, it locates the template with the provided PIN. Finally, it conducts a one-to-one matching between the newly processed data and the retrieved template to determine whether the claim is true or false. This process can be described more formally as follows. Given an input (a feature vector, α, and a claimed identity, id), decide whether the combination (α, id) matches the pre-registered template (β, id) or not. If a matching score between α and β is within certain range, the claim is reported to be true otherwise it is false. This score can describe similarity or dissimilarity between α and β. Without loss of generality, we assume the matching score represents similarity and its value is normalized to be in range (0, 1) where 0 means 'different' and 1 means 'identical'. Thus, the decision can be written as:

$$decide(\alpha, id) = \begin{cases} True & \text{if } score(\alpha, \beta) \geq Th \\ False & \text{otherwise} \end{cases} \tag{2.1}$$

where Th is a predetermined threshold value between 0 and 1.

2.2.2 Identification Mode

Here, the goal is to determine the identity of a person. The system recognizes a person by capturing only his biometric data and matching it with all available templates in the database. A comparison against all pre-registered templates is required since there is no claimed PIN. In closed systems, where all users are pre-registered, the system declares the identity associated with the most similar template. However, in open systems, where some persons may not have been seen before, it either declares the identity of the most similar one, or it declares failure when the highest matching score is below a certain threshold. More formally it can be described as follows. Given an input feature vector, α,

determine the most likely identity id_ω, where $\omega = \{1, 2, ..., N\}$ and N is the total number of users. For closed systems, the decision rule can be written as:

$$decide(\alpha) = id_{\omega^*} \ \text{ where } \omega^* = \arg\max_{\omega=1..N}\{\text{score}(\alpha, \beta_\omega)\} \tag{2.2}$$

whereas for and open system the decision rule can be written as follows:

$$decide(\alpha) = \begin{cases} id_{\omega^*} \text{ where } \omega^* = \arg\max_{\omega=1..N}\{\text{score}(\alpha, \beta_\omega)\} & \text{if } \text{score}(\alpha, \beta_{\omega^*}) \geq Th \\ failure & \text{otherwise} \end{cases} \tag{2.3}$$

where *Th* is a predetermined threshold value between 0 and 1.

2.3   Evaluation Criteria

Each biometric trait can have strengths and weaknesses which in turns affects the system performance. Thus, it is required to benchmark different biometric traits and systems to select the most suitable for the application at hand. Jain et al. [4] listed several evaluation criteria that can be used for this purpose. These criteria are as follows:

a) Universality: All potential users must possess that chosen biometric trait.

b) Distinctiveness: The chosen biometric trait should have sufficient discriminant information to distinguish among different users.

c) Permanence: Almost all biometric traits are changing over time which is known aging. This criterion is concerned with how fast is the change of the chosen biometric trait.

d) Collectability: The chosen biometric trait must be quantitatively measurable. It should be easy to collect and not affected much by the imperfectness of the

capturing device or environmental conditions such as poor lighting or external noise.

e) Performance: This measure is concerned with the system accuracy and speed within the available computation resources.

f) Acceptability: This criterion is related to the end-users satisfaction and ease of use. A biometric trait is required to be non-intrusive and easily used.

g) Circumvention: The biometric system should have some immunity against the determined attackers.

h) Cost: A biometric system should also be affordable.

We will shed the light more on the important evaluation measures for the performance of a biometric system. The system may expose some errors due to the inter-class similarity and/or the intra-class variations. For example, two persons may look similar (inter-class similarity), yet they have different identities. On the other hand, the biometric captured from the same person may look different (intra-class variation), yet the identity is still the same. To measure these errors, there are two main statistical metrics that have been broadly used in the biometric domain. These are the False Acceptance Rate (FAR), i.e., the proportion of imposter users recognized as genuine, and the False Rejection Rate (FRR), i.e., the proportion of genuine users who have been recognized as imposter. There is a tradeoff between these two metrics depending on the setting of the threshold value. Usually the biometric system will have some errors, and the system performance can be adjusted to an acceptable level of errors for the given application domain. The system may act flexible and increase the accepting rate of the newcomers or it may act sharply

and rejects any suspicious newcomers. Consequently, system designers could apply more

restrictions over the matching criteria to decrease accepting users by mistake, or relax the

matching conditions to allow flexibility. Figure 3 shows two distributions of genuine and

imposter users on a range of similarity scores and the tradeoff between FAR and FRR.

FAR and FRR can be computed from the distributions as follows:

$$FAR(Th) = \int_{Th}^{1} p(s \mid imposter)ds \qquad (2.4)$$

$$FRR(Th) = \int_{0}^{Th} p(s \mid genuine)ds \qquad (2.5)$$
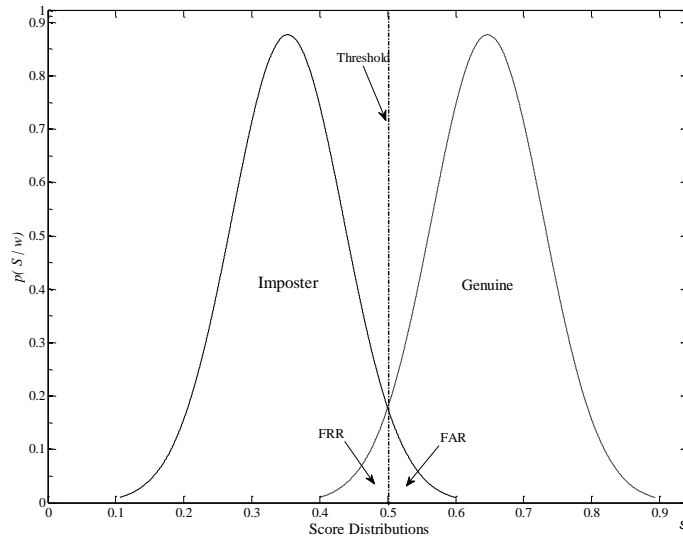
Figure 3 Genuine and imposter distribution, $w \in \{imposter, genuine\}$

To visualize the tradeoff between FAR and FRR at different threshold values, a Receiver

Operating Characteristic (ROC) curve can be plotted. The ROC curve plots FAR against

Genuine Acceptance Rate (GAR) which equals $1 - FRR$. Each point on the ROC curve is

indicating different operating performance. Among all ROC operating points, there is a

11

specific point on the curve where FAR equals FRR that called Equal Error Rate (EER).
Computing EER from the data may not be precise due to the discrete values of the FAR
and FRR. Therefore, it may need a large number of test samples to estimate EER more
accurately. Nevertheless, some authors have tried to estimate the EER value from a given
reasonable set of FAR and FRR. For example, Cheng and Wang [6] have proposed a
method to estimate EER based on the samples without running the system using log
likelihood. Another estimation of the EER has been suggested by Stylianou et al. [7].
They have computed the EER according to the following:

$$Ind_{EER} = \arg\min_{Ind}\left[FRR(Ind) - FAR(Ind)\right] \qquad (2.6)$$

$$EER = \frac{FRR(Ind) + FAR(Ind)}{2} \qquad (2.7)$$

where Ind_{EER} is the index of the minimum difference of FRR and FAR along all
evaluated points Ind = 1, 2, …,n. Figure 4 shows examples of the evaluation measures,
ROC, FAR, FRR, and EER.

(a)   (b)
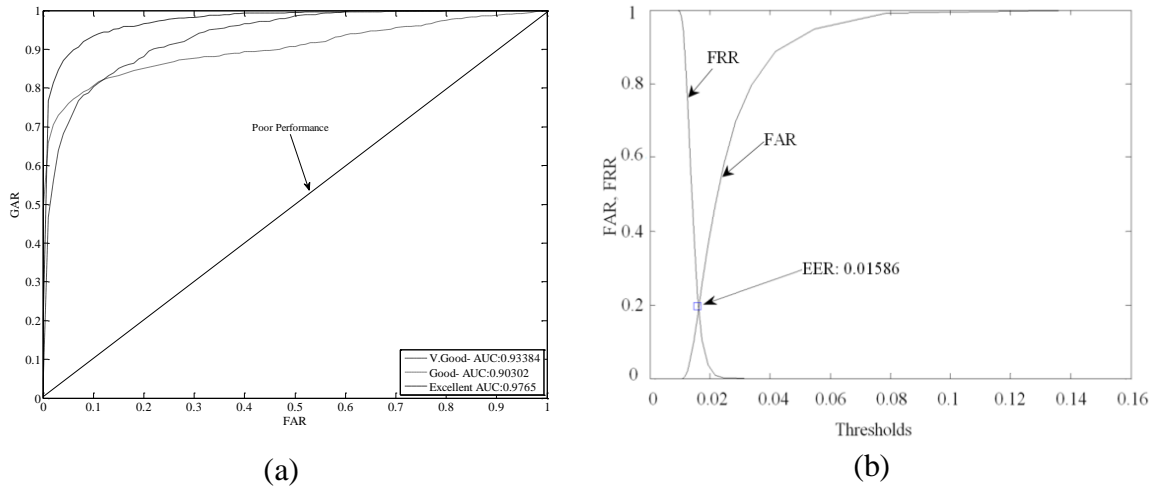
Figure 4 Biometric system evaluation measures a) ROC, b) FAR, FRR, EER

12

2.4   Multibiometric Systems

2.4.1   Information Sources

In multibiometric systems, there are five sources of information that can be integrated to solidify the evidence for personal recognition. These sources can be grouped into five categories [1] as illustrated in Figure 5: (1) multi-bio sensors, in which multiple input data of the same biometric trait are acquired using different biometric devices (e.g., capacitive, optical or thermal), (2) multi-algorithm, using various feature extraction or matching algorithms on a single biometric trait, (3) multi-instance, such as capturing the index fingerprint of both hands (left and right), (4) multi-sample, unlike the previous source, the multi-sample is considering two or more samples of the same biometric trait to enhance biometric representation, and (5) multibiometric, multiple but different biometric traits are used to strengthen evidence towards better recognition.
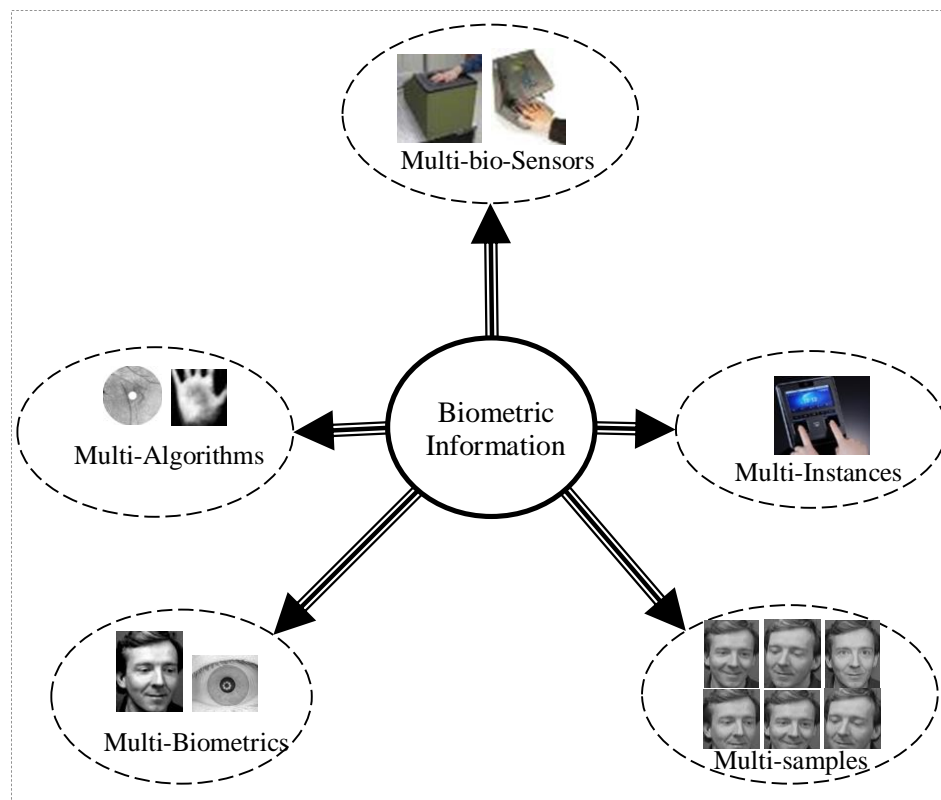
Figure 5 Multiple biometric information sources categories

2.4.2 Fusion Techniques

Integrating different biometric traits can take place at four different levels: sensor level, feature-extraction level, matching-score level or decision level [2]. The information exists at each level decreases gradually from the sensor level to the decision level, but the simplicity and smoothness increase. Therefore, fusion at earlier stages is expected to have more useful information, but it requires more computational resources (time and space). Moreover, data can be noisy and the relationship of different biometrics may not be so obvious. Figure 6 shows the availability and difficulty of the information fusion at each level. In the following subsections, we will review some of the commonly used techniques for each of these fusion levels.
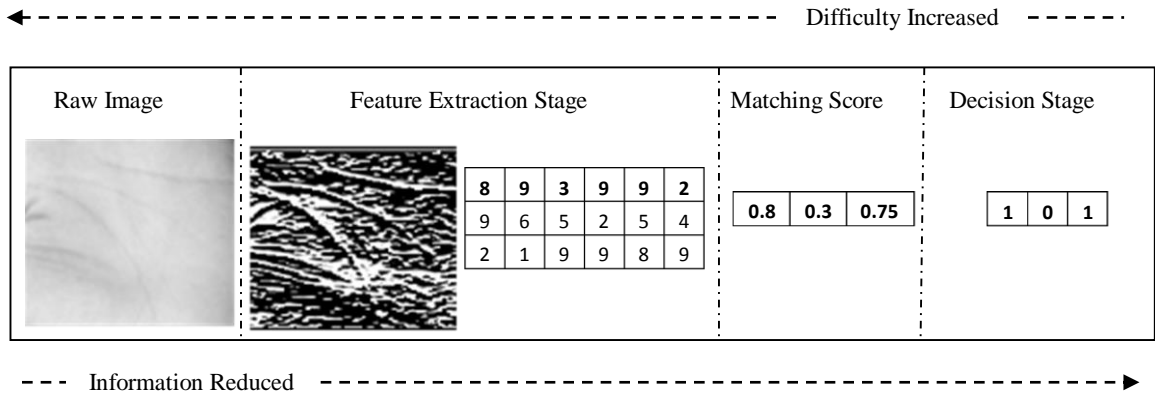
Figure 6 Biometric information against and fusion difficulty

A) Feature-Level Fusion

Typically the fusion at this level is proposed to update, enhance or solidify the feature representation of one or more biometric traits or samples. Updating the representation of the same biometric can be made easily by an averaging technique of the existing representation and the newly acquired representation. The subsequent modules of the

14

biometric system will remain unchanged. This can be an important step for certain biometrics which may vary frequently due to aging or acquisition conditions. Figure 7 illustrates the updating approach using the averaging technique for two feature vectors.
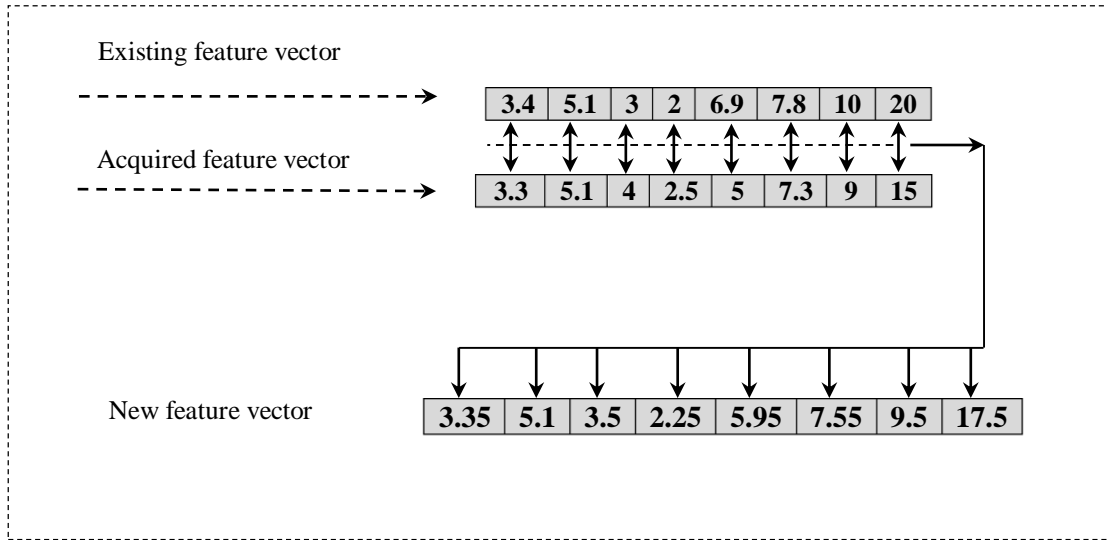
Figure 7 Feature update using the averaging technique

Voting is another approach that can be utilized in multi-sample biometric recognition systems for discrete features. In this case, the feature vectors extracted from different samples are compared and the best candidate value for each feature is selected by a majority vote. A third approach for feature-level fusion is augmentation or concatenation of two or more vectors. This approach is very useful for integrating features coming from different biometric traits or samples that are not related or with unclear relationship. However, the increased dimensionality of this approach may discourage its use or require other techniques for feature selection.

15

B) Matching-Score Level Fusion

The matching-score level fusion is one way to express the human behavior for associating evidence to increase confidence and make a better decision. Fusion at this level can be divided into two main subcategories: classification and combination [2]. The classification based fusion techniques are based on machine learning and neural network methods. The scores of different experts are treated as classifier inputs. Then, based on the learning approach, the trained classifier will determine the scores' class (genuine or imposter). Secondly, the combination techniques are those that depend on the stored templates and computed threshold to identify a person such as statistical combination using sum, product, min and max rules [1]. These rules assume data independence of the multibiometric sources. Therefore, they are found to be strong and usually produce good performance. Table 1 summarizes the formulas for the common statistical fusion rules.

Fusion at this level is considered be a challenging task because of several reasons. Firstly, different biometric experts may produce heterogeneous scores. Secondly, scores may fall into different ranges. Moreover, score probability distributions may be different. So, to integrate different matching scores, it is necessary to have all scores in a common domain using normalization. The normalization is a process to transform the scores from their specific domains to a common one (i.e., change scale and location). A good normalization technique has to be insensitive to outliers; this property is called robustness [1]. It also should be efficient in the way of retaining the original probability distributions.

Table 2 illustrates various normalization techniques [60],[62],[63].

Table 1 Statistical fusion rules

Fusion rule	Formula
Sum	$s_F = s_1 + s_2 + s_3 + \ldots + s_n$
Weighted sum	$s_F = x s_1 + y s_2 + \ldots + z s_n$ where $x, y, \ldots, z$ are weights
Product	$s_F = s_1 \times s_2 \times s_3 \times \ldots \times s_n$
Minimum	$s_F = \min(s_1, s_2, \ldots s_n)$
Maximum	$s_F = \max(s_1, s_2, \ldots s_n)$
Median	$s_F = median(s_1, s_2, \ldots s_n)$

Table 2 Normalization techniques

Normalization Technique	Formula
Min-Max	$$\overline{s}_i = \frac{s_i - \min\left(\{s_1 \ldots s_n\}\right)}{\max\left(\{s_1 \ldots s_n\}\right) - \min\left(\{s_1 \ldots s_n\}\right)}$$
Decimal Scaling	$$\overline{s}_i = \frac{s_i}{10^{\left(log_{10}\left(\max(\{s_1, \ldots, s_n\})\right)\right)}}$$
Z-score	$$\overline{s}_i = \frac{s_i - \mu}{\sigma}$$ where μ and σ are the mean and standard deviation of the scores
Median Absolute Deviation (MAD)	$$\overline{s}_i = \frac{s_i - median(\{s_1 \ldots s_n\})}{median(\{|s_j - median(\{s_1 \ldots s_n\})| : j = 1..n\})}$$
Double Sigmoid	$$\overline{s}_i = \begin{cases} \dfrac{1}{1 + \exp\left(-2(s_i - \eta)/\alpha_1\right)} & if \ s_i < \eta \\[2ex] \dfrac{1}{1 + \exp\left(-2(s_i - \eta)/\alpha_2\right)} & otherwise \end{cases}$$ where η is the reference operating point, α_1 and α_2 are left and right edges of the region

Table 2 (Cont.)

Normalization Technique	Formula
Tanh	$$\overline{s}_i = 0.5\left(\tanh\left(0.01\left(\frac{s_i - \mu}{\sigma} \right) \right) + 1 \right)$$ where μ and σ are the mean and standard deviation of the scores
Two-Quadrics (QQ)	$$\overline{s}_i = \begin{cases} \dfrac{1}{c} s_i^2, & \text{if } s_i \leq c \\\\ c + \sqrt{(1-c)(s_i - c)}, & otherwise \end{cases}$$ where c is the center of the overlap area
Quadric-Linear-Quadric (QLQ)	$$\overline{s}_i = \begin{cases} \dfrac{1}{c - \frac{w}{2}} s_i^2 & \text{if } s_i \leq \left(c - \frac{w}{2} \right) \\\\ s_i & \text{if } \left(c - \frac{w}{2} \right) < s_i \leq \left(c + \frac{w}{2} \right) \\\\ \left(c + \frac{w}{2} \right) + \sqrt{\left(1 - c - \frac{w}{2} \right)\left(s_i - c - \frac{w}{2} \right)} & otherwise \end{cases}$$ where s_i is the score normalized using Min-Max, c is the center of the overlapped area, and w is the width.

C) Decision-Level Fusion

At the final stage of any biometric recognition system is a decision module. At this stage, the multibiometric system may have multiple decisions out of its single subsystems. Therefore, the fusion can take place to finalize the decision. The information presented at this level could be either zero or one (accept or reject). Therefore, a logical AND/OR or majority voting could be used to have better decision [87]. Moreover, multibiometric decision-level fusion can be supported by some external information such as eye and skin color, face and hand scares, gender, etc. which are called soft-biometrics [63].

18

CHAPTER 3

LITERATURE SURVEY

In this chapter, we will review the state-of-the-art of face, iris, and hand recognition systems. We will discuss and summarize the work that has been done for unimodal and multimodal for these biometric traits.

3.1   Face Recognition

Face as a biometric trait was heavily studied in the literature for security (verification and identification) based systems. This human trait has a strong connection to a wide range of real world applications such as access control, human-computer interaction, multimedia management and forensic applications [8].

During the preprocessing stage, the system can use segmentation and alignment to locate the face image and regions of interest and to adjust its orientation and position [10]. Mittal and Sasi [9] have proposed a face detection technique that is able to locate faces with beards using an elimination algorithm. The features that could be extracted from a human face are divided into two main categories, local and global.

Local face features are based on the geometrical measurements of specific facial locations. It starts via locating specific points on the face by using a searching window to locate the position of the mouth, eyes, nose and eyebrows. Brunelli and Poggio [11] found that geometrical facial features can produce satisfactory results provided that four conditions should be met: 1) geometrical feature estimation ought to be doable and easy,

2) effect of illumination must be minor, 3) small changes in facial expression should not affect performance, and 4) discriminative information should be high as much as possible. Another work by Jiao et al. [12] have reduced the computation needed by the searching window to find the local features by using Gabor jets for location estimation.

On the other hand, global features (also called holistic) of human faces are those extracted using the whole image to produce biometric features. We could divide the holistic approaches into subspace and transformation algorithms. There are several algorithms that have been previously proposed to address face recognition based on subspace such as Principle Component Analysis (PCA), Independent Component Analysis (ICA) and Linear Discriminate Analysis (LDA) [8], [10], [13]. Transformation techniques attempt to change the original face image space into a special domain. These techniques can ease the search space for the discriminant feature sets within the transformed domain; such as Discrete Cosine Transform (DCT), Discrete Fourier Transform (DFT), and Wavelet Transform (WT) [13], [14], [15].

Extracting face features using DCT is one of the common techniques that have been tested on face recognition. Pan and Bolouri in [16] have reported a high recognition speed when using some DCT coefficients for face recognition instead of using the raw face image. However, this kind of feature normally has higher dimensionality than the previous category. Therefore, feature reduction of the DCT space is needed. The DCT components can be fed into a back-propagation neural network classifier to model the classification. Another work by Er et al. [17] has analyzed the DCT space using a clustering technique to select the most discriminative DCT components for face recognition. Recently, Akrouf et al. [13] have combined PCA with DCT to carry out

face recognition. They have transformed face images into DCT space. Then, they have reduced the working space by selecting 9 components of each DCT block (8×8). After that, they have applied PCA to reduce the feature space. Figure 8 shows some global and local face features.
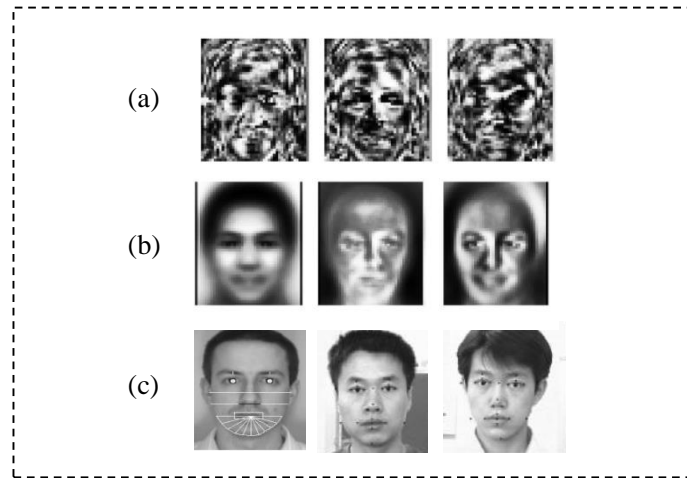
Figure 8 Face recognition global and local techniques
a) subspace LDA, b) eigenfaces [10], c) local features (geometrical) [11],[12]

3.2   Iris Recognition

Within a human eye, there is a powerful and distinctive trait called iris. It has multiple distinguishing characteristics of different scales that can be processed using image processing techniques. Iris features may include ligaments, furrows ridges, freckles, rings and zigzag collarette [23].

Several techniques have been proposed for iris recognition that could be divided into three categories: phase-based, zero-crossing, and texture analysis [18]. Phase-based techniques are mainly based on John Daugman pioneer work that has been patented in 1994 [20]. He described the iris recognition by first determining the center coordinates

and radius of both the pupil and the iris. Then, a coarse-to-fine integro-differential operator has been used as a circular edge detector to find the pupil and iris boundaries. Moreover, the same technique has been used to detect the upper and lower eyelid boundaries. Then, a two-dimensional wavelet demodulation is applied to extract a phase representation of size 256 bytes to represent the Iriscode. Finally the encoded feature set was matched using hamming distance for personal recognition. Figure 9 shows an overview of Daugman's iris feature extraction.
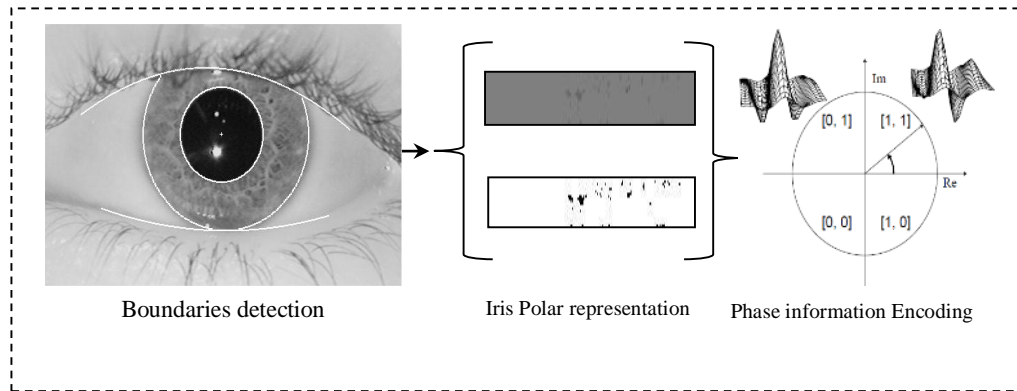
Figure 9 Iris feature extraction and encoding (Daugman Approach)

Zero-crossing feature extraction has been proposed by Boles and Boashash [21]. They have extracted features from the iris at different levels of resolution based on fine-to-coarse approximations. They have used dyadic wavelet transform on concentric iris circles to transform the iris images into a special domain. The resultant was analyzed to extract a zero-crossing representation. Finally, a simple distance measure was used in the matching process.

Texture-based iris recognition has been addressed by Ma et al. [19]. They have proposed a texture analysis algorithm that started by locating the iris. Then, they have applied a spatial filter on 8×8 blocks on the iris to analyze local spatial patterns that have frequency

and orientation information. For each block, they have extracted the mean, average absolute deviation and the magnitude. Finally, they have reduced the feature dimensionality using LDA. A more recent texture analysis approach has been proposed by Ng et al. [22]. The authors have divided the normalized iris into 3 equal zones. The first zone represents the area that directly surrounds the pupil. The second zone is the middle area of the iris and the third zone is the area of the iris that contacts the eyelids and eyelashes. After that, a one dimensional log-Gabor filter was applied to transform the iris texture to the frequency domain. On recognition, each zone is weighted according to its contribution to the accuracy of the system. Another recent technique has been proposed by Zhu et al. [24]. They have applied a region-based scale-invariant feature transform (SIFT) which was basically proposed to tackle iris recognition with off-centered iris position, and to extract reliable iris features that have an accurate location. SIFT has three main phases: 1) Producing the difference of Gaussian pyramid images, 2) Detecting local extreme points, 3) Assigning the leading orientation of feature points before generating the feature matrix.

3.3   Hand Recognition

Hand based biometric is an attractive technology to establish a recognition system. It has three main modalities: Fingerprint, hand geometry and palmprint [64]. Each of these biometric traits has its own advantages and disadvantages. For instance, fingerprint technology has shown robust and high accuracy, but it could be spoofed by using gummy fingers [25]. Hand geometry is a highly accepted technology due to its non-intrusive characteristic, but it may not be unique across a large number of users. Palmprint

technology is considered among the most attractive biometric traits to researchers due to the various types of features that can be extracted. As far as we are concerned in this thesis, we will focus next on palmprint and hand geometry.

3.3.1 Palmprint Recognition

In palmprint recognition, fingerprint similar features can be extracted such as minutiae, but it requires high resolution palmprint images [86]. Another type of features that can be extracted is to use techniques similar to face and iris such as subspace algorithms, texture analysis, or transformation techniques. Some authors also used palmprint geometrical features such as palm lines [26], [27], [28]. Extracting fingerprint similar features can be difficult whereas extracting face and iris like features can have high dimensionality, and using geometrical features can lack uniqueness when the system has a large number of users.

The subspace techniques such as PCA, ICA and LDA have been successfully applied on palmprint in a similar way to face recognition. There are some research papers proposing subspace techniques for palmprint, for instance, Shang et al. [32] have used Winner-Takes-All (WTA) ICA algorithm to extract features that are statistically independent of the image pixels. They treated the problem in two scenarios: 1) The palmprint images have been used as random variables while their pixels are considered to be observations, 2) They have treated the palmprint images as observations and their pixels as random variables. The resultant features of WTA-ICA technique have been classified using Radial-Basis Function Neural Network (RBFNN).

Finally, texture-based techniques have also been applied to extract discriminating features from the palmprint biometric. Texture patterns such as orientation and frequency can be computed using statistical measurements such as the mean and variance. The palmprint recognition may also use local and global statistical features. In local statistical features, the palmprint image is transformed into a special domain. Then, it divided into smaller regions, so the statistical measurements. The same is true with the global statistical features measurements except that there is no need to divide the transformed images into small regions [26]. Examples of the statistical features have been conducted by Kumar and Shen [29]. They have extracted the mean and variance features from a concentric circular band of a gray level palmprint image. Another example by Noh and Rhee [30] extracted invariant moments of level 2 and 3 from the whole space to represent palmprint image. Fusion of multiple textures of palmprint has also been proposed using neural network approach [81].

The structural features of a palmprint such as line-based approach have been addressed using edge detection techniques [26]. For example, Huang et al. [27] have proposed a verification system based on palmprint principal lines. The technique used a Modified Finite Radon Transform (MFRAT) that can detect principal palmprint lines easily even if there were strong wrinkle lines. Other work has been proposed by Wu et al. [28] for palmprint classification. Their algorithm defines a group of starting points for the principal lines explicitly. Then, it recursively detects and extracts the principal lines out from the palmprint. They have classified the palmprint lines into 6 categories based on the number of principal lines and the number of intersections. Moreover, it has been proposed by Wu et al. [31] to use a fuzzy logic to estimate the palmprint lines. The

authors have calculated fuzzy directional element energy features (FDEEF) via estimating the line orientation as a membership function to represent palmprint lines statistically with two main features (Global FDEEF and Block Edge Energy feature). At the same time, they have retained the characteristics of the lines such as thickness and length to support the palmprint features.

3.3.2 Hand Geometry

Hand geometry is another attractive biometric technology that has been used mostly in affordable authentication mode. During the past decade, hand shape authentication was uncomfortable technology due to the restrictions applied during the biometric acquisition procedure. The most common scenario to acquire a hand image was requesting a user to hold his hand on a fixed platform with small stands (pegs). The pegs were used as a guide to position the hand correctly. Although these pegs were providing some aid to the process of feature extraction, the applied restrictions were annoying to end users. As an example of such systems, Sanchez-Reillo [33] has proposed a biometric recognition system based on hand geometry. His acquisition design consists of a camera and a platform with six pegs in order to guide the users to the right position. Also, he has included a mirror on one side of the platform to obtain the width of the hand. Another example of the pegged platform was developed by Jain and Duta [34]. They have proposed a deformable matching technique that operates during the alignment phase. The hand geometry recognition has been addressed using other machine learning techniques including probabilistic neural networks [82], abductive neural networks [83], and support-vector machines [84].

More recently, peg-free and contactless hand geometry based authentication has formed a new trend in the hand based biometric technology. The new direction has added more challenges and difficulties to the hand based biometric recognition. The main force in this direction is the low level of acceptance to the pegged platform design. Examples of the peg-free and contactless designs [35]–[37]. Figure 10 shows pegged and peg-free hand geometry acquisition devices.

Using hand shape, different geometrical measurements can be computed. They are mainly the measurements of the hand shape such as finger lengths and widths, palm length and width, hand length, hand area and contour, etc. These measurements mainly depend on the located hand land marks.
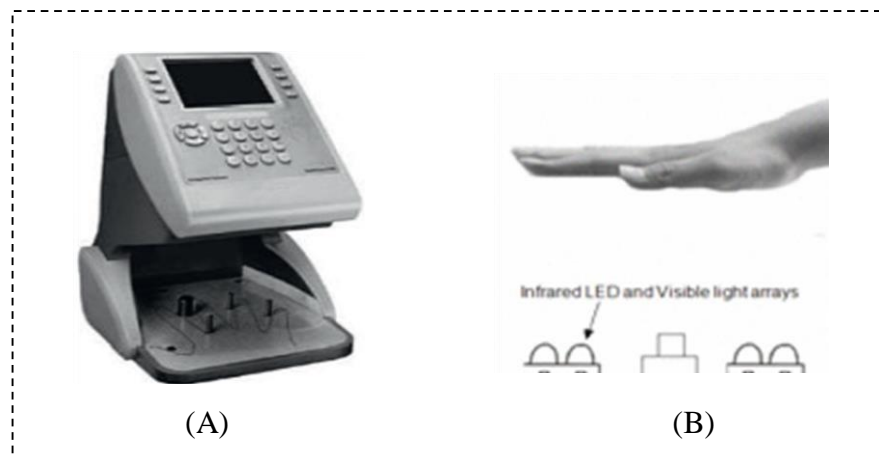
Figure 10 Hand acquisition devices,
(A) With pegs [37], (B) Infrared LED towards contactless acquisition [38]

3.4   Multimodal Biometric

As we mentioned before, the limitations of the unimodal biometric systems has motivated many researchers to combine multiple biometrics or samples. Several approaches have

been proposed in the literature. In the following subsections, we will review the state-of-the-art biometric fusion system for various combinations of face, iris and hand.

3.4.1 Face & Iris Fusion

Most of the techniques for combining face and iris traits are at the feature level or the matching score level. Gan and Liu [38] have proposed an approach to integrate face and iris features to enhance the recognition performance. They have extracted low frequency components from the face and iris images by using Two-Dimensional Discrete Wavelet Transform (2D-DWT) and Kernel Fisher Discriminant Analysis (KFDA). The low frequency components have been found to retain most of the important information of the image. Besides that, only one quarter of the image information can be dedicated as a feature vector. Noticeably, the domain number of the face feature set and the iris is heterogeneous. For this reason, the z-score normalization technique was used to transform the resultant feature vectors to a common space. Then, the face and iris feature vectors have been concatenated. At the matching and decision modules, a K-Nearest Neighbor (K-NN) classifier was used to compute the scores and make final decisions. Another work by Chen and Chu [39] to combine face and iris at feature level. They have extracted one-dimensional energy features from both face and iris by the horizontal and vertical projections respectively. Then, a particle swarm optimization (PSO) algorithm has been adopted to find the learning parameters of the wavelet probabilistic neural network (WPNN) as their matching and decision module.

The matching-score-level fusion requires two separate biometric systems to produce biometric scores. Once scores have been produced by both biometric traits, they are

combined using different techniques such as statistical or machine learning techniques. Fakhar et al. [40] have extracted texture-based information from face and iris using a steerable pyramid (S-P) representation. The S-P can produce a multi-scale representation and retain orientation characteristics. Raw resultant of the algorithm was divided into blocks size of 8×8 and 16×16. Each of these blocks was further analyzed using statistical measurements to lower the complexity and space of feature vectors. Therefore, there were only four features been extracted from each block: mean, variance, energy and entropy of the energy distribution. The features from each block were concatenated to form one feature vector of each image (Face or Iris). Just before matching-score level fusion, the system has to compute the matching scores of each biometric technology. Then, the scores were prepared to be combined using z-score normalization. Finally, a strong statistical technique (sum rule) was used to consolidate the matching scores.

The classification fusion technique has been carried out to integrate face and iris. Examples of these approaches are the work in [41] and [42] where a support vector machine (SVM) classifier was used for score fusion. Regardless of the features extracted from face and iris traits, the fusion treated the scores of both technologies as input vectors to the two-class classifier to decide whether the user is genuine or imposter.

In comparison between the statistical and classification techniques, Wang et al. [43] have conducted some experiments to compare the performance of the statistical and classification techniques on multimodal biometric systems using face and iris. They have found that the classification approach can produce better results; which may be due to their strong generalization ability. Recently, there is a direction towards the multimodal design of face and iris with a single acquisition device. For instance, Zhang et al. [44]

29

have designed a high resolution Near Infrared (NIR) sensor to capture a single image containing both the face and iris.

3.4.2 Face & Hand Fusion

Combining face and hand (palmprint or hand geometry) is one of the earliest proposed multimodal biometric systems. For example, Lu et al. [45] have fused face and palmprint to enhance identification accuracy. They have applied two techniques for feature extraction. The first technique is a texture-analysis technique and has been applied on both traits to extract statistical properties such as mean, standard deviation, smoothness descriptor, third and fourth moment, and uniformity and entropy from a gray-level histogram. The second technique applied a two-dimensional PCA. Once the feature extraction is finished, a *K*-NN classifier is used to calculate the scores using city-block and Euclidean distances. Finally the score of each biometric system was fused using a minimal distance rule (MDR) as follows:

$$\text{MDR}_i = \min_j \left(s_{f_j^i} \right) + \min_j \left(s_{p_j^i} \right) \quad \text{where } i = \text{users and } j = \text{samples} \tag{3.1}$$

Face and palmprint have also been combined at the feature level. For instance, Ahmed et al. [46] have extracted face and palmprint features using a bank of Gabor filters. They have filtered the biometric images using Gabor filters in eight directions $\{0, 1 \ldots 7\} \times \pi/8$, and four scales $\{2, 4, 8 \text{ and } 16\}$. The dimensionality of the resultant feature vector was very high. Therefore, they have used PCA and LDA to reduce the feature vector dimensionality. After that, these feature sets were simply concatenated to form a fused feature vector.

As far as the hand biometric has more than one modality, there were some research works that conducted to fuse face with more than one hand biometric trait. For example, Chaudhary and Nath have carried out some experiments on the fusion of two modalities of hand (palmprint and fingerprint) with face biometric trait [47]. The extraction of features for the palmprint, fingerprint and face was executed independently. PCA has been used to extract face and palmprint feature vectors while minutiae-based approach has been adopted to extract fingerprint features. In the fusion, the weighted sum rule has been used to consolidate the scores of the three biometric technologies. Weights are assigned to each biometric score by taking into consideration the importance of each biometric type. For instance, the authors used 0.6, 0.3 and 0.1 for fingerprint, palmprint and iris to reflect their past experience with each trait.

To the best of our knowledge, face and hand geometry have not been given attention as much as other biometric combinations. Ross et al. [48] have conducted one of the earliest integration on face and hand geometry with the support of fingerprint. They have investigated the information fusion at feature and matching-score levels. The authors have studied different combinations of fusion techniques. First, they have extracted independent feature sets of each biometric trait. PCA has been used to extract discriminant features from face whereas fingerprint features have been extracted using two techniques: minutiae-based and appearance-based. In addition, they have adopted 14 hand geometry features. In the fusion phase, they have applied three fusion techniques namely sum rule, decision tree and LDA. More recent, Tsalakanidou et al. [49] have evaluated the combination of 3D face and hand geometry for robust user authentication. They have taken biometric images in real working environment that included

31

complicated backgrounds. In 2012, El-Alfy and Binmakhashen [88] presented an identification system based on the fusion of face and hand geometry at the feature level using a support vector machine approach.

3.4.3   Iris & Hand Fusion

Wu et al. [50] have fused scores of palmprint and iris using statistical combination methods (sum, product, min and max fusion rules). They have extracted the features by applying a Gaussian filter to encode the palmprint into DiffCode, while a 2D Gabor filter has been used to extract the Iriscode. Both palmprint and iris systems have adopted the Hamming distance to produce similarity scores. Wang et al. [51] investigated the fusion of palmprint and iris at score level. They have applied the Phase-Only-Correlation (POC) to match palmprint images and produce matching scores. Finally, Gaussian Mixture Model (GMM) was used to fuse the scores and estimate the genuine and imposter distributions. Recently, Meraoumia et al. [53] have conducted a fusion of iris and palmprint in identification mode. They have suggested minimum average correlation energy (MACE) filter to produce matching scores of iris and palmprint systems. Most of the previous work was conducted between iris and palmprint with very little research to investigate the combination of iris and hand geometry. An example of this work can be found in [52] using statistical rules.

3.4.4   Hand Geometry & Palmprint Fusion

There are some studies that have concentrated with integrating hand geometry and palmprint information. An example of combining hand geometry and palmprint [54] was

motivated by using one sensor for both the acquisition of both biometrics; thus leading to more user convenience. Once the hand image is captured, the system carries out a process to locate the ROI. Then, feature extraction phase has to be started to get hand geometry and palmprint features. The hand geometry features are measurements of the lengths and widths of the fingers, the area of the hand, etc. For the palmprint, they used the principal line directional features. The fusion of hand geometry and palmprint has been carried on at feature and score levels separately. Other research works such as [55]–[58] have a common factor which improving the palmprint biometric systems via incorporating hand geometry statistical features at score-level and feature-level fusion.

3.4.5   Face, Iris and Hand Fusion

Fusion of the three modalities (face, iris and hand) is rarely found in the literature. Fenghua and Jiuqiang [59] have proposed a biometric system based on three modalities (face, iris and palmprint). They have tested the system with the available biometric traits using a selector. Therefore, their design can work with one, two or three modalities. Moreover, they found that combining the three modalities can enhance the system performance when using parallel SVM, but it can have a bad impact when using a static SVM as a classification technique.

3.5   Summary of Literature

We summarize the main related work in the literature in two tables. Table 3 illustrates the single biometric systems from 1998 to 2009 while Table 4 summarizes the multimodal systems from 2003 to 2012.

Table 3 Literature survey summary for unimodal biometric systems

Year, Ref	S/U[+]	Biometric	Technique	Results (%)
1999, [16]	10/40	face	DCT, neural network	Acc: 91–94.5
2002, [12]	10/40		geometrical	Acc: 94.5
2005, [17]	10/40		DCT, RBF	Avg Err[++]: 2.45
2009, [13]	12/23		PCA+DCT	Acc: 72.77
1998, [21]	1/11	iris	zero-crossing	-
2003, [18]	-/213		phase-based, Hamming	Acc: 98.06
2006, [24]	7/108		SIFT	Acc: 92
2008, [22]	7/108		Log-Gabor, Hamming	Acc: 98.62
2002, [29]	9/50	palmprint	fuzzy logic, principal lines	Acc:97.2
2004, [31]	20/40		statistical local	Acc: 97.5
2004, [28]	20 /690		principal lines	Acc:96.03
2005, [32]	2/189		statistical global	FAR:0.04; GAR:98
2008, [27]	20/386		principal lines	FAR:0.49; FRR:0.565
1999, [34]	2-15/53	hand geometry	alignment matching	Acc: 96
2000, [33]	10/20		GMM	Acc: 96; EER: 4.9

[+] S/U: Samples/Users, [++] Avg Err: Average Error

Table 4 Literature Survey Summary (Multimodal Biometric systems)

Year, Ref	S/U[+]	Biometric Modalities	Fusion level	Results (%)
2003, [54]	10/100	hand geometry/palmprint	feature, score	FAR:5.08, FRR:2.25 FAR:0, FRR: 1.41
2003, [48]	10/50	face/hand geometry		FAR:0.03, FRR:2.18
2004, [56]	30/50	palmprint/hand geometry	decision	FAR: 3.7–36.3; FRR: 1.6–5.3
2005, [39]	7/40	face/iris	feature	Avg Err[++]: 0.33
2006, [58]	10/100	palmprint/hand geometry	feature, score	FAR:0–5.3; FRR: 8.3, 1.41
2006, [52]	7/96	iris/hand geometry	score	CER: 1.67
2007, [57]	10/100	palmprint/hand geometry		FAR:0.43–0.32; FRR:0.6 EER:0.6
2007, [49]	-/50	face /hand geometry		EER: 0.82
2007, [55]	7/30	palmprint/hand geometry	feature	Acc: 94 – 98
2007, [50]	5/120	iris/palmprint	score	EER: 0.06; MTR: 0.012
2008, [59]	7/40	face/iris/palmprint		EER: 16–24
2009, [42]	10/40	face/iris		EER: 0.35
2009, [51]	6/100	iris/palmprint		EER; 1.75
2009, [47]	-	face/palmprint /fingerprint		ROC Curve
2009, [45]	10/40	face/palmprint		Acc: 96–98
2010, [46]	10/40	face/palmprint	feature	Acc: 99.5
2011, [41]	8/40	face/iris	score	MTR: 0.044
2011, [40]	4,7/108	face/iris		Acc: 99.5
2011, [61]	8/100	fingerprints	score, decision	ROC Curve
2012, [53]	6/100	iris/palmprint	score	Acc:99.75

[+]S/U: Samples/Users, [++]Avg Err: Average Error

CHAPTER 4

THE PROPOSED BIOMETRIC SYSTEM

In this chapter, we describe the proposed multibiometric recognition system using face, iris and hand. We start with an overview of the system components. Then, we discuss the preprocessing of the acquired images followed by the feature-extraction techniques for various biometrics. After that, we describe a bio-inspired technique for dimensionality reduction of the extracted features based on the particle swarm optimization algorithm. Finally, we discuss the fuzzy integral fusion technique.

4.1   An Overview of the Proposed Biometric System

In our proposed biometric system, we have considered three main biometric traits: face, iris and hand. For each of these human traits, the system starts by collecting some biometric images from the designated users and a user profile is created. During this enrollment phase, the system will do some preprocessing on the raw data to locate the ROI for each biometric image; and if it fails, the system recaptures the user's biometric. This process will be repeated until the system accepts the input. After that, the system will use the DCT and Gabor filter bank to extract different feature sets for each biometric. These feature sets will be stored in the system database to be used later during the identification/verification operation mode. At the operation phase, the system performs the same steps from collecting biometric images for the user to be identified/verified to feature extraction and the resultant feature vector will be compared with the pre-stored feature sets to identify/verify the coming user. Figure 11 shows the layout of the biometric system. Later, we will investigate the performance of each biometric separately and different combinations of two and three biometrics.
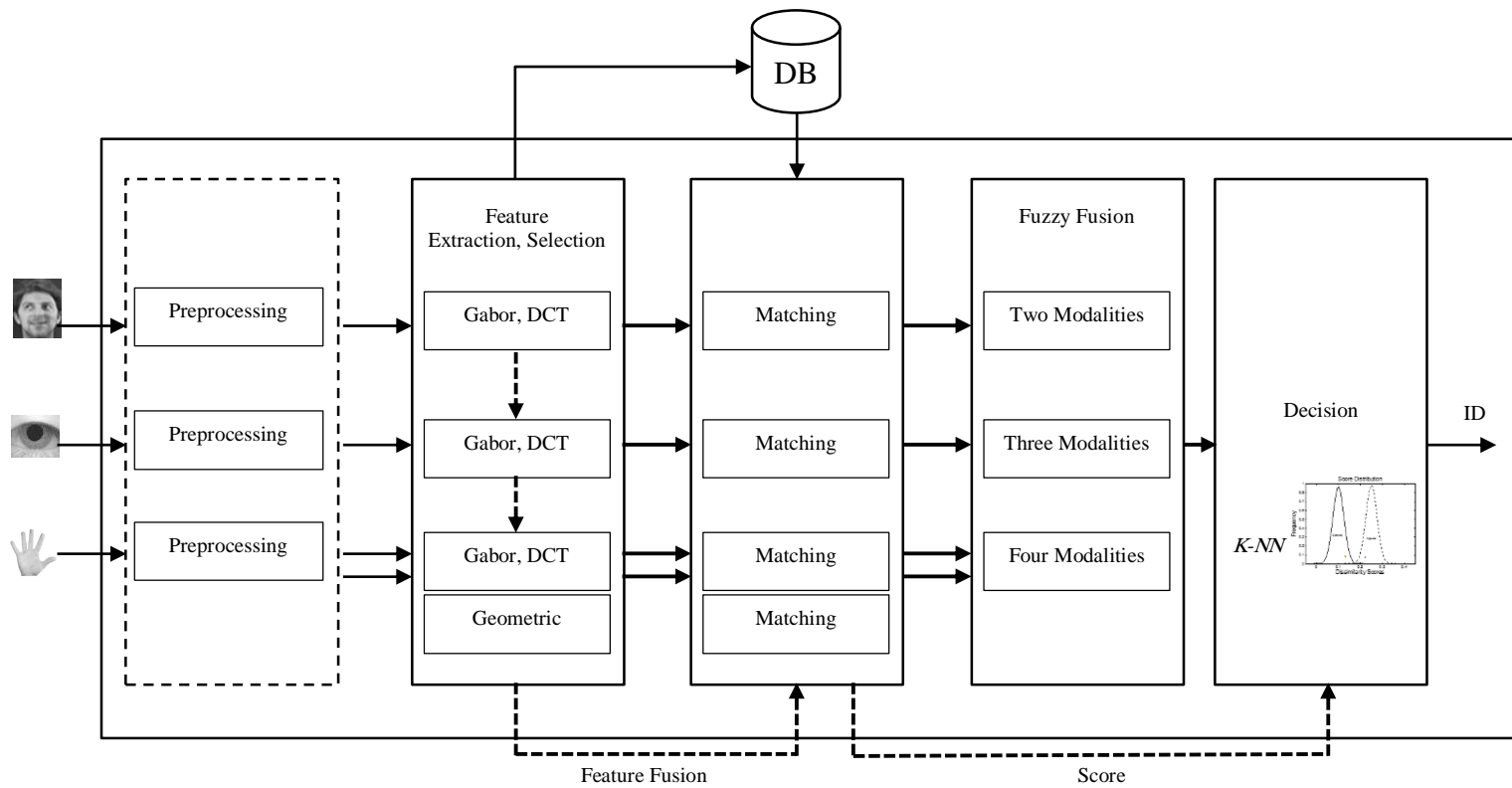
Figure 11 Layout of the biometric system

4.2   Preprocessing

In a real implementation of the proposed system, the acquired images for face, hand and iris may need some preprocessing to enhance their quality and extract ROI before applying the techniques of the following steps. Since we have used available benchmarking databases that were created by other authors, we have not done much at this stage for face and hand other than some unification of the user *ids* and number of samples per user. This was needed because the adopted iris database has fewer samples. However, for the iris database, it is required to locate and isolate the iris from the rest of the image. We applied two techniques: segmentation and normalization. Similar to the work by Libor Masek [65], the segmentation has been done using circular Hough transform and parabolic Hough transform. It has five main steps to extract the ROI:

a) Use Canny edge detection to generate an edge map.

b) Find circle parameters (center point and radius) from the output of the first step. Based on the iris database, the system has to be provided with the tentative radii (for the pupil from 28 to 75 and for the iris from 80 to 150 pixels). This information has been utilized by circular Hough transform to find circular shapes. After that, the Hough transform space has to be searched to find the parameters with the largest radius. Finally, the coordinates of that point has to be returned.

c) Detect the inner and outer iris boundaries. The inner boundary defines a circular edge with the pupil, while the outer boundary defines a circular edge with the sclera. Starting from a point on the circle surface, the outer boundary has to be computed by gradient biased in the vertical direction only. The inner boundary can be detected using the same method on the vertical and horizontal direction.

d) Exclude eyelids by applying a linear Hough transform for fitting a line to the upper and lower eyelid. These lines have two conditions. First, the line is not fitted if and only if the maximum value in the Hough space is less than a predefined threshold. Second, any fitted line has to be outside the pupil but it could be in the iris region.

e) Exclude eyelashes; this is database dependent. For the adopted iris database, the CASIA database, it has been found that the eyelashes were quite darker. Therefore, a simple thresholding technique can be used to eliminate the distortion within the iris region. On the other hand, when the detection of eyelashes is hard, it is advisable to leave the iris region without further processing. This is because thresholding may exclude some important information if it is not carefully implemented.

Assuming perfect iris localization and segmentation, the iris texture has to be normalized into a polar coordinate (See Figure 12). A mapping of each point in the dimensionless polar coordinates into a normalized polar coordinate was computed using a method called radial resolution. The radial resolution is based on Daugman rubber sheet model with a modification that allows the computation of the iris region, in the presence of pupil dilation, is more reliable.
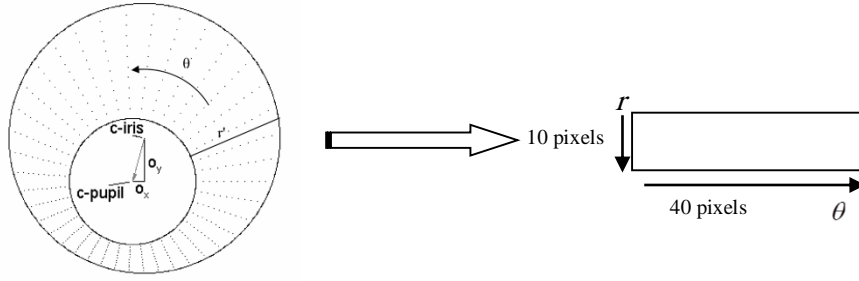
Figure 12 Radial resolution approach [65]

A formula is defined to model the radial resolution depending on the angle around the circle as follows [65]:

$$\bar{r} = \sqrt{\alpha}\beta \pm \sqrt{\alpha\beta^2 - \alpha - r_I^2} \qquad (4.1)$$

where r_I is the radius of the iris, and $\bar{r}$ is the distance between the edge of the iris and the edge of the pupil at angle θ; and α, β are given by:

$$\alpha = o_x^2 + o_y^2$$
$$\beta = \cos\left[\pi - \tan^{-1}\left(\frac{o_y}{o_x}\right) - \theta\right] \qquad (4.2)$$

where o_x and o_y is the displacement of the center of the pupil relative to the center of the iris in the x- and y- directions.

40

4.3 Feature Extraction Techniques

We have adopted two image processing techniques for feature extraction namely Two-Dimensional Discrete Cosine Transform (DCT) and Gabor filter in addition to the hand geometry. The coming subsections present the theoretical facts behind each of these techniques.

4.3.1 Two-dimensional Discrete Cosine Transform (2D-DCT)

It is a widely-known technique in the field of image and video processing [13], [66], [67]. It has been suggested by Ahmed, Natarajan and Rao in 1974 and standardized for JEPG image compression in 1992. Basically, the DCT transforms the image from a spatial domain into its frequency representation. The subsequent space has a specific structure, which allows the most important information to be concentrated in a small region. More preciously, the correlation between the pixels in the spatial domain is mapped into uncorrelated DCT space. This fact permits the redundant information in the high dimensional image space to be filtered in a way that the most important information is retained. On the other hand, the redundant information is actually not perceived by the human eye. Therefore, discarding such information is unnoticeable. The information kept by the DCT is in three bands: low, medium and high. The low band can be realized by the human visual system [67]; thus it is used for feature extraction.

DCT is basically similar to the discrete Fourier transform that operates on the real numbers. There are several DCT forms, but 2D is a commonly-used form in image processing. Consider a digital image represented by the intensity function $f(x,y)$ in the

41

spatial domain where $x, y = 0, 1, 2, \ldots, M - 1$. The coefficients of a 2D-DCT are given by:

$$Coef(u,v) = \alpha(u).\alpha(v) \sum_{x=0}^{M-1} \sum_{y=0}^{M-1} f(x,y).\cos\left[\frac{\pi u(2x+1)}{2M}\right].\cos\left[\frac{\pi v(2y+1)}{2M}\right] \qquad (4.3)$$

where (u, v) represents a point in the image frequency domain; $u, v = 0, 1, 2, \ldots, M - 1$; and $\alpha(u)$ and $\alpha(v)$ are computed as follows:

$$\alpha(u), \alpha(v) = \begin{cases} \sqrt{\dfrac{1}{M}} & \text{for} \quad u, v = 0 \\ \sqrt{\dfrac{2}{M}} & \text{Otherwise} \end{cases} \qquad (4.4)$$

The coefficient computed at $u, v = 0$ (called DC component) is one important component in the DCT space because it represents the average of the DCT window that applied on the image block.

In our work, we have extracted the DCT features from the biometric images by following two strategies. The first strategy, denoted as DCT_W, considers the whole image as one piece of texture. The second strategy, denoted as DCT_B, starts by dividing the face image into blocks and calculates the DCT coefficients from each block separately. We have used the standard block size of JPEG image compression, *i.e.* 8×8. Figure 13 (a) and (b) illustrate these two strategies applied on a face image. The features that have been extracted from DCT_W are read in a zigzag manner as illustrated in Figure 13 (c).
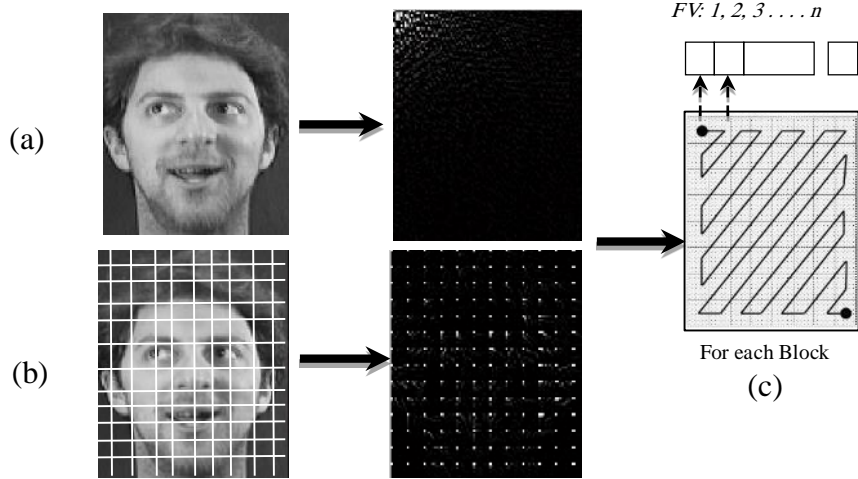
Figure 13 Feature extraction using DCT
(a) DCT$_W$ technique, (b) DCT$_B$ technique (8×8), (c) Zigzag algorithm

4.3.2 Gabor Filter Bank

This is one of the most powerful techniques that have been studied in the image processing field [68]. The Gabor filter is a combination of two functions: Gaussian and sinusoidal functions. It allows flexibility through adjusting its parameters to achieve multi-resolution image analysis. The filter can work as an excellent band-pass filter for one-dimensional and two-dimensional data. Usually a complex Gabor filter is defined using a complex sinusoid (carrier), $s(x, y)$, and a Gaussian kernel (envelope), $\omega(x, y)$, as follows:

$$g(x,y) = s(x,y)\omega(x,y) \tag{4.5}$$

The real and imaginary parts of a complex sinusoid are defined as follows:

$$Re\left[s(x,y)\right] = \cos\left(2\pi\left(u_0 x + v_0 y\right) + P\right) \tag{4.6}$$

$$Im\left[s(x,y)\right] = \sin\left(2\pi\left(u_0 x + v_0 y\right) + P\right) \tag{4.7}$$

43

where (u_0, v_0) and P are the spatial frequency and phase of the sinusoid in the Cartesian coordinates. In polar coordinates the magnitude and direction are given as follows:

$$F_0 = \sqrt{u_0^2 + v_0^2} \tag{4.8}$$

$$\omega_0 = \tan^{-1}\left(\frac{v_0}{u_0}\right) \tag{4.9}$$

alternatively,

$$u_0 = F_0 \cos\omega_0 \tag{4.10}$$

$$v_0 = F_0 \sin\omega_0 \tag{4.11}$$

Thus, the complex sinusoid is:

$$s(x, y) = \exp\left(j\left(2\pi F_0\left(x\cos\omega_0 + y\sin\omega_0\right) + P\right)\right) \tag{4.12}$$

where $j = \sqrt{-1}$. On the other hand, the Gaussian envelope can be calculated with the following equation:

$$w(x, y) = K \exp\left(-\pi\left(a^2\left(x - x_0\right)_r^2 + b^2\left(y - y_0\right)_r^2\right)\right) \tag{4.13}$$

where (x_0, y_0) is the peak of the function, a and b are scaling parameters of the Gaussian, r stands for a Θ-rotation such that

$$\begin{bmatrix} \left(x - x_0\right)_r \\ \left(y - y_0\right)_r \end{bmatrix} = \begin{bmatrix} \cos\theta & \sin\theta \\ -\sin\theta & \cos\theta \end{bmatrix}\begin{bmatrix} x - x_0 \\ y - y_0 \end{bmatrix} \tag{4.14}$$

The Gabor filter is tuned to reduce the effect of brightness by adjusting the DC to zero with the application of the following formula:

$$g'(x, y) = g(x, y) - \frac{1}{(2M+1)^2} \sum_{i=-M}^{M} \sum_{j=-M}^{M} g(i, j) \tag{4.15}$$

Its 2D Fourier transform is as follows:

$$G(u, v) = \frac{K}{ab} \exp\left(j\left(-2\pi\left(x_0\left(u - u_0 \right) + y_0\left(v - v_0 \right) \right) + P \right) \right) \exp\left(-\pi\left(\frac{\left(u - u_0 \right)_r^2}{a^2} + \frac{\left(v - v_0 \right)_r^2}{b^2} \right) \right) \tag{4.16}$$

from which the magnitude and phase components are:

$$\text{Magnitude}\left[G(u, v) \right] = \frac{K}{ab} \exp\left(-\pi\left(\frac{\left(u - u_0 \right)_r^2}{a^2} + \frac{\left(v - v_0 \right)_r^2}{b^2} \right) \right) \tag{4.17}$$

$$\text{Phase}\left[G(u, v) \right] = -2\pi\left(x_0\left(u - u_0 \right) + y_0\left(v - v_0 \right) \right) + P$$

or alternatively the real and imaginary components are:

$$Im\left[G(u, v) \right] = \text{Magnitude}\left[G(u, v) \right] \sin\left(\text{Phase}\left[G(u, v) \right] \right)$$

$$Re\left[G(u, v) \right] = \text{Magnitude}\left[G(u, v) \right] \cos\left(\text{Phase}\left[G(u, v) \right] \right) \tag{4.18}$$

To extract the biometric feature vectors, a Gabor filter is applied on the biometric images at four directions with three different scales and frequencies. Thus, twelve Gabor filters are used to filter the biometric images and the final output will be computed using the maximum of the filters outputs for each element in the Gabor feature vector.

4.3.3 Hand Geometry

Hand geometry is a little different; it holds only geometrical measurements as features. Once a hand image is acquired, the image is binarized using thresholding and an ROI is extracted to separate the hand shape from its background and noise [37], [54], [58], [70].

The system then locates specific points at the hand that are called landmarks. The landmark points can be varied from design to another. Usually, hand landmarks are located within four positions: finger tips, the in-between finger valleys, hand wrist and middle of the hand (palm point) [71]. Figure 14 shows some examples of hand landmarks.
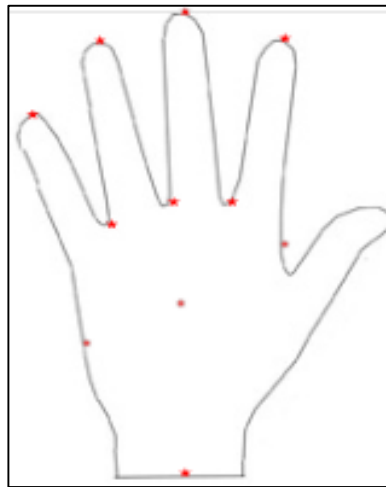
Figure 14 Hand landmarks

After these major points been determined, feature extraction has to be carried out to measure various distances between landmarks, e.g., lengths of fingers which are the distances between valley points to the associating fingertip points. As depicted in Figure 15, we have adopted 17 conventional hand geometry features. Finger length (FL) was extracted from four fingers except the thumb. Finger width (FW) measurement was taken at two different latitudes of each finger. Palm width (PW) was measured from the middle point of the line between the thumb and the index finger to the end of the other side of the palm. Hand and Palm lengths (PL, HL) were computed based on the wrest landmark point and the middle-finger valley and tip landmark points respectively. The last two features were the hand-contour length and area (HCL, HA) [72].
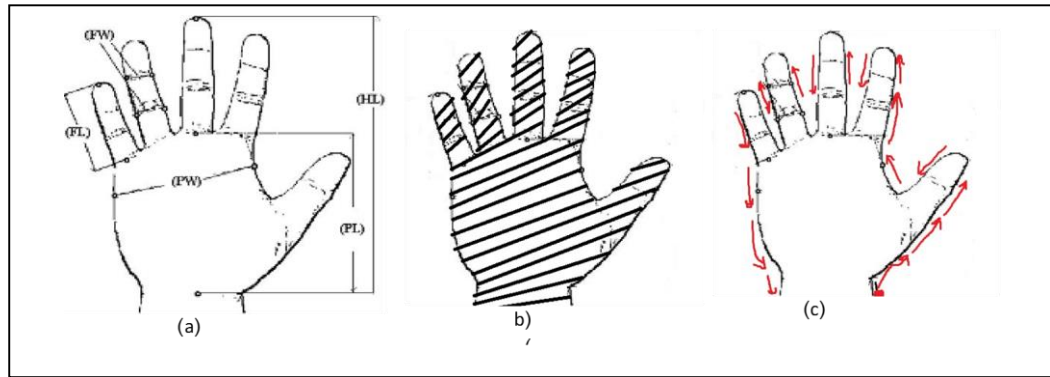
Figure 15 Hand geometry features extraction
(A) 15 features, (B) Hand contour, (C) Hand area

4.4 Bio-inspired Feature Selection

One of the major problems in the recognition of a biometric pattern is the curse of dimensionality, especially with the fusion of multiple biometrics. The difficulty of this problem is due to: 1) Too many features may include noise, 2) Increasing the size of the feature dimensionality may need more samples to carry out better recognition operation, and 3) High computation and large storage are needed. According to the analysis conducted by Silverman [73], the estimated ideal number of samples required as a function of the number of dimensions is as shown in Table 5; it is clear that this number is growing exponentially.

Table 5 Ideal number of samples per dimension

Dimensionality	Required Sample Size
1	4
2	19
5	786
7	10,700
10	842,000

Feature selection and reduction is an essential process to determine a subset of a given feature set for the application of a learning algorithm [74]. This subset should contribute to enhance or stabilize the system performance. There are two main strategies for feature selection: Forward and backward. Forward selection, as the name suggests, it starts with a small amount of features and subsequently grow this number by adding one or more features until reaching reasonable performance. Backward feature selection is completely the opposite version of the previous approach. It starts with the complete feature vector space. Then, it continues by taking out one by one of the feature space and evaluates the current feature vector until the stop condition is met.

In our work we adopted a bio-inspired approach for feature selection based on Particle Swarm Optimization (PSO). We have chosen this technique because of two main reasons. First, it is unlike other techniques such as PCA which is required to be recomputed each time the system adds or drops a registered user. Secondly, the PSO algorithm needs to be run once for each biometric space and returns the best feature locations at the training stage. The PSO has been first introduced by Kennedy and Eberhart [75]. The idea was inspired by a flock of birds searching for a warmer location. Each bird can feel the temperature degree of the current location, perceive the other birds' current locations, and tell which bird's location is the warmest. There are three different decisions each bird can make to reach the target [76]:

1. Keep flying in the same direction and find a better place.

2. Return to the previous place where the temperature is better.

3. Change direction towards the neighboring bird's location that is warmer.

Finally, birds can manage to settle on a decision that has an optimal or best possible solution via information sharing.

The PSO is a population-based search heuristic technique. It starts by randomly initialized solutions (particles). Each particle has a position X and a velocity v. Moreover, particles can memorize their best local position ($P_{best,p}$) and tracking the global best position (G_{best}).

Figure 16 shows a general flowchart of the algorithm. Assume a solution vector has n dimensions and there are m particles. Let $X_p = \{x_{p,1}, x_{p,2}, \dots x_{p,n}\}$ denote the location (solution) of the p-th particle where $p = 1, 2, 3, \dots, m$. To decide the best position, a fitness function has to be evaluated for every solution (particle position). In PSO, particles' positions and velocities are normally updated repeatedly. The position of each particle is affected by the updated velocity. Each particle updates its velocity according to the following [89]:

$$V_p^{new} = w \times V_p^{old} + c_1 \times rand_1 \times (P_{best,p} - X_p^{old}) + c_2 \times rand_2 \times (G_{best} - X_p^{old}) \qquad (4.19)$$

where w is the inertia of the particle, c_1 and c_2 are stochastic acceleration terms to pull each particle towards $P_{best,p}$ and G_{best}; usually $c_1, c_2 = 2$, $rand_1$ and $rand_2$ are two random numbers from a uniform distribution in a range of [0 1]. The velocity should have a maximum and minimum boundaries; this is to avoid trapping a particle in a local minima. Moreover, the maximum velocity should not be set to a very small value to avoid such problem. In the other hand, the particle may pass over the global minimum when using a large velocity. Therefore, velocities should be within a predefined range [V_{min}, V_{max}].

A binary version of PSO is used in the implementation of the feature reduction process. Primarily, particles are represented in binary modes (0, 1). The mode {1} indicates a selection of the corresponding attribute in the feature space, and {0} indicates a discarding of the corresponding attribute. The position of each particle is updated using the new computed velocity as:

$$x_{p,i}^{new} = \begin{cases} 1 & rand < \dfrac{1}{1+\exp\left(-v_{p,i}^{new}\right)} \\ 0 & otherwise \end{cases} \tag{4.20}$$

where $v_{p,i}^{new}$ is the new velocity of particle p in the i-th direction.

Each PSO particles may start randomly from any position on the feature space such as $x_1=\{1,0,1,1,0,0,1,1\}$ that selects 5 features out of 8. Suppose this particle current fitness value is 0.8, then this particle is trying to move into another position as $\underline{x}_1=\{0,0,1,1,1,0,1,1\}$ but its fitness value is 0.6. Therefore, this particle decision will be to roll back to old place. Moreover, the particle's new position is affected by the global best position found so far. Therefore, each particle will update its parameters to find the right direction and settle in the best found position.

The fitness function that we have used depends on the relationship between the selected feature attributes (particle position) and its corresponding accuracy using K-NN. The objective of the PSO is maximizing the system performance while reducing the number of features. The fitness value is obtained according to the following formula:

$$Obj(X_p) = (1 - \alpha) \times Eval(X_p) + \alpha \times (\ (F_{all} - F_{selected}) / F_{all}\ ) \qquad (4.21)$$

where α is a balancing factor for favoring the performance or features solution, $F_{selected}$ is the number of features that has been selected by the particle, and F_{all} is the total number of features. The $Eval(.)$ is the evaluation of the particle.

There are two scenarios to find the best solution in the biometric feature space. The first scenario is to select the subset feature of the feature vector from each single biometric. The second scenario considers the concatenation of the feature vectors of multiple biometric traits before searching the feature vector space. Figure 17 shows an example of how the feature selection can take place.
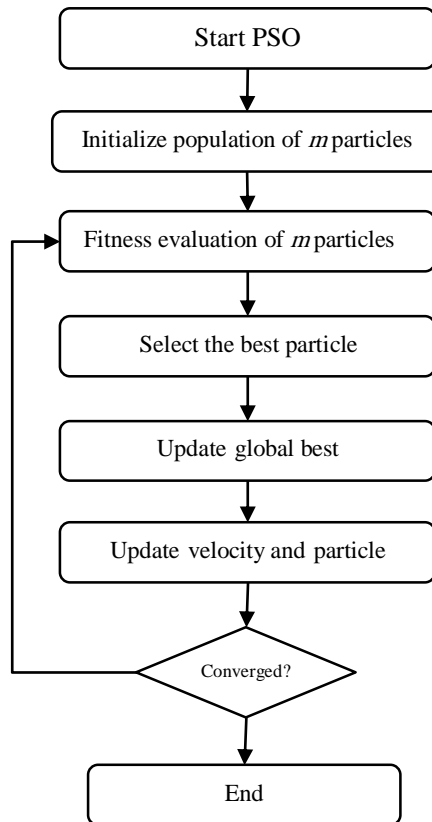
Figure 16 General PSO flowchart
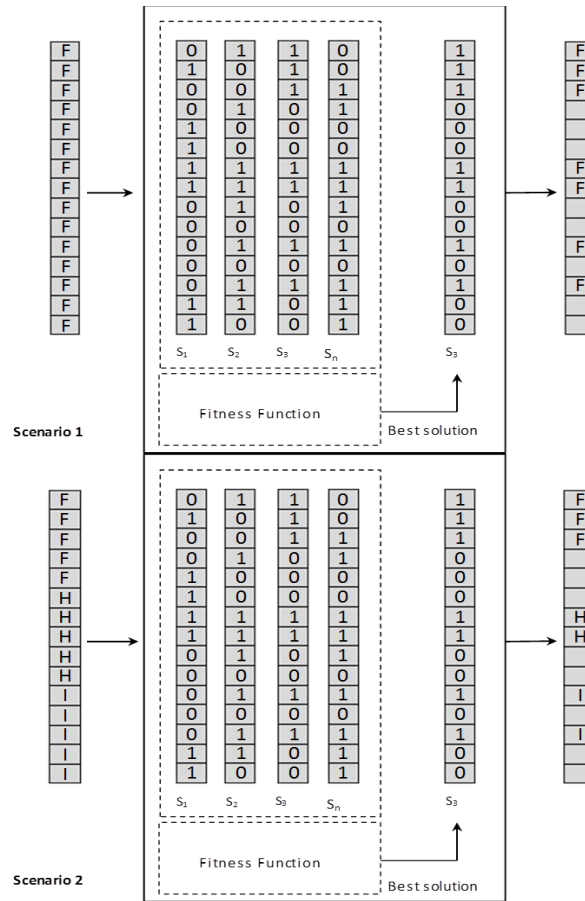
Figure 17 Binary PSO: two scenarios for feature selection
F: Face, H: Hand, I: Iris

4.5   Matching Score Evaluation

The system has set to use similarity-based measurements for generating the scores based on the city-block distance between a given biometric feature vector and the pre-stored feature vector. After computing the distance, we used min-max normalization then the normalized value is subtracted from 1 to convert it to similarity score; as follows:

52

$$\bar{s} = 1 - \frac{d - d_{\min}}{d_{\max} - d_{\min}} \qquad (4.22)$$

where d is the computed distance, $\bar{s}$ is the corresponding normalized similarity score, and $d_{\min}$, $d_{\max}$ are the lower and upper bounds on the distance measure.

4.6   Fuzzy Fusion

Fuzzy logic has been developed to handle imprecision in the description. Basically, it tries to describe the vagueness or ambiguity in natural languages (linguistic, lexical or semantic uncertainty). Fuzzy logic is mainly suggested for human subjective evaluation problems. For example, the phrases 'wide street' or 'best price' may have different meanings based on the person's background. For a European person, 'wide street' may refer to a street with four lanes, but it may mean a street with three lanes for an Asian person. The same is true for 'best price' when we infer the meaning from a poor or rich person [78]. It has been applied successfully on several decision problems [79].

The fuzzy integral can be thought of as an average membership value of fuzzy sets which is related to fuzzy measures. It has been applied successfully on several decision problems [79].

As an aggregation operator, fuzzy integrals are well-known to be among those techniques that are powerful yet flexible to aggregate information under different assumptions of source independence [61], [80]. Most of the work that has been found using fuzzy fusion in biometrics is concerned with the decision level fusion [77], [63], [91]. This supports the fact of uncertainty in the ownership of biometric traits. Also the fusion could be supported by soft characteristics such as (eye colors, facial marks, gender, weight etc.).

Chetty et al. [63] has tired a fuzzy integral to combine information of face and voice in verification mode.

The fuzzy integrals are nonlinear functional operators which defined relative to the fuzzy measures [94]. Let $X = \{x_1, x_2, \ldots, x_n\}$ be a finite set that may have some interactions with each other, and $P(X) = 2^X$ denote the family of all subsets of X which is also known as the power set. The fuzzy measure on X can be defined as a set of functions $f : P(X) \rightarrow [0, 1]$ with the following axioms:

1) The measure has a boundary: $f(\phi) = 0, f(X) = 1$

2) The measure is monotonically increasing: $f(A) \leq f(B)$, if $A \subseteq B$ and $A, B \in P(X)$

3) The fuzzy measure is continuous:

$$\lim_{i \to \infty} f(A_i) = f\left(\lim_{i \to \infty}(A_i)\right), \text{if } A_i \in P(X) \text{ and } A_1 \subseteq A_2 \subseteq A_3 \subseteq \ldots\ldots$$

Starting from this definition, Sugeno [93] has introduced a so-called λ-fuzzy measure that has an additional axiom as follows:

$$f_\lambda(A \cup B) = f_\lambda(A) + f_\lambda(B) + \lambda f_\lambda(A) f_\lambda(B) \tag{4.23}$$

for all $A, B \subseteq X$, $A \cap B = \phi$ and for some λ > −1. It is obvious that when λ=0 the Sugeno fuzzy measure turns out to be the standard probability.

The value of λ for a given set $X = \{x_1, x_2, \ldots, x_n\}$ can be computed by solving the following polynomial equation:

$$\lambda + 1 = \prod_{i=1}^{n}(1 + \lambda f_\lambda(x_i)), \lambda \neq 0 \tag{4.24}$$

54

The root of interest should satisfy the condition that $\lambda > -1$. Based on the solution of equation (4.24), there are three cases according to [79]:

$$
\begin{cases}
\text{if } \displaystyle\sum_{i=1}^{n} f(x_i) > f(X) = 1, & then \quad -1 < \lambda < 0 \\[4mm]
\text{if } \displaystyle\sum_{i=1}^{n} f(x_i) = f(X) = 1 & then \quad \lambda = 0 \\[4mm]
\text{if } \displaystyle\sum_{i=1}^{n} f(x_i) < f(X) = 1 & then \quad \lambda > 0
\end{cases}
\tag{4.25}
$$

As given in [94], the fuzzy integral of a function $h(.)$ computed over P(X) of the function h with respect to a fuzzy measure $f(.)$ is defined as follows:

$$
\int_{Y=P(X)} h(y) \circ f(.) \triangleq \sup_{\alpha \in [0,1]} \Big[\min\big[\alpha, f(\{y : h(y) \geq \alpha\})\big] \Big]
\tag{4.26}
$$

when the values of $h(.)$ are ordered in decreasing sequence such that $h(x_1) \geq h(x_2) \geq \ldots \geq h(x_n)$, the Sugeno integral becomes

$$
\int_{Y=P(X)} h(y) \circ f(.) \triangleq \max_{i=1\ldots n} \Big[\min\big[h(y_i), f(A_i)\big] \Big]
\tag{4.27}
$$

where $A_i = \{y_1, y_2, \ldots, y_i\}$ denotes a subset of the universe of discourse. The value of $f(A_i)$ are assumed to the fuzzy measure and can be determined recursively from:

$$
\begin{cases}
f(A_1) = f(\{y_1\}) = f_1 \\
f(A_i) = f_i + f(A_{i-1}) + \lambda f_i f(A_{i-1}), & \text{for } 1 < i \leq n
\end{cases}
\tag{4.28}
$$

Murofushi and Sugeno have explained that if the above measure is additive the expression does not return the integral [85]. For this reason, they have proposed a Choquet fuzzy integral that can be computed using the following equation:

$$\int_{Y=P(X)} h(y) \circ f(.) \triangleq \sum_{i=}^{n} \left[h(y_i) - h(y_{i+1}) \right] f(A_i), \quad \text{where} \quad h(y_{n+1}) = 0 \qquad (4.29)$$

To demonstrate the above procedure in the context of a biometric fusion example, suppose we have four biometrics to be combined *a, b, c* and *d*. Their systems have produced these scores $f(\{a\})=0.6, f(\{b\})=0.7, f(\{c\})=0.9$ and $f(\{d\})=0.8$, respectively. In addition, the expert person has assigned belief values to these systems as $h(\{a\})=0.9,$ $h(\{b\})=0.85, h(\{c\})=0.99,$ and $h(\{d\})=0.8$ in order. First, the system sorts the scores to be combined so that the $h(.)$ are in decreasing order. Then, it computes λ and applies Equation (4.28), recursively, then computes the integral either by Sugeno or Choquet.

4.7   Decision Making Module

During training an optimal threshold value is determined. During the verification mode, the system compares the computed score (whether for a single biometric or after fusion of multiple biometrics) with the pre-calculated threshold. If the score is greater than the threshold, then the system accepts the claim. Otherwise, the claim is false.

For identification mode, the system compares repeats the calculation of similarity scores and comparison with the pre-calculated threshold for each for each of the pre-registered users. Then, the system uses a *K*-NN approach to make the final decision as follows:

a) All nearest neighbors have the same PIN, the system reports this PIN for the user.

b) Apply the majority vote and declare the PIN accordingly.

c) If PINs are different for the k nearest neighbors, then report the PIN with the highest score; similar to 1-NN.

CHAPTER 5

EXPERIMENTAL WORK AND RESULTS

In this chapter, we start with a description of the adopted biometric databases followed by the performance metrics. Then we describe the conducted experimental work and results for the unimodal-biometric systems based on face, iris and hand for two reasons, 1) It will be used as a benchmark for the proposed system, and 2) It will be studied to understand the strengths and weakness for each unimodal system. After that, we present the experimental work for various multimodal-biometric systems using two and three combinations of face, iris and hand. Finally, we give some experimental results of the fusion at the feature level to identify the successful combinations of those biometric features. In addition, the results of this feature level fusion are compared with matching score level fusion. We should also mention that the feature-level fusion has been conducted on randomly selected features of each biometric trait. This is because, the number of the generated data files with feature vector concatenation is so huge (> 600 data files) with a total size of 23.4GB.

5.1   Biometric Databases

Before we discuss the performance of the biometric systems, we have to describe the biometric databases. Most of the multimodal biometric researchers have assumed an independence of the human biometric traits. According to this assumption, a virtual

multimodal biometric database can be composed of multiple independent databases. In this work, we have built our virtual database using public biometric databases that are available online as described next.

A. *Face Database:* The face images have been adopted from ORL database of faces [90]. The database has been developed by Olivetti Research Laboratory Cambridge, UK. This database has been reported in many researches such as [38], [39], [41], [43], [45]. It contains images with different facial expressions (e.g., smiling, not smiling, and open or closed eyes), facial details, and varying illuminations. Figure 18 shows some images of two users.
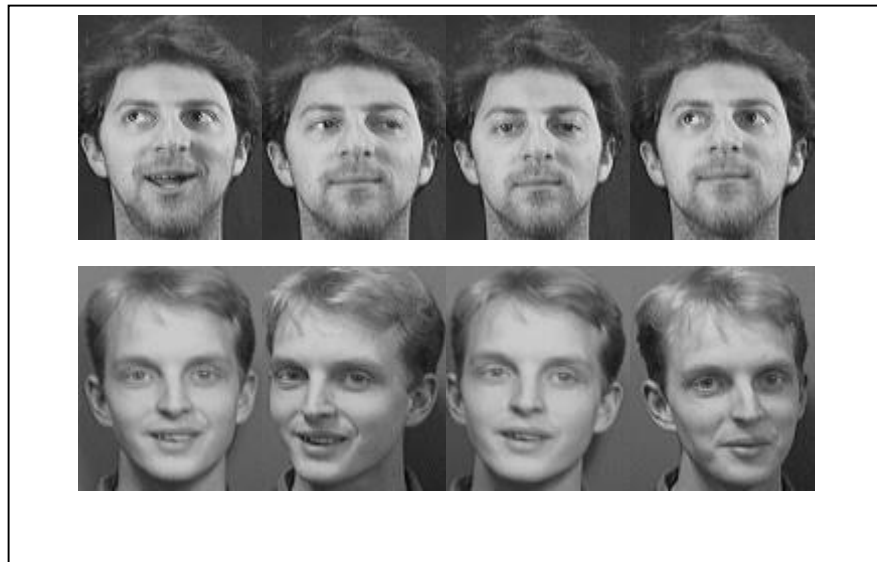
Figure 18 Eight images of two users in the ORL database of faces

The size of each image is 92×112 with 256 gray levels per pixel. The database contains 400 images of 40 users and 10 samples for each user. It has been built specifically for face recognition. The preprocessing has been manually conducted to each image to locate only the face and eliminate noise.

B. *Iris Database:* We have used CASIA database version 1 (CASIA-Iris V1) [92]. The database is well-known and available for research purposes. It consists of 756 iris images that have been taken from 108 users. Each user has contributed 7 images. The iris images have been captured in two sessions. Three images were collected in the first session whereas four images were taken in the second session. Near-infrared sensor was used to capture eye images. All images have a dimension of 320×280 and are stored as bitmap type. The iris images have some noisy information such as eyelids and eyelashes. The noisy information may reduce the recognition performance. Moreover, some images have non-centered iris positions. Figure 19 shows 6 iris images of 2 users.
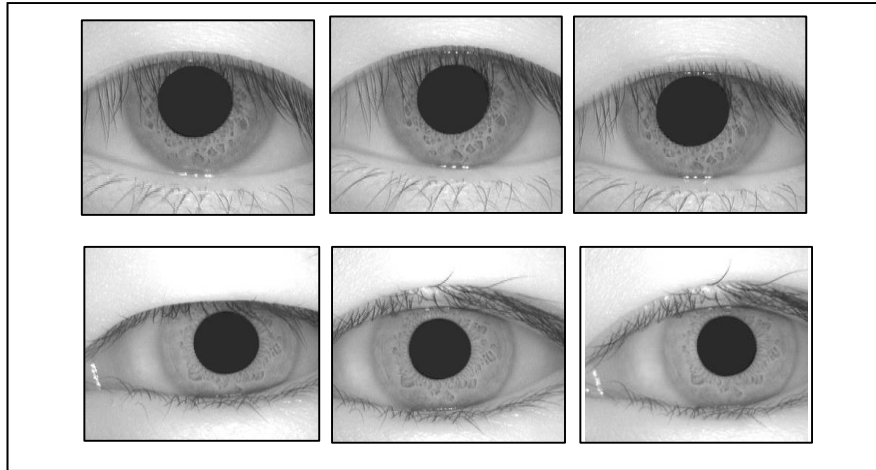
Figure 19 Six images of two users in the CASIA-Iris V1 database

C. *Hand Database:* We adopted two databases one for the hand geometry and the other for the palmprint from [72]. The hand geometry database contains 1000 hand images of 100 subjects, each subject contributed with 10 left hand images. The images were captured in peg-free mode using a digital camera. Hand orientation was determined using the binary version of the hand in the preprocessing phase. Then hand geometry features were computed using the preprocessed binary version of the hand images, this was needed to ensure that similar feature positions will be located and extracted for all

users [58]. Moreover, hand images have been preprocessed and ROI (palmprint) was extracted. The palmprint-images have different image sizes (445×442 and 404×400). The images have been stored as text files and provided publicly for free. These text files can be converted to palmprint images again using special software. The adopted database is in gray level scale with different illumination. Figure 20 shows a sample of palmprint images of two users in different illumination
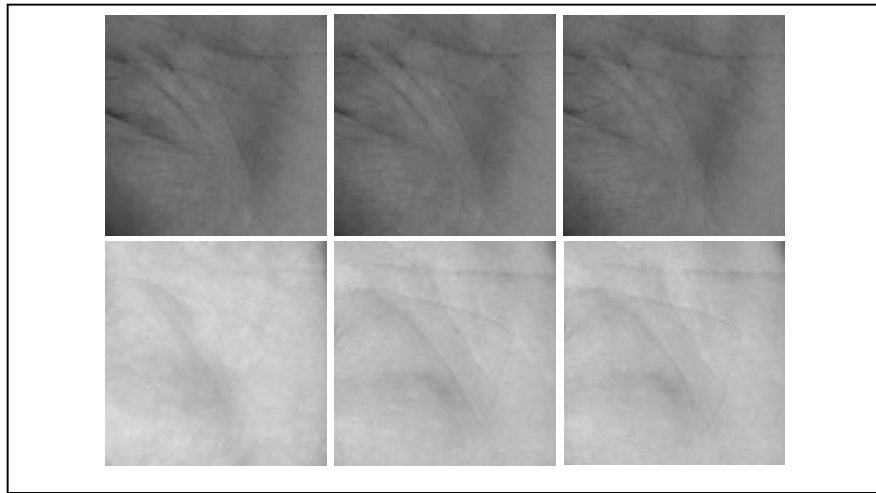
Figure 20 Six images of two users in the palmprint database

5.2   Performance Metrics

In our biometric recognition system, the performance is measured in two methods; ROC measurement and single threshold testing. In the ROC, we have run the system on the complete data repeatedly. Then, a matching is carried out at various thresholds, where the FRR and FAR are computed. The performance is also compared according to the AUC values. In the second method, a single threshold is computed over the training subset. Then, a test is carried out using k-fold cross-validation with $k = 7$. Therefore, each biometric database is divided into 7 subsets and the system is trained on six of them and tested on the last. Each experiment is repeated 7 times with different subsets for training

and testing. Therefore, seven different data subsets are used in training and testing on each execution. The total reported system performance is the average of all seven experiments. In feature extraction using Gabor filter bank, we used the parameters shown in Table 6 (these parameters we found by trial and error on the palmprint database).

Table 6 Gabor filter bank parameters

Filters	F	a,b	θ
First	0.1	0.24	270°
	0.1	0.24	180°
	0.1	0.24	90°
	0.1	0.24	0
Second	0.2	0.48	270°
	0.2	0.48	180°
	0.2	0.48	90°
	0.2	0.48	0
Third	0.6	1.44	270°
	0.6	1.44	180°
	0.6	1.44	90°
	0.6	1.44	0

5.3   Unimodal Biometric Systems

We started by considering a single biometric system as illustrated in the framework shown in Figure 11. We run the system to prepare the feature sets from different biometrics. After the features been computed, the system saves these features in a database. Then, we carried out two main experiments; the first experiment is carried on the feature sets without feature reduction. The second uses a reduced feature set generated by the particle swarm. Table 7 tabulated different feature sets and their sizes before and after feature selection.

Table 7 Feature sizes (with and without feature selection)

Biometric	Features Type	Without F.S.	With F.S.
Face	Im (Imaginary)	10304	2246
	Re (Real)	10304	2255
	Angles	10304	1495
	Mag (Magnitude)	10304	2236
	DCT_B	64	18
	DCT_W	64	18
Iris	Im (Imaginary)	4800	1014
	Re (Real)	4800	753
	Angles	4800	746
	Mag (Magnitude)	4800	703
	DCT_B	90	26
	DCT_W	64	28
Palmprint	Im (Imaginary)	16385	4126
	Re (Real)	16385	4000
	Angles	16385	4044
	Mag (Magnitude)	16385	5275
	DCT_B	256	95
	DCT_W	64	17
Hand geometry	Geometric	17	5
Feature-Level Fusion	FF_1: $\text{Mag}^{\text{face}} + DCT_W^{\text{iris}}$	10368	2592
	FF_2: $\text{Mag}^{\text{face}} + DCT_W^{\text{palm}}$	10368	2558
	FF_3: $\text{Mag}^{\text{face}} + \text{Angles}^{\text{palm}}$	26688	6621
	FF_4: $\text{Mag}^{\text{face}} + \text{Hand}$	10321	3735
	FF_5: $DCT_W^{\text{iris}} + DCT_W^{\text{palm}}$	128	44
	FF_6: $DCT_W^{\text{iris}} + \text{Angles}^{\text{palm}}$	16448	5862
	FF_7: $DCT_W^{\text{palm}} + \text{Hand}$	81	13
	FF_8: $\text{Angles}^{\text{Palm}} + \text{Hand}$	10321	2540
	FF_9: $DCT_W^{\text{iris}} + \text{Hand}$	81	22
	FF_{10}: $\text{Mag}^{\text{face}} + DCT_W^{\text{iris}} + DCT_W^{\text{palm}}$	10432	2609
	FF_{11}: $\text{Mag}^{\text{face}} + DCT_W^{\text{iris}} + \text{Angles}^{\text{palm}}$	26752	6568
	FF_{12}: $\text{Mag}^{\text{face}} + DCT_W^{\text{iris}} + \text{Hand}$	10385	2597
	FF_{13}: $DCT_W^{\text{iris}} + DCT_W^{\text{palm}} + \text{Hand}$	145	27

5.3.1 Face Recognition

For unimodal face recognition, the results of the experiments for verification and identification modes for different types of features without and with feature selection are shown in Table 8 and Table 9, respectively. We can clearly observe that the system performance during the verification mode is higher than its performance during identification mode. Without feature selection (No F. S.), the best results we could have observed for face recognition is up to 98.93±0.02% in verification mode and 87.86±0.05% in identification mode. Using the reduced the feature sets resulting from PSO feature selection (F.S.), the results show some enhancement of the performance in verification and identification modes using some Gabor bank features. However, for DCT features the performance is reduced; this can be attributed to the huge reduction of the feature space (see Table 7).

Table 8 Face recognition results (No F.S.)

Features	Verification (%)			Identification (%)		
	ACC	FAR	FRR	ACC	FAR	FRR
Imaginary	98.57± .01	0± 0	1.47± .01	**87.86± .04**	**12.14± .04**	**0± 0**
Real	96.07± .03	0± 0	4.03± .03	85.71± .05	14.29± .05	0± 0
Magnitude	97.86± .02	0± 0	2.2± .02	84.29± .07	15.71± .07	0± 0
Angles	93.21± .04	0± 0	6.96± .04	82.5± .05	17.5± .05	0± 0
DCT_B	**98.93± .02**	**0± 0**	**1.1± .02**	**87.86± .05**	**12.14± .05**	**0± 0**
DCT_W	96.43± .03	0± 0	3.66± .03	82.86± .06	17.14± .06	0± 0

Table 9 Face recognition results (F.S.)

Features	Verification (%)			Identification (%)		
	ACC	FAR	FRR	ACC	FAR	FRR
Imaginary	**98.57± .01**	**0± 0**	**1.47± .01**	**88.21± .02**	**11.79± .02**	**0± 0**
Real	97.14± .02	0± 0	2.93± .02	86.07± .04	13.93± .04	0± 0
Magnitude	98.21± .02	0± 0	1.83± .02	83.93± .05	16.07± .05	0± 0
Angles	93.57± .03	0± 0	6.59± .03	82.5± .07	17.5± .07	0± 0
DCT_B	98.21± .02	0± 0	1.83± .02	85.36± .05	14.64± .05	0± 0
DCT_W	91.43± .03	0± 0	8.79± .03	78.21± .04	21.79± .04	0± 0

5.3.2   Iris Recognition

Unlike Libor Masek's system, we have suggested applying Gabor and DCT directly on the normalized iris images without any masks to avoid the overhead for the recognition system. The system has been built based on the model depicted in Figure 11. Table 10 shows the results of the verification and identification modes. We have found in verification mode that the magnitude-based features have achieved the best performance result. In addition, the results of the identification mode have experienced low performance. However, the error rates are not balanced; it showed better FAR over FRR.

Although we were expecting to have better results for the iris system, we were surprised to see these results. So, we further investigate on this problem and found out that some iris images have not been localized properly or non-centric which apparently negatively affect the system performance. Figure 21 shows some examples of the iris localization problem. In another experiment, we used feature selection and Table 11 shows the results. We can observe that half of Gabor filter based features have produced better performance while the other retain the performance in comparison with the former experiment in verification mode. The same is true in the identification mode.
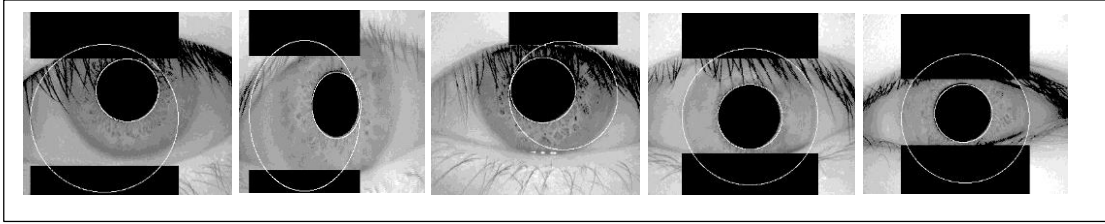
Figure 21 Mislocalized and noisy iris samples

Table 10 Iris recognition results (No F.S.)

Features	Verification (%)			Identification (%)		
	ACC	FAR	FRR	ACC	FAR	FRR
Imaginary	88.57± .07	0± 0	11.72± .07	73.57± .07	26.43± .07	0± 0
Real	86.43± .07	0± 0	13.92± .07	76.43± .03	23.57± .03	0± 0
Magnitude	**90.36± .03**	**0± 0**	**9.89± .03**	72.5± .07	27.5± .07	0± 0
Angles	84.29± .04	0± 0	16.12± .04	65.36± .04	34.64± .04	0± 0
DCT$_B$	89.29± .03	0± 0	10.99± .03	**79.64± .04**	**20.36± .04**	**0± 0**
DCT$_W$	83.93± .02	0± 0	16.48± .02	73.21± .06	26.79± .06	0± 0

Table 11 Iris recognition results (F.S.)

Features	Verification (%)			Identification (%)		
	ACC	FAR	FRR	ACC	FAR	FRR
Imaginary	88.21± .03	0± 0	12.09± .03	**76.07± .05**	**23.93± .05**	**0± 0**
Real	86.07± .03	0± 0	14.29± .03	73.93± .07	26.07± .07	0± 0
Magnitude	**91.07± .04**	**0± 0**	**9.16± .05**	75.36± .04	24.64± .04	0± 0
Angles	85.36± .06	0± 0	15.02± .06	63.93± .08	36.07± .08	0± 0
DCT$_B$	86.07± .02	0± 0	14.29± .02	71.79± .05	28.21± .05	0± 0
DCT$_W$	84.64± .02	0± 0	15.75± .02	68.57± .03	31.43± .03	0± 0

5.3.3 Hand Recognition

*Hand Geometry Recognition***:** In this subsection, we are discussing and reporting the performance of a hand geometry biometric system in verification and identification modes. In verification mode, we could achieve a high performance of $97.86 \pm 0.016\%$ with no feature reduction and $98.21 \pm 0.02\%$ with feature reduction. In the identification mode, the system performance is reduced. In comparison between the full feature set and the reduced version, we could recommend to use the full feature set in identification mode, because the subset of the features are not enough for identification testing. Although the features selected by PSO are very few, the system was able to achieve good results in verification mode. This is because the system after feature reduction has shown better rejection errors while retains the perfect false acceptance error. On the other hand the performance was dropped from $93.57 \pm 0.05\%$ to $77.86 \pm 0.05\%$ in identification mode. Table 12 shows the verification and identification results. The hand shape suffers a large inter-similarity in the real world and these results can clarify why hand shape is very attractive for low-medium level security systems.

Table 12 Hand geometry Recognition Results

F. Type	Verification (%)			Identification (%)		
	ACC	FAR	FRR	ACC	FAR	FRR
No FS	97.86±0.016	0±0	2.2±0.016	93.57±0.05	6.43±0.055	0±0
FS	98.21±0.02	0±0	1.83±0.023	77.86±0.05	22.14±0.05	0±0

Palmprint Recognition: Table 13 and Table 14 shows the results for the palmprint experiments in verification and identification modes before and after feature selection. In verification mode, the accuracy can reach up to 99.64± 0.01% in case of all features of DCT_W. On the other hand, the other feature types can achieve more than 90% accuracy in verification mode. In identification mode, the best system performance can reach up to 96.07% with DCT_W.

Table 13 Palmprint recognition results (No F.S.)

Features	Verification (%)			Identification (%)		
	ACC	FAR	FRR	ACC	FAR	FRR
Imaginary	93.57± 0.03	0± 0	6.59± 0.04	87.14± 0.02	12.86± 0.02	0± 0
Real	92.86± 0.04	0± 0	7.33± 0.04	85± 0.06	15± 0.06	0± 0
Magnitude	92.14± 0.04	28.57± 0.45	7.33±0.04	84.29± 0.05	15.71± 0.05	0± 0
Angles	87.5± 0.04	0± 0	12.82± 0.05	78.21± 0.05	21.79± 0.05	0± 0
DCT_B	91.79± 0.05	0± 0	8.42± 0.05	81.79± 0.06	18.21± 0.06	0± 0
DCT_W	**99.64± 0.01**	**0± 0**	**0.37± 0.01**	**96.07± 0.03**	**3.93± 0.03**	**0± 0**

Table 14 Palmprint recognition results (F.S.)

Features	Verification (%)			Identification (%)		
	ACC	FAR	FRR	ACC	FAR	FRR
Imaginary	95± .03	71.43± .45	3.3± .03	87.14± .02	12.86± .02	0± 0
Real	92.86± .04	0± 0	7.33± .04	82.5± .06	17.5± .06	0± 0
Magnitude	92.86± .04	0± 0	7.33± .04	81.07± .08	18.93± .08	0± 0
Angles	86.43± .04	0± 0	13.92± .04	77.5± .05	22.5± .05	0± 0
DCT_B	91.79± .05	14.29± .35	8.06± .06	80.71± .03	19.29± .03	0± 0
DCT_W	**97.86± .02**	**0± 0**	**2.2± .03**	**95± .02**	**5± .02**	**0± 0**

We also used ROC curves to compare the performance for different unimodal systems as shown in Figure 22 and 23 using full and reduced feature sets, respectively. We observed that the best results have been achieved using palmprint with DCT_W in both cases. Most of the AUC results are more than 90%.
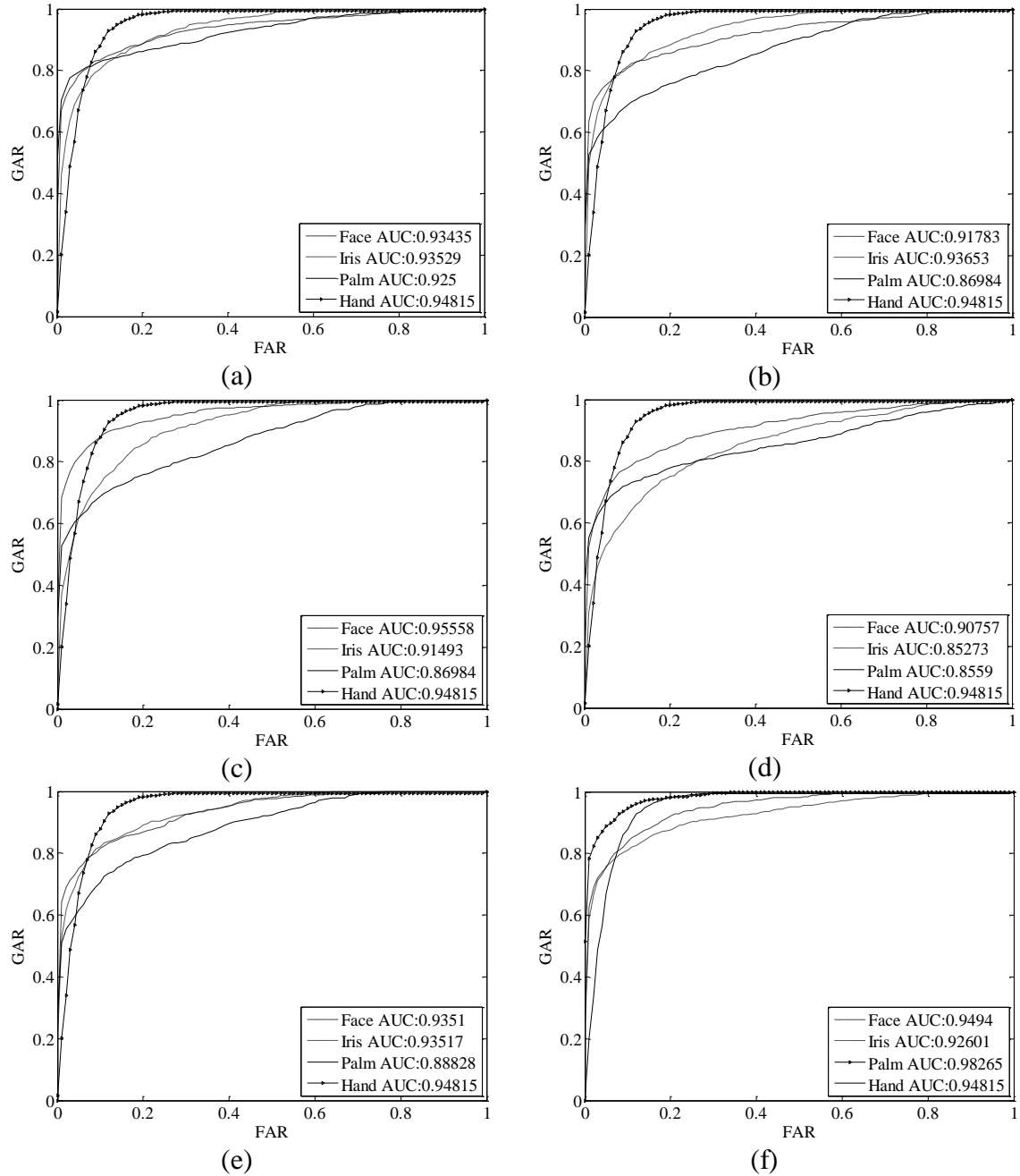
Figure 22 Single Biometric ROCs (No F.S.)

a) *Imaginary*, b) *Re*, c) Magnitude, d) Angles, e) DCT_B, f) DCT_W
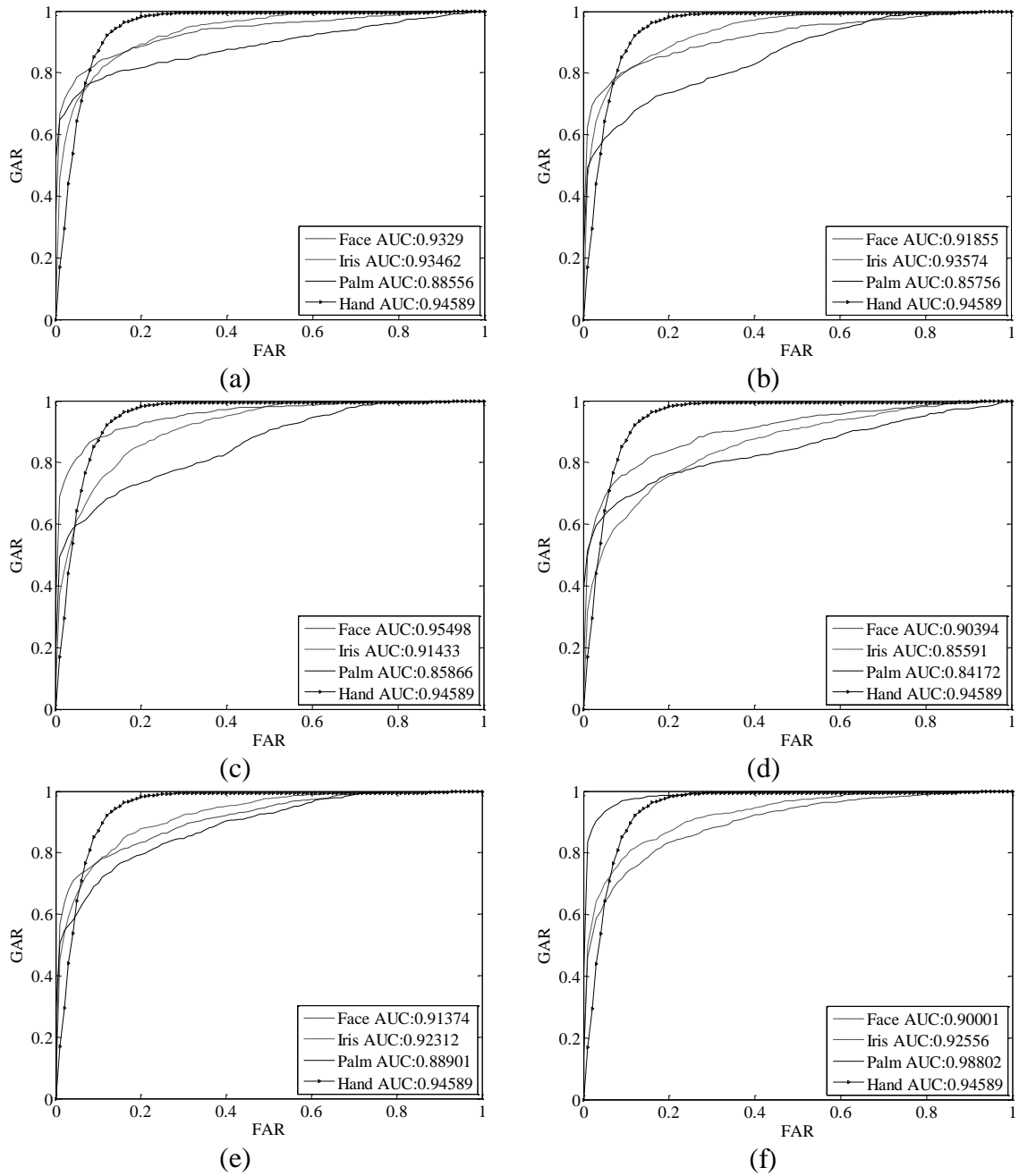
Figure 23 Single Biometric ROCs (F.S.)

a) *Imaginary*, b) *Re*, c) **Magnitude**, d) **Angles**, e) **DCT**$_B$, f) **DCT**$_W$

5.4 Multimodal Biometric Experiments

We conducted several experiments on score-level fusion based on two different methodologies of fuzzy integral to study the performance of the fusion against the unimodal systems. First, the integration of two modalities of the same feature type was conducted and the results are tabulated in the following subsections. Each biometric trait, except the hand geometry, contributed with the Imaginary and DCT_W feature types. We chose these features randomly, because the unimodal system shows fluctuated results on all feature types. Therefore, some of these features achieve high results such as DCT_W of the palmprint in verification mode while the same feature type of the iris has showed the worst results in verification mode. In multimodal biometric experiments, we have investigated six different integrations. We also compared the results with other traditional fusion techniques including sum, max, and product. Moreover, feature-level fusion has been carried out on a selected number of feature types of face, iris and palmprint. Table 15 shows the chosen feature types of the biometric traits. The fusion at this level has taken place on two and three combinations using concatenation.

Table 15 Selected features for feature-level fusion

Biometric trait	Verification	Identification
Face	Magnitude	Magnitude
Iris	DCT_W	DCT_W
Palmprint	DCT_W	Angles
Hand	Geometrical	Geometrical

5.4.1 Bimodalities Fusion

The performance of Sugeno and Choquet fuzzy integrals has been compared to the single biometric system and other strong fusion methods such as sum, product and max rules. We have reported the system performance following the same strategy as the single biometric system.

A. *Face & Palmprint Fusion:* One of the recent trends on biometric fusion that have been conducted to enhance the system performance is based on face and palmprint.

B. Table 16 shows performance results of face and palmprint without feature selection. In this experiment, the system was able to achieve perfect accuracy using fuzzy fusion techniques in verification mode of the Imaginary feature type. In the identification experiment, the performance has dropped to $80.36 \pm 0.03\%$ using Sugeno fuzzy integral, but the best results has been achieved by Choquet fuzzy integral. The system shows high performance using DCT_W than the unimodal system. It is also observed that the system can operate better in identification mode with the combination of face and palmprint. We repeated the experiment using the reduced features and the results are shown in

Table 17. The system achieves the same performance on verification mode using Choquet and Sugeno fuzzy integrals on Imaginary features.

Using the ROC curves, the system performance has shown that Choquet fuzzy integral fusion has better AUC than other techniques in both modes (with and without feature reduction). Figure 24 and 25 show the ROCs of fusing scores without and with feature reduction respectively. The AUC has nearly perfect value using DCT_W.

Table 16 Face and palmprint fusion results (No F.S.)

Feature Type	F. T	Verification			Identification		
		ACC	FAR	FRR	ACC	FAR	FRR
Imaginary	Sum	99.64± .01	0± 0	0.37± .01	97.14± .02	2.86± .02	0± 0
	Product	97.86± .02	0± 0	2.2± .02	95.36± .04	4.64± .04	0± 0
	Max	98.93± .01	0± 0	1.1± .01	95.36± .03	4.64± .03	0± 0
	Sugeno	**100± 0**	**0± 0**	**0± 0**	80.36± .03	19.64± .03	0± 0
	Choquet	**100± 0**	**0± 0**	**0± 0**	**97.5± .01**	**2.5± .01**	**0± 0**
DCT$_W$	Sum	**100± 0**	**0± 0**	**0± 0**	98.93± .01	1.07± .01	0± 0
	Product	**100± 0**	**0± 0**	**0± 0**	97.86± .02	2.14± .02	0± 0
	Max	**100± 0**	**0± 0**	**0± 0**	99.64± .01	0.36± .01	0± 0
	Sugeno	**100± 0**	**0± 0**	**0± 0**	97.5± .02	2.5± .02	0± 0
	Choquet	**100± 0**	**0± 0**	**0± 0**	**100± 0**	**0± 0**	**0± 0**

Table 17 Face and palmprint fusion results (F.S.)

| Feature Type	F. T	Verification			Identification		
		ACC	FAR	FRR	ACC	FAR	FRR
Imaginary	Sum	99.29± .01	0± 0	0.73± .01	95.36± .04	4.64± .04	0± 0
	Product	98.93± .01	0± 0	1.1± .01	95± .04	5± .04	0± 0
	Max	99.29± .01	0± 0	0.73± .01	95.71± .02	4.29± .02	0± 0
	Sugeno	**100± 0**	**0± 0**	**0± 0**	86.43± .04	13.57± .04	0± 0
	Choquet	**100± 0**	**0± 0**	**0± 0**	**97.5± .04**	**2.5± .04**	**0± 0**
DCT$_W$	Sum	**100± 0**	**0± 0**	**0± 0**	98.21± .03	1.79± .03	0± 0
	Product	**100± 0**	**0± 0**	**0± 0**	96.43± .04	3.57± .04	0± 0
	Max	99.64± .01	0± 0	0.37± .01	**98.93± .02**	**1.07± .02**	**0± 0**
	Sugeno	99.64± .01	0± 0	0.37± .01	86.43± .03	13.57± .03	0± 0
	Choquet	**100± 0**	**0± 0**	**0± 0**	**98.93± .01**	**1.07± .01**	**0± 0**

(a)

(b)
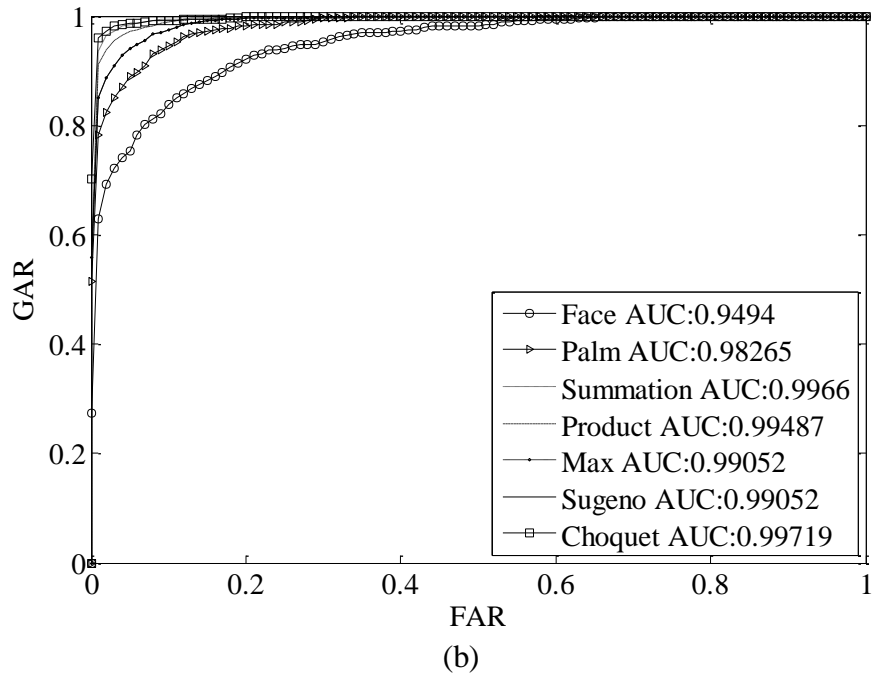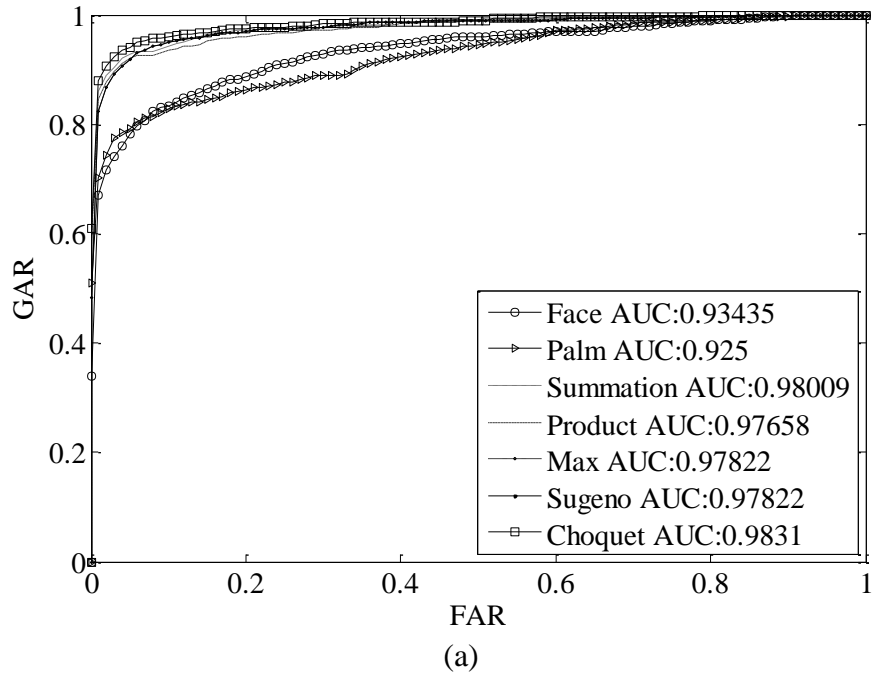
Figure 24 Face & palmprint and fusion ROCs (No F.S.), (a) *Imaginary*, (b) DCT*w*

(a)

(b)

Figure 25 Face & palmprint fusion ROCs (F.S.), (a) *Imaginary*, (b) DCT*w*

74

C. *Iris & Palmprint Fusion***:** As we noted before, the iris unimodal system performance was low. When fused with palmprint features using Choquet fuzzy integral, the results as shown in Table 18 are enhanced for the Imaginary and DCT$_W$ feature types in verification and identification modes. Moreover, the fusion of these modalities has increased the system performance more than 10% enhancement.

Table 19 shows the results of the experiment of the system when the reduced feature set is used. In comparison with the first experiment, the system shows an enhancement over the most of the fusion techniques using Imaginary feature type in verification mode. A slight reduction has been observed for identification mode in the second experiment.

Table 18 Iris & palmprint fusion results (No F.S.)

Feature Type	F. T	Verification			Identification		
		ACC	FAR	FRR	ACC	FAR	FRR
Imaginary	Sum	95.71± .02	0± 0	4.4± .02	87.14± .03	12.86± .03	0± 0
	Product	95.36± .02	0± 0	4.76± .02	87.14± .03	12.86± .03	0± 0
	Max	88.57± .05	0± 0	11.72± .05	76.79± .06	23.21± .06	0± 0
	Sugeno	95± .06	42.86± .49	4.03± .07	85± .03	15± .03	0± 0
	Choquet	**99.64± .01**	**0± 0**	**0.37± .01**	**93.93± .04**	**6.07± .04**	**0± 0**
DCT$_W$	Sum	98.57± .02	0± 0	1.47± .02	97.14± .02	2.86± .02	0± 0
	Product	98.57± .02	0± 0	1.47± .02	95.36± .02	4.64± .02	0± 0
	Max	99.29± .01	0± 0	0.73± .01	96.43± .02	3.57± .02	0± 0
	Sugeno	**99.64± .01**	**0± 0**	**0.37± .01**	97.14± .03	2.86± .03	0± 0
	Choquet	**99.64± .01**	**0± 0**	**0.37± .01**	**98.93± .02**	**1.07± .02**	**0± 0**

Table 19 Iris & palmprint fusion results (F.S.)

Feature Type	F. T	Verification			Identification		
		ACC	FAR	FRR	ACC	FAR	FRR
Imaginary	Sum	96.07± .03	0± 0	4.03± .03	86.79± .03	13.21± .03	0± 0
	Product	96.07± .03	0± 0	4.03± .03	**88.21± .03**	**11.79± .03**	**0± 0**
	Max	92.86± .04	0± 0	7.33± .04	78.93± .07	21.07± .07	0± 0
	Sugeno	97.14± .04	0± 0	2.93± .04	86.79± .03	13.21± .03	0± 0
	Choquet	**98.57± .02**	**0± 0**	**1.47± .02**	86.43± .05	13.57± .05	0± 0
DCT$_W$	Sum	97.5± .01	0± 0	2.56± .01	92.86± .04	7.14± .04	0± 0
	Product	96.43± .01	0± 0	3.66± .01	90.71± .05	9.29± .05	0± 0
	Max	98.57± .03	0± 0	1.47± .03	96.43± .02	3.57± .02	0± 0
	Sugeno	**99.64± .01**	**0± 0**	**0.37± .01**	88.57± .03	11.43± .03	0± 0
	Choquet	99.29± .02	0± 0	0.73± .02	**97.14± .02**	**2.86± .02**	**0± 0**

Figure 26 and Figure 27 also show the ROC curves of the full and reduced feature sets experiments. The fuzzy fusion of palmprint and iris demonstrated better results than the unimodal biometric systems. The AUC of the fusion techniques shows that the Choquet fuzzy integral fusion has the best performance results over the other traditional fusion techniques. This is due to the fact that the fuzzy integral can be tuned with some parameters to favor one unimodal over the other with respect to the quality of the scores.
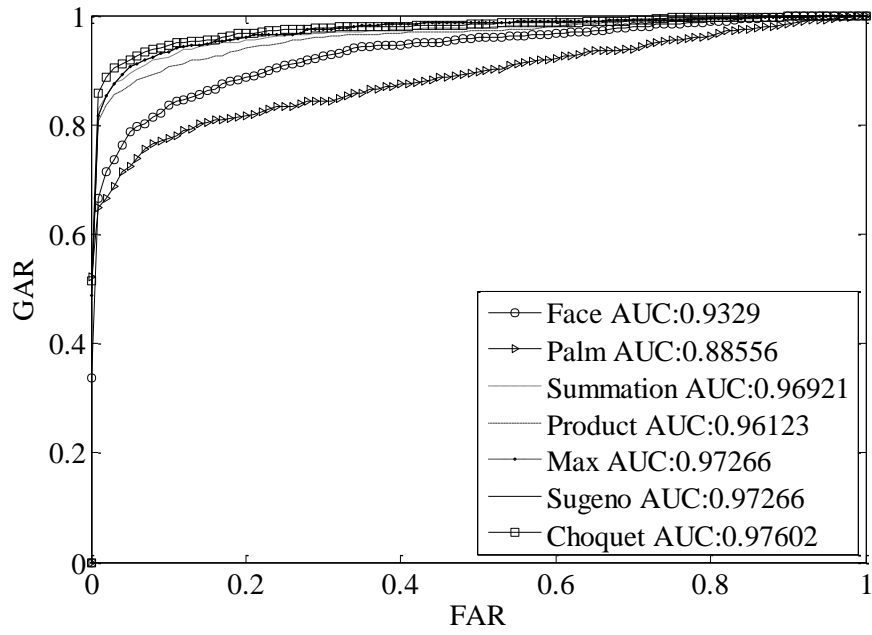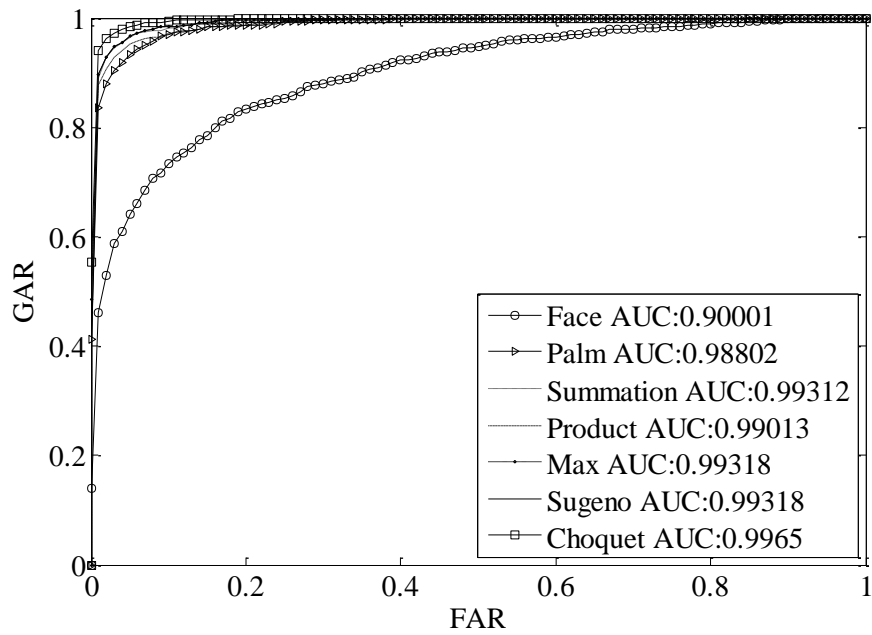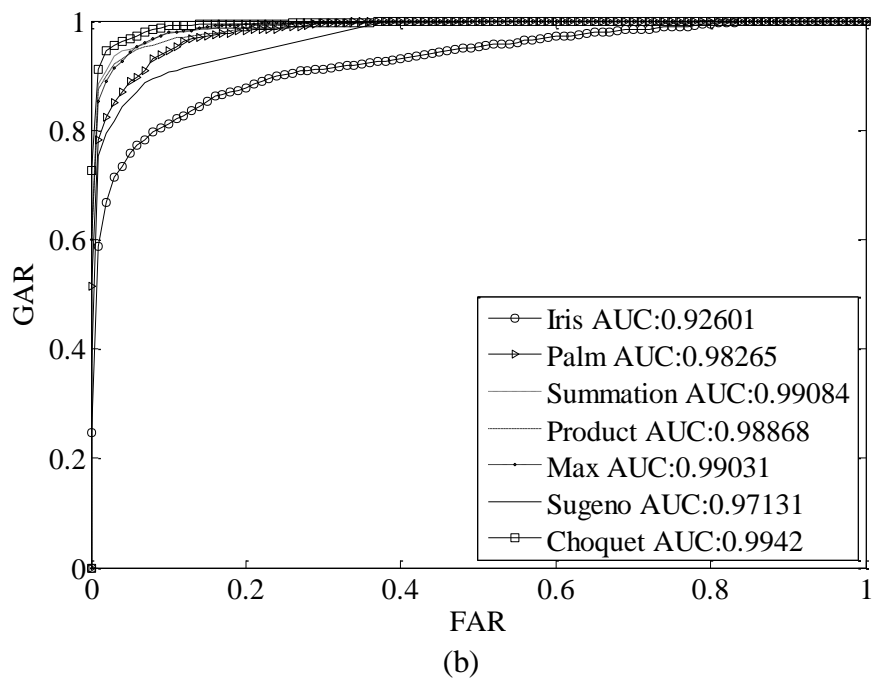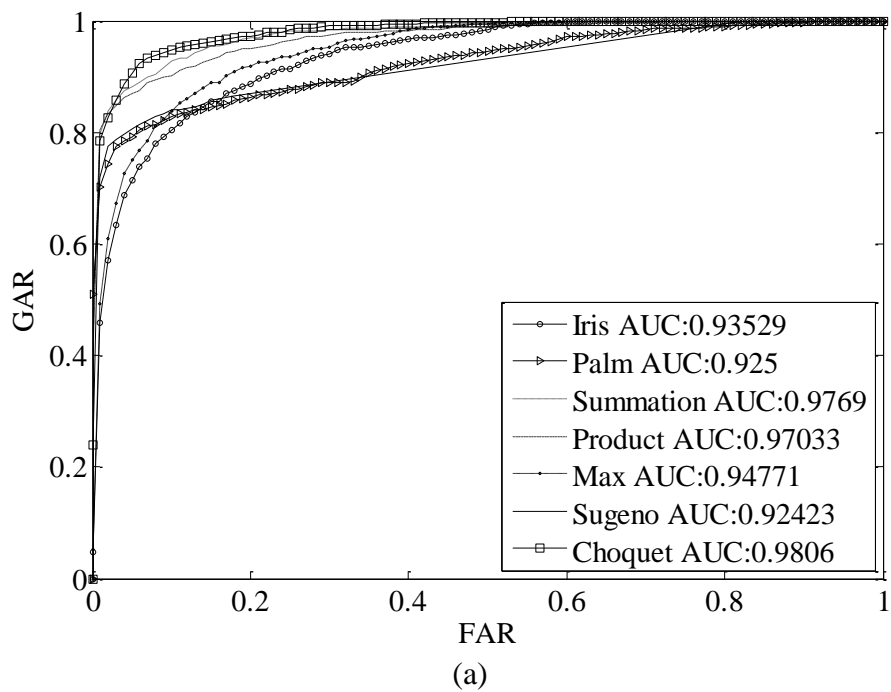
(a)

(b)

Figure 26 Iris & palmprint fusion ROCs (No F.S.), (a) *Imaginary*, (b) DCT*w*

(a)

(b)
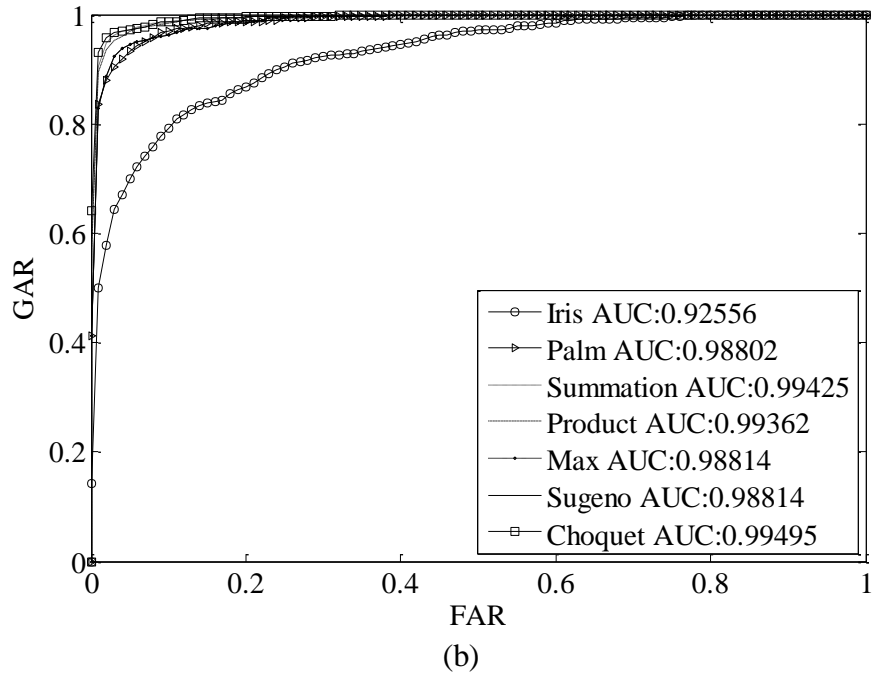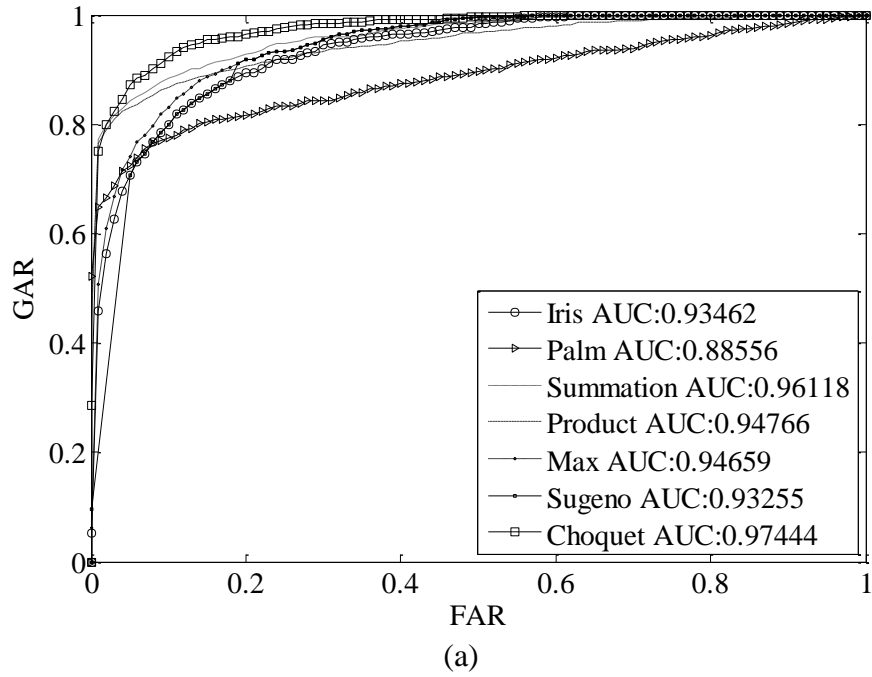
Figure 27 Iris & palmprint fusion ROCs (F.S.), (a) *Imaginary*, (b) DCT*W*

D. *Iris & Hand Geometry Fusion***:** It is obvious from the results presented in Table 20 that the fusion of iris and hand geometry achieves good performance than unimodal systems using Imaginary and DCT$_W$ feature types using the Max rule. In the identification mode, most of the fusion techniques have better performance than unimodal systems. However, the Sugeno fuzzy integral is not successful as the other techniques. The Choquet fuzzy fusion integral is able to reach up to 97.86 ± 0.02% and 96.07± 0.02% accuracy in verification using Imaginary and DCT$_W$ feature types. In identification mode, the system achieves up to 97.14± 0.03% using Choquet integral, which is not achieved by neither iris nor hand geometry in single mode testing.

Table 20 Iris & hand geometry fusion results (No F.S.)

Iris Features	F. T	Verification (%)			Identification (%)		
		ACC	**FAR**	**FRR**	**ACC**	**FAR**	**FRR**
Imaginary	Sum	97.5± .02	0± 0	2.56± .02	96.07± .03	3.93± .03	0± 0
	Product	97.5± .02	0± 0	2.56± .02	95.71± .03	4.29± .03	0± 0
	Max	**98.21± .01**	**0± 0**	**1.83± .01**	96.07± .03	3.93± .03	0± 0
	Sugeno	95± .04	0± 0	5.13± .04	87.5± .03	12.5± .03	0± 0
	Choquet	97.86± .02	0± 0	2.2± .02	**97.14± .03**	**2.86± .03**	**0± 0**
DCT$_W$	Sum	92.5± .05	0± 0	7.69± .05	87.14± .04	12.86± .04	0± 0
	Product	90.71± .05	0± 0	9.52± .05	86.07± .03	13.93± .03	0± 0
	Max	**97.86± .02**	**0± 0**	**2.2± .02**	**93.93± .03**	**6.07± .03**	**0± 0**
	Sugeno	85.36± .13	57.14± .49	13.55± .15	62.5± .05	37.5± .05	0± 0
	Choquet	96.07± .02	0± 0	4.03± .02	93.21± .04	6.79± .04	0± 0

On the other hand, the performance accuracy in another experiment using the reduced feature set is enhanced with most techniques in verification mode as depicted in Table 21. This is reasonable because hand geometry has enhanced performance in single mode testing, while iris retains its performance using Imaginary feature type. In Figure 28 the AUC of the first experiment shows that Choquet fuzzy integral fusion has achieved the best system performance. In the second experiment as shown in Figure 29, the Sum and Product fusion rules have better performance than the first experiment (without feature reduction) while the Choquet fuzzy integral still achieves the best results.

Table 21 Iris & hand geometry fusion results (F.S.)

Iris Features	F. T	Verification (%)			Identification (%)		
		ACC	FAR	FRR	ACC	FAR	FRR
Imaginary	Sum	**98.57± .02**	**0± 0**	**1.47± .02**	**95.71± .02**	**4.29± .02**	**0± 0**
	Product	97.86± .03	0± 0	2.2± .03	95.36± .02	4.64± .02	0± 0
	Max	**98.57± .02**	**0± 0**	**1.47± .02**	81.07± .05	18.93± .05	0± 0
	Sugeno	96.79± .03	0± 0	3.3± .04	89.29± .05	10.71± .05	0± 0
	Choquet	98.21± .03	0± 0	1.83± .03	94.64± .02	5.36± .02	0± 0
DCT*w*	Sum	97.14± .03	0± 0	2.93± .03	90.36± .06	9.64± .06	0± 0
	Product	96.43± .02	0± 0	3.66± .02	89.29± .06	10.71± .06	0± 0
	Max	**98.21± .02**	**0± 0**	**1.83± .02**	77.86± .04	22.14± .04	0± 0
	Sugeno	72.86± .12	0± 0	27.84± .12	62.14± .08	37.86± .08	0± 0
	Choquet	97.86± .02	0± 0	2.2± .03	**95.36± .02**	**4.64± .02**	**0± 0**

(a)

(b)

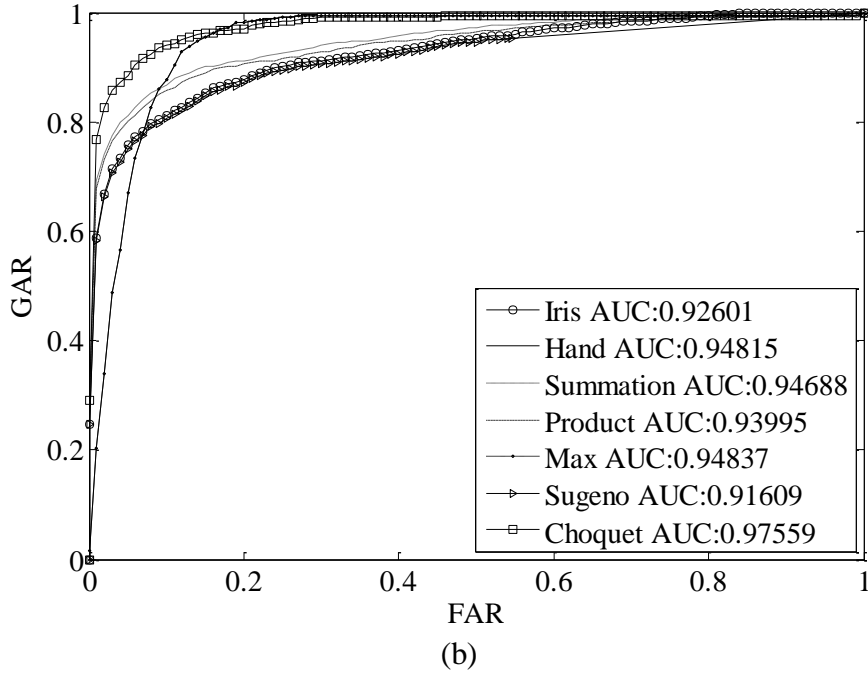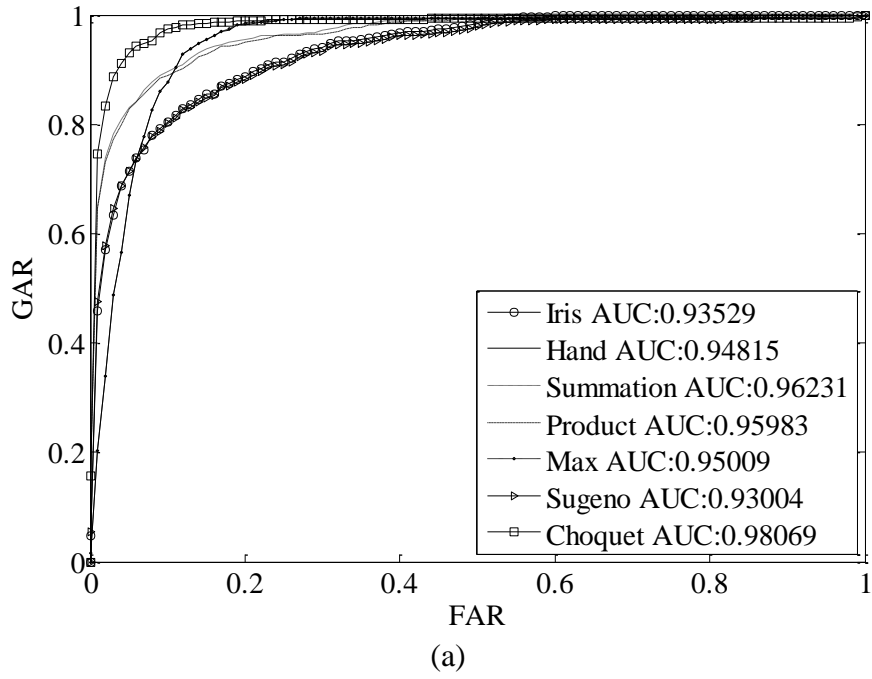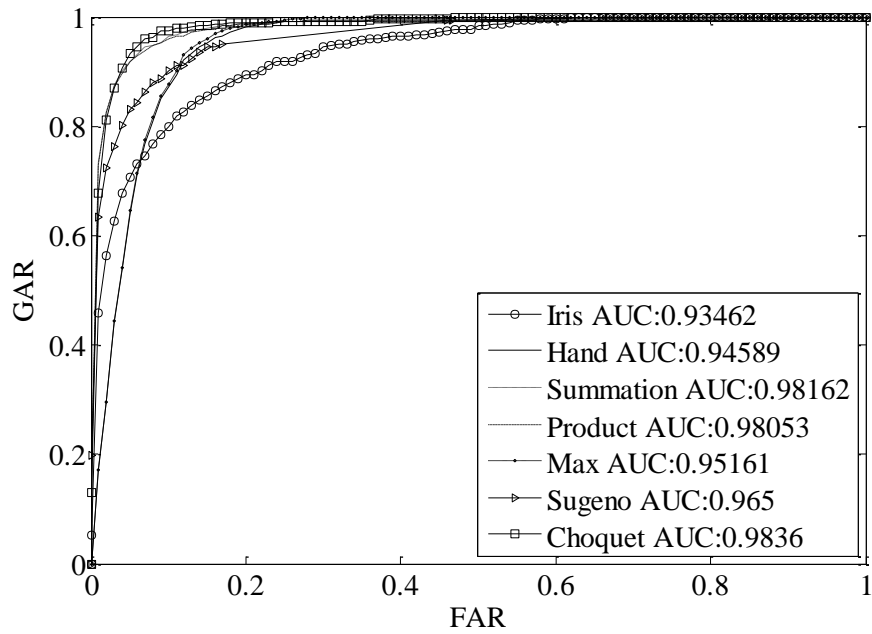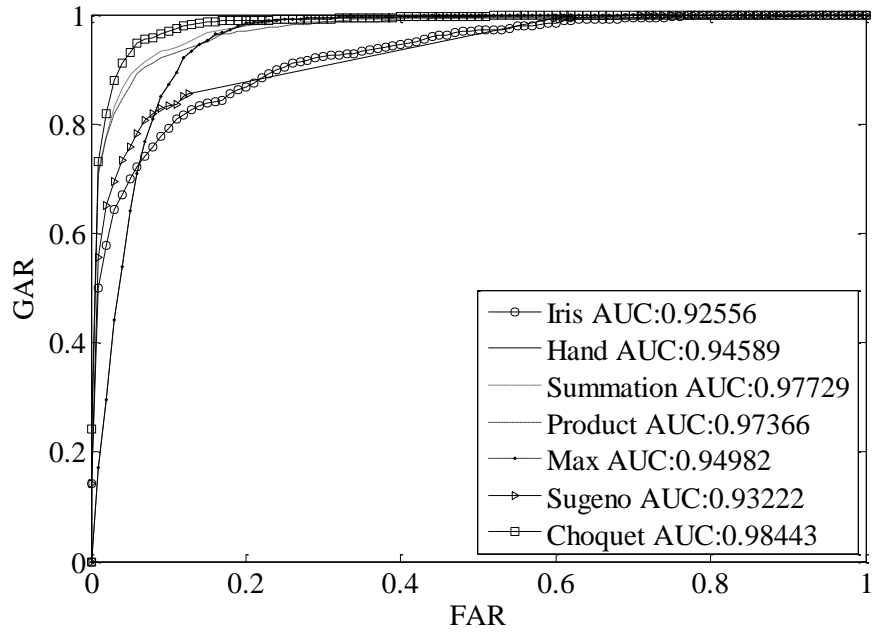**Figure 28 Iris & hand geometry fusion ROCs (No F.S.), (a)** *Imaginary***, (b) DCT***W*

(a)

(b)

Figure 29 Iris & hand geometry fusion ROCs (F.S.), (a) *Imaginary*, (b) DCT*w*

E. *Palmprint & Hand Geometry Fusion:* This integration has typically been suggested due to the relationship between the palmprint and the hand geometry. First, they are located on the same human body part (hand). Second, they usually can share the same image acquisition device. Therefore, such integration is found to be inexpensive. Additionally, the hand geometry can be applied in low-to-medium level security applications. However, by mixing it with palmprint, we bring in more security to the biometric system. Table 22 shows a high level of performance (98.93±0.01%) of the Choquet fuzzy integral fusion using Imaginary feature type, while Sugeno fuzzy integral fusion has showed a perfect accuracy with DCT_W feature type in verification mode. In identification mode, the Choquet fuzzy integral fusion has showed the best results for both the Imaginary and DCT_W (98.21± 0.02% and 98.93± 0.02% respectively).

Table 22 Palmprint & hand geometry fusion results (No F.S.)

Iris Features	F. T	Verification (%)			Identification (%)		
		ACC	FAR	FRR	ACC	FAR	FRR
Imaginary	Sum	98.21± .02	0± 0	1.83± .02	93.57± .05	6.43± .05	0± 0
	Product	96.79± .03	0± 0	3.3± .04	92.14± .05	7.86± .05	0± 0
	Max	97.86± .02	0± 0	2.2± .02	94.29± .03	5.71± .03	0± 0
	Sugeno	91.79± .12	0± 0	8.42± .13	55.36± .06	44.64± .06	0± 0
	Choquet	**98.93± .01**	**0± 0**	**1.1± .01**	**98.21± .02**	**1.79± .02**	**0± 0**
DCT_W	Sum	99.64± .01	0± 0	.37± .01	**98.93± .01**	**1.07± .01**	**0± 0**
	Product	99.64± .01	0± 0	.37± .01	98.21± .02	1.79± .02	0± 0
	Max	98.57± .02	0± 0	1.47± .02	95± .03	5± .03	0± 0
	Sugeno	**100± 0**	**0± 0**	**0± 0**	95± .04	5± .04	0± 0
	Choquet	99.64± .01	0± 0	.37± .01	**98.93± .02**	**1.07± .02**	**0± 0**

The results of the system using a reduced feature version are shown in Table 23. This experiment is showing an enhancement over all techniques using Imaginary feature type in the verification mode. On the other hand, the Sugeno fuzzy integral fusion has better performance in the first experiment than the second. It has very low performance in the identification mode with respect to the other fusion techniques. The ROC curves have also conveyed a similar conclusion of the system performance using the fusion of hand shape and palmprint. Figure 30 and Figure 31 illustrate the ROCs of the system performance without and with feature reduction, respectively. The Choquet fuzzy integral has better AUC in comparison with the others.

Table 23 Palmprint & hand geometry fusion results (F.S.)

Iris Features	F. T	Verification (%)			Identification (%)		
		ACC	FAR	FRR	ACC	FAR	FRR
Imaginary	Sum	98.57± .02	0± 0	1.47± .02	96.07± .03	3.93± .03	0± 0
	Product	97.86± .03	0± 0	2.2± .03	93.57± .04	6.43± .04	0± 0
	Max	98.57± .01	0± 0	1.47± .01	79.29± .07	20.71± .07	0± 0
	Sugeno	94.29± .09	0± 0	5.86± .1	68.57± .05	31.43± .05	0± 0
	Choquet	**98.93± .01**	**0± 0**	**1.1± .01**	**97.14± .03**	**2.86± .03**	**0± 0**
DCT$_W$	Sum	**99.64± .01**	**0± 0**	**0.37± .01**	**97.86± .02**	**2.14± .02**	**0± 0**
	Product	99.29± .01	0± 0	0.73± .01	97.14± .02	2.86± .02	0± 0
	Max	98.57± .01	0± 0	1.47± .01	79.29± .08	20.71± .08	0± 0
	Sugeno	95.36± .03	0± 0	4.76± .03	94.29± .03	5.71± .03	0± 0
	Choquet	98.21± .01	0± 0	1.83± .01	97.5± .02	2.5± .02	0± 0
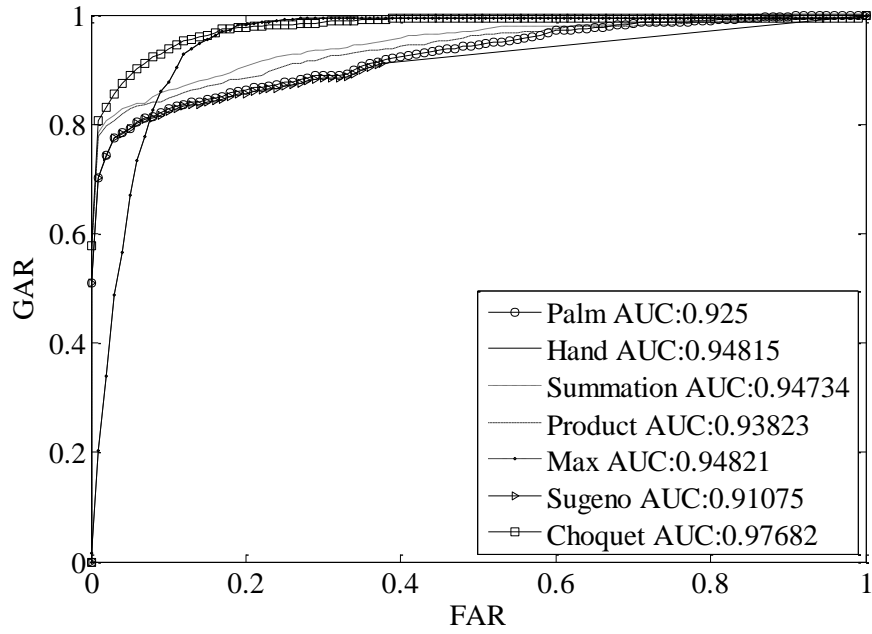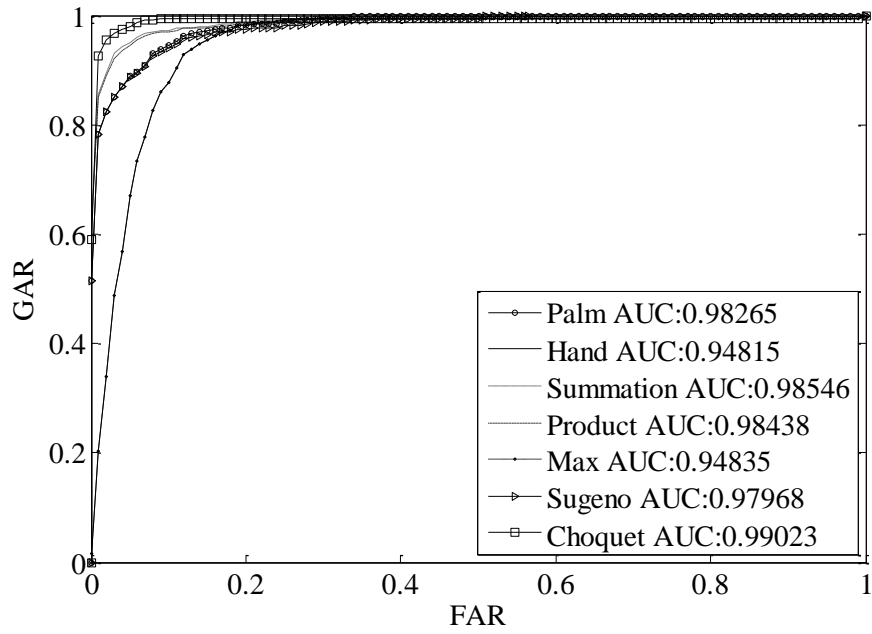
Figure 30 Palmprint & hand geometry fusion ROCs (No F.S.), (a) *Imaginary***, (b) DCT***W*

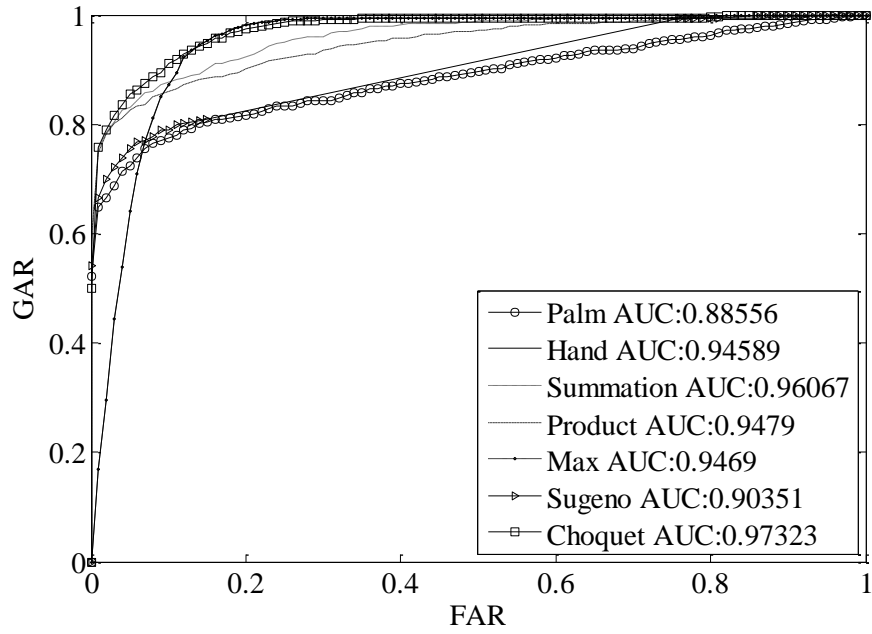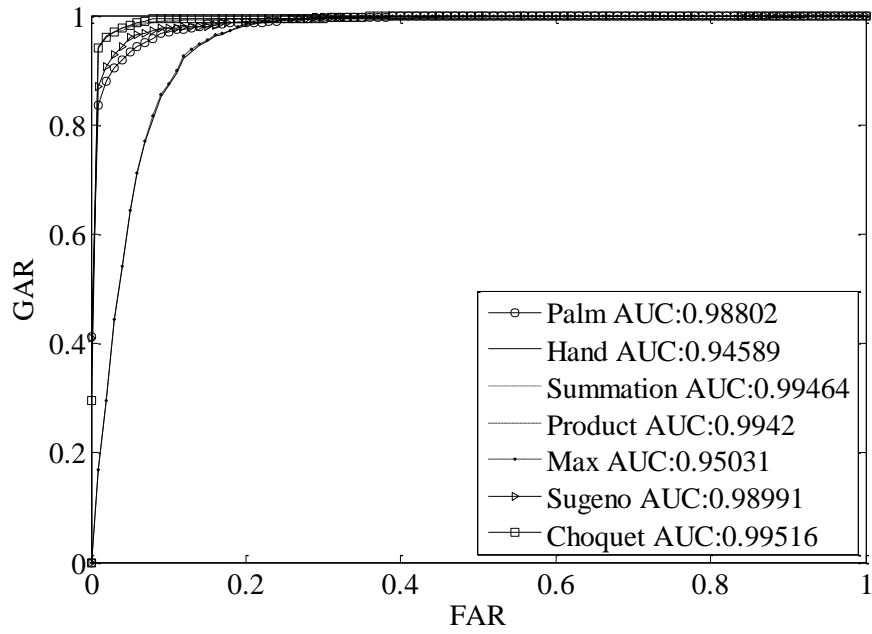**Figure 31 Palmprint & hand geometry fusion ROCs (F.S.), (a) *Imaginary*, (b) DCT*w***

5.4.2 Three Modalities Fusion

A. *Face, Iris & Palmprint Fusion:* The integration of these three biometric modalities has many attractive reasons. First, the face biometric is considered to be non-intrusive and highly accepted technology. Moreover, face and iris can be acquired by the same acquisition device [44]. The results of this integration have shown high performance. In Table 24, a perfect performance is reported in verification mode for both Imaginary and DCT$_W$ feature types using the Sum, Product and Choquet and Sugeno fuzzy integrals. In Identification mode, the Choquet fuzzy integral fusion has achieved the same level of accuracy using DCT$_W$.

Table 24 Face, iris & palmprint fusion results (No F.S.)

Feature Type	F. T	Verification			Identification		
		ACC	**FAR**	**FRR**	**ACC**	**FAR**	**FRR**
Imaginary	Sum	**100± 0**	0± 0	0± 0	**99.29± .01**	**0.71± .01**	**0± 0**
	Product	**100± 0**	0± 0	0± 0	97.5± .02	2.5± .02	0± 0
	Max	97.86± .03	0± 0	2.2± .03	87.86± .05	12.14± .05	0± 0
	Sugeno	98.21± .02	0± 0	1.83± .02	97.86± .03	2.14± .03	0± 0
	Choquet	**100± 0**	**0± 0**	**0± 0**	98.93± .01	1.07± .01	0± 0
DCT$_W$	Sum	99.64± .01	0± 0	0.37± .01	99.29± .02	0.71± .02	0± 0
	Product	99.64± .01	0± 0	0.37± .01	98.93± .02	1.07± .02	0± 0
	Max	99.29± .01	0± 0	0.73± .01	98.57± .01	1.43± .01	0± 0
	Sugeno	**100± 0**	**0± 0**	**0± 0**	96.43± .03	3.57± .03	0± 0
	Choquet	**100± 0**	**0± 0**	**0± 0**	**100± 0**	**0± 0**	**0± 0**

In another experiment using the reduced feature sets, the system performance was degraded slightly over some techniques with respect to the first experiment. On the other hand, the Choquet fuzzy integral achieves the best results in identification mode ($99.29\pm 0.01\%$ and $99.64\pm 0.01\%$). It also achieves perfect accuracy in verification mode using DCT_W (see Table 25). If we compare between the bimodal systems ("Face-Palmprint integration" and "Iris-Palmprint integration") with the three modalities fusion, we can observe that the Choquet fuzzy integral fusion achieves better performance than the two combinations in identification mode with respect to "Face-Palmprint integration". Moreover, it has better results in verification and identification modes if we compare it with 'Iris-Palmprint integration'. The performance of face, iris and palmprint integration can be further depicted using ROC plots as shown in Figure 32 and Figure 33. We observed that most of the fusion techniques have achieved high AUC.

Table 25 Face, iris and palmprint fusion results (F.S.)

| Feature Type	F. T	Verification			Identification		
		ACC	FAR	FRR	ACC	FAR	FRR
Imaginary	Sum	**100± 0**	**0± 0**	**0± 0**	**99.29± .02**	**0.71± .02**	**0± 0**
	Product	99.64± .01	0± 0	0.37± .01	98.93± .02	1.07± .02	0± 0
	Max	97.14± .02	0± 0	2.93± .03	90.71± .05	9.29± .05	0± 0
	Sugeno	98.57± .01	0± 0	1.47± .01	96.79± .02	3.21± .02	0± 0
	Choquet	99.64± .01	0± 0	0.37± .01	**99.29± .01**	**0.71± .01**	**0± 0**
DCT_w	Sum	98.93± .02	0± 0	1.1± .02	97.14± .03	2.86± .03	0± 0
	Product	98.57± .02	0± 0	1.47± .02	96.07± .02	3.93± .02	0± 0
	Max	99.64± .01	0± 0	0.37± .01	99.29± .01	0.71± .01	0± 0
	Sugeno	98.93± .02	28.57± .45	0.37± .01	98.21± .03	1.79± .03	0± 0
	Choquet	**100± 0**	**0± 0**	**0± 0**	**99.64± .01**	**0.36± .01**	**0± 0**

(a)

(b)
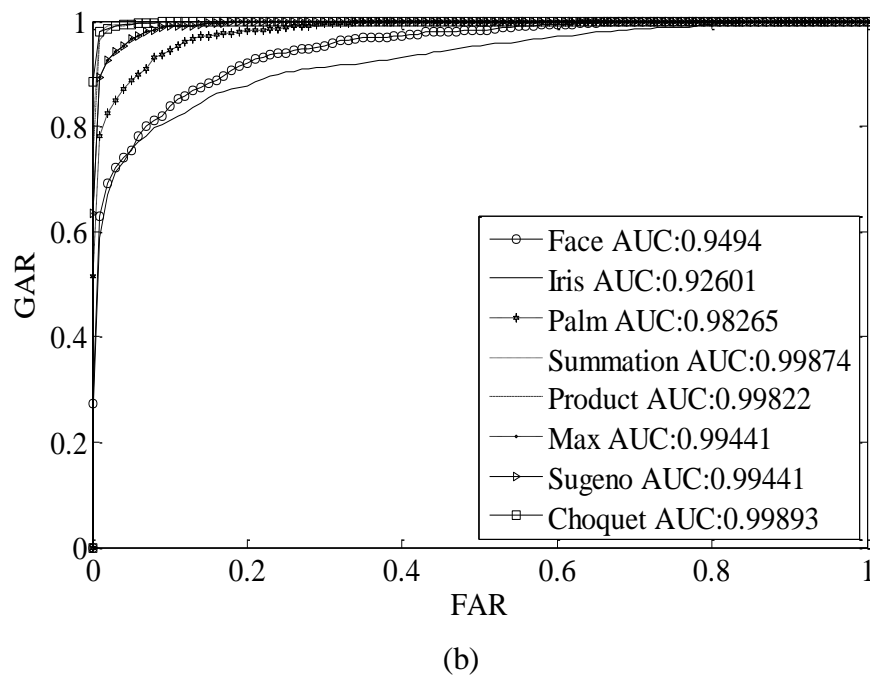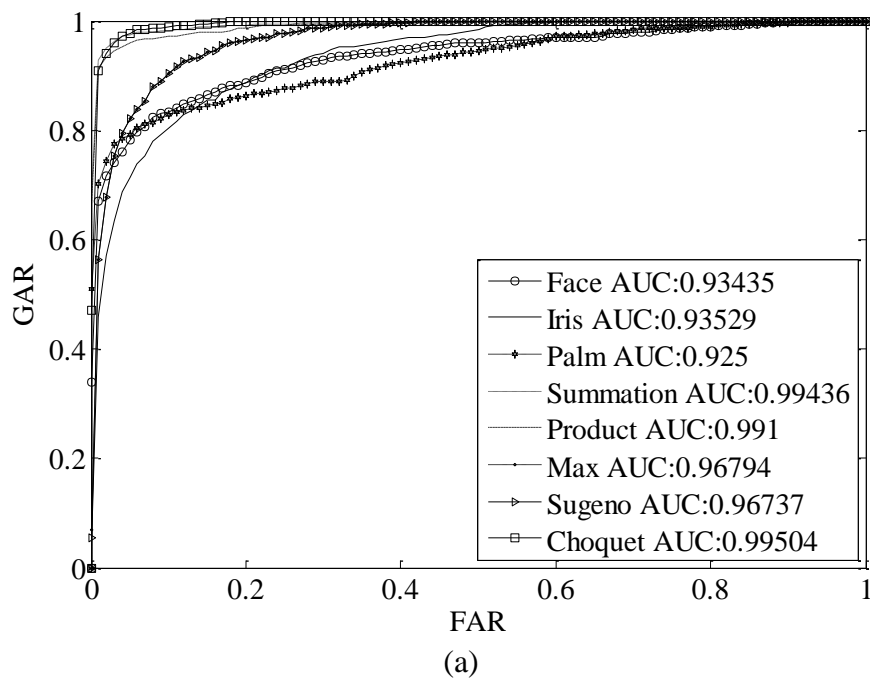
Figure 32 Face, Iris & Palmprint ROCs (No F.S.), (a) *Imaginary***, (b) DCT***w*
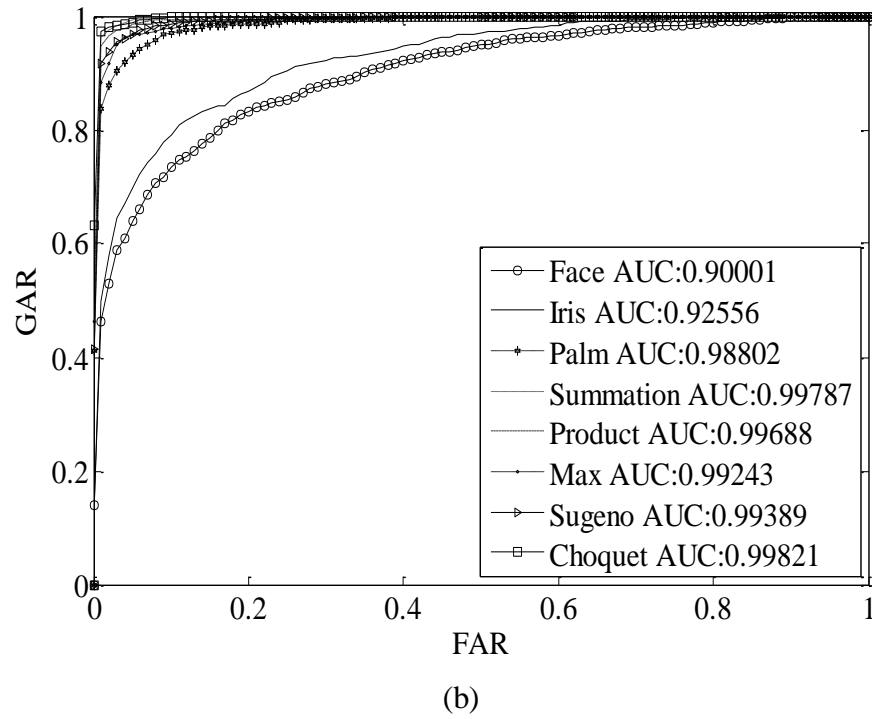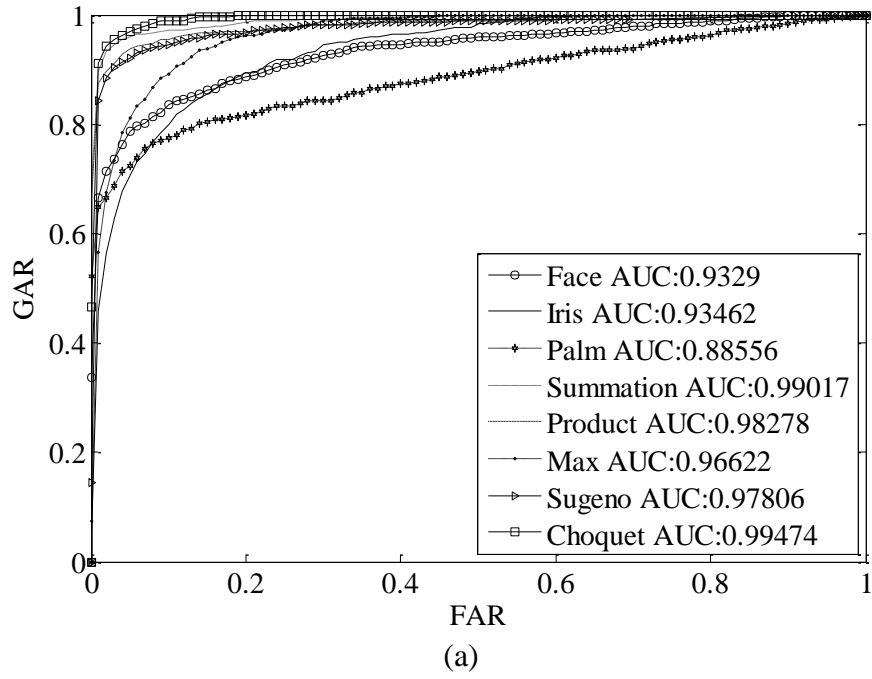
(a)

(b)

Figure 33 Face, Iris & Palmprint ROCs (F.S.), (a) *Imaginary*, (b) DCT*w*

B. *Face, Palmprint & Hand-Geometry Fusion:* To the best of our knowledge, the performance of the integration of these three biometric modalities has not been reported yet. This combination has shown a high performance in testing for both verification and identification modes. Table 26 illustrates the system performance without feature reduction. Comparing the results with the two modality fusion ("Face and Palmprint integration"), we observed that the Sugeno fuzzy integral has retained its performance in both experiments, while the Sum rule has enhanced the performance in verification mode using Imaginary feature type. Moreover, the system has better performance when using three modality fusion than the two modality fusion ("Palmprint Hand geometry integration").

Table 26 Face, palmprint & hand geometry fusion results (No F.S.)

Feature Type	F. T	Verification			Identification		
		ACC	FAR	FRR	ACC	FAR	FRR
Imaginary	Sum	100± 0	0± 0	0± 0	**98.93± .01**	**1.07± .01**	**0± 0**
	Product	99.29± .01	0± 0	0.73± .01	97.5± .01	2.5± .01	0± 0
	Max	98.93± .02	0± 0	1.1± .02	94.64± .03	5.36± .03	0± 0
	Sugeno	**100± 0**	**0± 0**	**0± 0**	95.71± .02	4.29± .02	0± 0
	Choquet	99.29± .02	0± 0	0.73± .02	**98.93± .01**	**1.07± .01**	**0± 0**
DCT$_W$	Sum	**100± 0**	**0± 0**	**0± 0**	**100± 0**	**0± 0**	**0± 0**
	Product	99.29± .01	0± 0	0.73± .01	98.93± .01	1.07± .01	0± 0
	Max	98.57± .02	0± 0	1.47± .02	95.36± .02	4.64± .02	0± 0
	Sugeno	99.29± .01	0± 0	0.73± .01	98.21± .02	1.79± .02	0± 0
	Choquet	99.64± .01	0± 0	0.37± .01	98.93± .02	1.07± .02	0± 0

Table 27 shows the results of the experiment executed using feature reduction. A high system performance is reported using the Sugeno fuzzy integral for the verification mode. However, when compared with the first experiment we can perceive marginal degradation to the system performance in some cases. Figure 34 and Figure 35 show the ROC curves of the system. The Choquet fuzzy integral fusion has realized the best AUC.

Table 27 Face, palmprint & hand geometry fusion results (F.S.)

| Feature Type	F. T	Verification			Identification		
		ACC	FAR	FRR	ACC	FAR	FRR
Imaginary	Sum	99.29± .01	0± 0	0.73± .01	**98.21± .03**	**1.79± .03**	**0± 0**
	Product	99.29± .01	0± 0	0.73± .01	97.5± .03	2.5± .03	0± 0
	Max	98.21± .02	0± 0	1.83± .02	79.64± .03	20.36± .03	0± 0
	Sugeno	**100± 0**	**0± 0**	**0± 0**	96.79± .02	3.21± .02	0± 0
	Choquet	98.93± .01	0± 0	1.1± .01	**98.21± .03**	**1.79± .03**	**0± 0**
DCT$_w$	Sum	**100± 0**	**0± 0**	0± 0	**99.29± .01**	**0.71± .01**	**0± 0**
	Product	**100± 0**	**0± 0**	0± 0	98.93± .01	1.07± .01	0± 0
	Max	98.57± .01	0± 0	1.47± .01	80± .04	20± .04	0± 0
	Sugeno	99.29± .02	0± 0	0.73± .02	98.93± .02	1.07± .02	0± 0
	Choquet	99.29± .01	0± 0	0.73± .01	98.93± .01	1.07± .01	0± 0

(a)

(b)
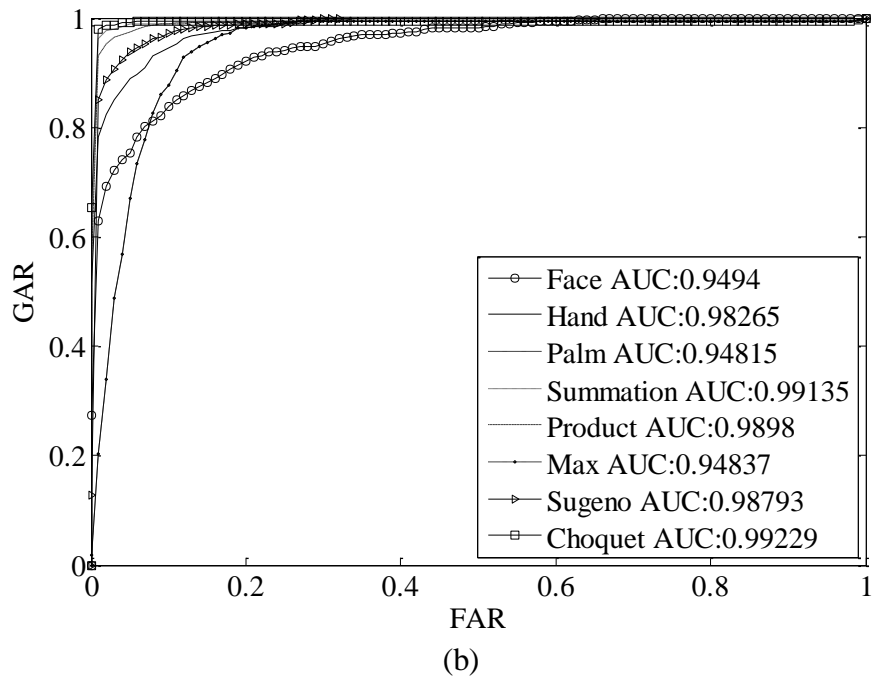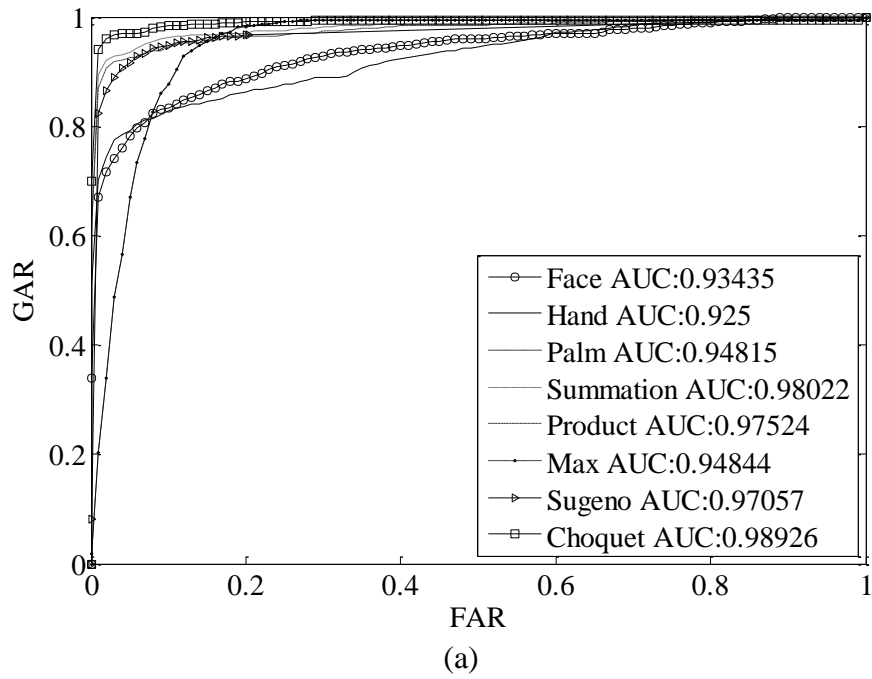
Figure 34 Face, palmprint & hand geometry ROCs (No F.S.), (a) *Imaginary*, (b) DCT*w*

(a)

(b)
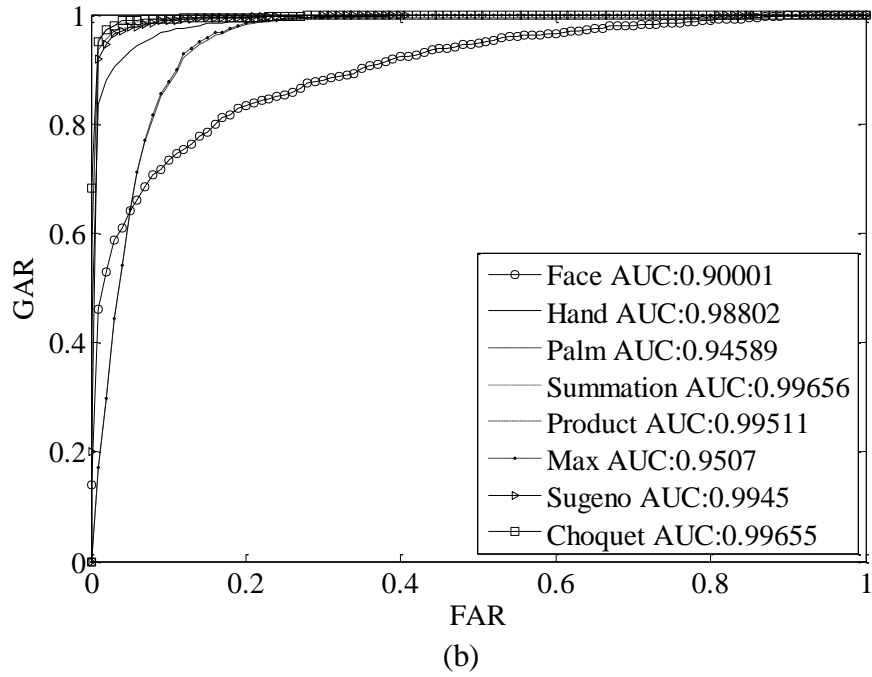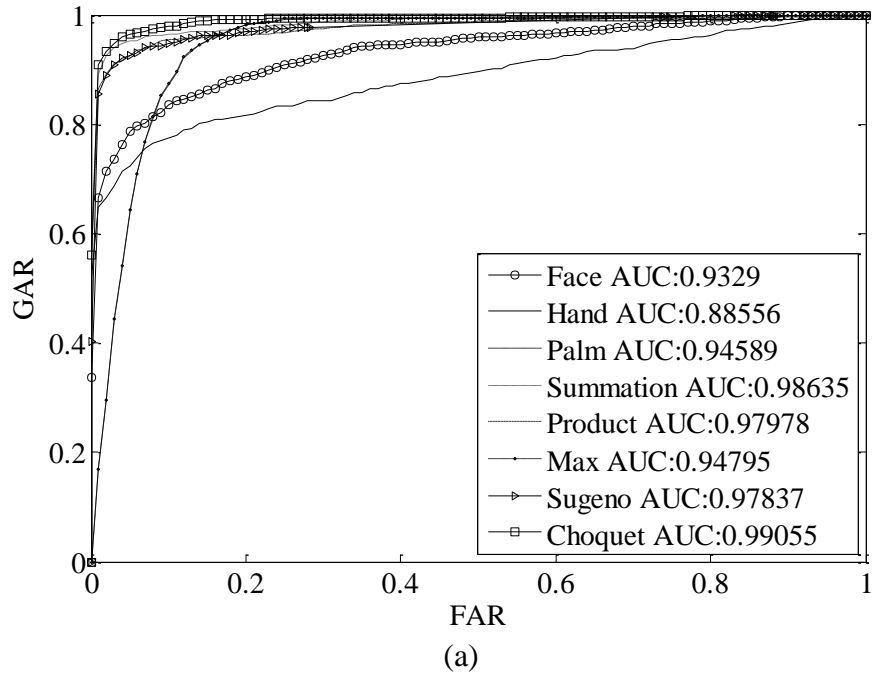
Figure 35 Face, palmprint & hand geometry ROCs (F.S.), (a) *Imaginary***, (b) DCT**$_W$

5.4.3   Feature-level Fusion

As mentioned before, we have selected some feature types randomly of each biometric trait. Then, a fusion has been carried out using concatenation. We have conducted two experiments at this level of fusion. First, the augmented features are passed through the system as if it came from a single biometric. Then, a normal matching (verification or identification) has been executed. In the second experiment, we reduced the number of features using PSO. After that, the normal recognition operation has been done (as single system). The results of these experiments are shown in Table 28 and

Table 29, respectively. It is clear that FF_4, FF_5 FF_7 and FF_{12} have good performance in the verification mode. On the other hand, FF_3, FF_6, FF_{11} and FF_{13} have good performance in the identification mode. Comparing the first and second experiments, we can make the following conclusions: most combinations have relatively degraded performance in the second experiment, only FF_7 has retained performance in verification, and FF_3, FF_{11}, FF_{13} have good performance in the identification mode.

Table 28 Feature-level fusion (No F.S.)

Features	Verification			Identification		
	ACC	FAR	FRR	ACC	FAR	FRR
FF_1	96.07±0.009	16.25±0.04	0.00±0.00	94.29±0.005	5.71±0.05	0.00±0.00
FF_2	95.72±0.02	15.36±0.05	0.94±0.01	-	-	-
FF_3	-	-	-	98.93±0.000	1.07±0.000	0.00±0.00
FF_4	97.16±0.02	2.84±0.02	2.82±0.03	84.68±0.04	15.32±0.04	0.00±0.00
FF_5	97.84±0.01	8.83±0.04	0.00±.000	-	-	-
FF_6	-	-	-	98.90±0.01	1.1±0.01	0.00±0.00
FF_7	**98.91±0.01**	**2.96±0.02**	**0.48±0.006**	-	-	-
FF_8	-	-	-	93.12±0.03	6.68±0.03	0.00±0.00
FF_9	96.13±0.02	9.8±0.04	1.87±0.01	95±0.004	5±0.004	0.00±0.00
FF_{10}	96.45±0.012	12.98±0.07	0.48±0.007	-	-	-
FF_{11}	-	-	-	**99.28±0.01**	**0.72±0.01**	**0.00±0.00**
FF_{12}	98.26±0.09	7.13±0.04	0.00±0.00	-	-	-
FF_{13}				98.59±0.013	1.41±0.013	0.00±0.00

Table 29 Feature-level fusion (F.S.)

Features	Verification			Identification		
	ACC	FAR	FRR	ACC	FAR	FRR
FF_1	84.58±0.12	15.48±0.12	15.55±0.2	61.58±0.2	42±0.2	0.00±0.00
FF_2	95.1±0.03	18.5±0.01	0.47±0.01	-	-	-
FF_3	-	-	-	99.28±0.01	0.72±0.01	0.00±0.00
FF_4	94.78±0.04	11.7±0.08	3.03±0.04	87.12±0.04	12.88±0.04	0.00±0.00
FF_5	95.08±0.04	19.75±0.2	0.00±0.00	-	-	-
FF_6	-	-	-	96.43±0.01	3.57±0.01	0.00±0.00
FF_7	98.19±0.01	2.9±0.02	1.46±0.01	-	-	-
FF_8				88.23±0.02	11.77±0.02	0.00±0.00
FF_9	94.6±0.01	14.14±0.07	2.36±0.01	90.05±0.03	9.95±0.025	0.00±0.00
FF_{10}	94.62±0.01	12.1±0.08	3.29±0.02	-	-	-
FF_{11}	-	-	-	97.5±0.01	2.5±0.01	0.00±0.00
FF_{12}	93.94±0.003	22.83±0.03	0.5±0.007	-	-	-
FF_{13}	-	-	-	97.12±0.01	2.88±0.01	0.00±0.00

CHAPTER 6

CONCLUSION AND FUTURE WORK

In this chapter, we summarize our contributions and highlight the limitations to pinpoint some directions for future research.

6.1 Concluding Remarks

Motivated by the abundant success of the application of the biometric technology for security systems, we investigated the performance of several unimodal systems and proposed a new approach for score-level fusion of biometric traits. The proposed approach is based on two methodologies for fuzzy integral and particle swarm optimization. We conducted intensive experiments using two feature extraction methods and tested various combinations of feature sets extracted from three biometric traits, namely face, iris and hand. We also compared the performance of the proposed system for verification and identification modes with three traditional fusion techniques. Based on our research findings, we can draw the following conclusions:

- The performance of the biometric systems is highly correlated to the database and the feature extraction method.

- Multimodal fusion has significantly improved the results of the unimodal systems in terms of accuracy, false acceptance rate, false rejection rate and area under the curve.

- The fuzzy integral has demonstrated good performance in most of the cases as compared to the other traditional fusion techniques. In addition, it has more flexibility in handling imprecision taking prior knowledge of a domain expert into

consideration. However, its performance depends on proper setting of the parameters.

- Fusion of three biometrics has slightly enhanced the performance, but in some cases it was worse than the bimodal system; this may be due to the increased dimensionality of the feature space and the limited number of biometric samples in the datasets.

- In general, the performance for the verification mode was better than that for the identification mode.

6.2 Future work

We have adopted databases with some restrictions on users during the acquisition of biometric data. As a future trend, it would be good to investigate the performance under uncontrolled acquisition environments, e.g. capturing face images while in motion. It will also be interesting to investigate other fuzzy techniques such as t-norms in the fusion of biometric data. Other directions might be using multi-resolution for feature extraction, combining multiple samples of the same biometric, and exploring the impact of facial expressions, gender, and soft biometrics on the performance.

REFERENCES

[1]   A. Ross, A. Jain, and K. Nandakumar, *Handbook of Multibiometrics*, Springer, 2006.

[2]   A. Ross and A. Jain, "Multimodal Biometric: An Overview," in *Proc. of the 12th European Single Processing Conference*, pp. 1221-1224, 2004.

[3]   A. Jain, P. Flynn, and A. Ross, Eds., *Handbook of Biometrics*. Springer, 2008.

[4]   A. Jain, A. Ross, and S. Prabhakar, "An Introduction to Biometric Recognition," *IEEE Transactions on Circuits and Systems for Video Technology*, vol. 14, no. 1, pp. 4– 20, 2004.

[5]   "Technical Document about FAR, FRR and EER." SYRIS Technology Corp. ver 1.0, 2004.

[6]   J. Cheng and H. Wang, "A Method of Estimating the Equal Error Rate for Automatic Speaker Verification," in *Proc.of the international Symposium on Chinese Spoken Language Processing*, pp. 285-288, 2004.

[7]   Y. Stylianou, Y. Pantazis, F. Calderero, et al. (2005), GMM-Based Multimodal Biometric Verification, [Online]. Available: http://www.enterface.net

[8]   L. Stan and A. Jain, *Handbook of Face Recognition*. Springer, 2011.

[9]   G. Mittal and S. Sasi, "Robust Preprocessing Algorithm for Face Recognition," in *Proc* of *the 3rd Canadian Conference on Computer and Robot Vision,* p. 57, 2006.

[10] W. Zhao, R. Chellappa, P. Phillips, and A. Rosenfeld, "Face Recognition: A Literature Survey," *ACM Computing Survey*, vol. 35, no. 4, pp. 399–458, 2003.

[11] R. Brunelli and T. Poggio, "Face Recognition: Features Versus Templates," *IEEE Transactions on Pattern Analysis and Machine Intelligence,* vol. 15, no. 10, pp. 1042 –1052, 1993.

[12] F. Jiao, W. Gao, X. Chen, G. Cui, and S. Shan, "A Face Recognition Method Based on Local Feature Analysis," in *Proc. of 5th Asian Conference on Computer Vision,* pp. 23-25, 2002.

[13] S. Akrouf, M. A. Sehili, A. Chakhchoukh, M. Mostefai, and C. Youssef, "Face Recognition Using PCA and DCT," in *Proc. of the 5th International Conference on MEMS, NANO, and Smart Systems*, pp. 15-19, 2009.

[14] P. Yuela, D. Dai, and G. Feng, "Wavelet-Based PCA for Human Face Recognition," in *Proc. of IEEE Southwest Symposium on Image Analysis and Interpretation*, pp. 223-228, 1998.

[15] A. Samra, S. El Taweel Gad Allah, and R. Ibrahim, "Face Recognition Using Wavelet Transform, Fast Fourier Transform and Discrete Cosine Transform," in *Proc. of IEEE 46th Midwest Symposium on Circuits and Systems,* vol. 1, pp. 272-275, 2003.

[16] Z. Pan and H. Bolouri, "High Speed Face Recognition Based on Discrete Cosine Transforms and Neural Networks," Univ. of Hertfordshire, Hatfield, Tech. Rep., 1999.

[17] M. Er, W. Chen, and S. Wu, "High-speed Face Recognition Based On Discrete Cosine Transform And RBF Neural Networks," *IEEE Transactions on Neural Networks*, vol. 16, no. 3, pp. 679 –691, 2005.

[18] J. Daugman, "How Iris Recognition Works," in *Proc. of the International Conference on Image Processing,* vol. 1, pp. 33-36, 2002.

[19] L. Ma, T. Tan, Y. Wang, and D. Zhang, "Personal Identification Based on Iris Texture Analysis," *IEEE Transactions on Pattern Analysis and Machine Intelligence*, vol. 25, no. 12, pp. 1519– 1533, 2003.

[20] J. Daugman, "Biometric Personal Identification System Based on Iris Analysis." US Patent 5291560, 1994.

[21] W. Boles and B. Boashash, "A Human Identification Technique Using Images of the Iris and Wavelet Transform," *IEEE Transactions on Signal Processing*, vol. 46, no. 4, pp. 1185–1188, 1998.

[22] R. Y. F. Ng, Y. H. Tay, and K. M. Mok, "Iris Recognition Algorithms Based on Texture Analysis," in *Proc. of the International Symposium on Information Technology,* vol. 2, pp. 1-5, 2008.

[23] R. Wildes, "Iris Recognition: An Emerging Biometric Technology," *Proceedings of the IEEE*, vol. 85, no. 9, pp. 1348 –1363, 1997.

[24] R. Zhu, J. Yang, and R. Wu, "Iris Recognition Based on Local Feature Point Matching," in *Proc.* of the *International Symposium on Communications and Information Technologies,* pp. 451 –454, 2006.

[25] T. Matsumoto, H. Matsumoto, K. Yamada, and S. Hoshino, "Impact of Artificial 'Gummy' Fingers on Fingerprint Systems," in *Proc. of SPIE*, vol. 4677, no. 1, pp. 275–289, 2002.

[26] A. Kong, D. Zhang, and M. Kamel, "A Survey of Palmprint Recognition," *Pattern Recognition*, vol. 42, no. 7, pp. 1408–1418, 2009.

[27] D.-S. Huang, W. Jia, and D. Zhang, "Palmprint Verification Based on Principal Lines," *Pattern Recognition*, vol. 41, no. 4, pp. 1316–1328, 2008.

[28] X. Wu, D. Zhang, K. Wang, and B. Huang, "Palmprint Classification Using Principal Lines," *Pattern Recognition*, vol. 37, no. 10, pp. 1987–1998, 2004.

[29] A. Kumar and H. Shen, "Palmprint Identification Using Palmcodes," in *Proc. of the 3rd International Conference on Image and Graphics,* pp. 258-261, 2004.

[30] J. Noh and K. Rhee, "Palmprint Identification Algorithm Using Hu Invariant Moments and Otsu Binarization," in *Proc. of the 4th Annual International Conference on Computer and Information Science,* pp. 94-99, 2005.

[31] X. Wu, K. Wang, and D. Zhang, "Fuzzy Directional Element Energy Feature (FDEEF) Based Palmprint Identification," in *Proc. of the 16th International Conference on Pattern Recognition,* vol. 1, pp. 95-98, 2002.

[32] L. Shang, D.-S. Huang, J.-X. Du, and Z.-K. Huang, "Palmprint Recognition Using ICA Based on Winner-Take-All Network and Radial Basis Probabilistic Neural Network," in *Advances in Neural Networks*, Wang et al., Eds., vol. 3972, Springer Berlin Heidelberg, pp. 216-221, 2006.

[33] R. Sanchez-Reillo, "Hand Geometry Pattern Recognition Through Gaussian Mixture Modelling," in *Proc. of the 15th International Conference on Pattern Recognition,* vol. 2, pp. 937-940 , 2000.

[34] A. Jain and N. Duta, "Deformable Matching of Hand Shapes for User Verification," in *Proc. of the International Conference on Image Processing,* vol 2, pp. 857-861, 1999.

[35] G. Amayeh, G. Bebis, A. Erol, and M. Nicolescu, "Peg-Free Hand Shape Verification Using High Order Zernike Moments," in *Proc. of the Conference on Computer Vision and Pattern Recognition Workshop,* pp.40- 40, 2006.

[36] A. Morales, M. A. Ferrer, F. Diaz, J. B. Alonso, and C. M. Travieso, "Contact-Free Hand Biometric System For Real Environment," in *Proc. of the European Signal Processing Conference,* vol. 16, 2008.

[37] C. Xin, X. Wu, Z. Qiushi, and T. Youbao, "A Contactless Hand Shape Identification System," in *Proc. of the 3rd International Conference on Advanced Computer Control (ICACC),* pp. 561-565, 2011.

[38] J.-Y. Gan and J.-F. Liu, "Fusion and Recognition of Face and Iris Feature Based on Wavelet Feature and KFDA," in *Proc. of the International Conference on Wavelet Analysis and Pattern Recognition,* pp. 47-50, 2009.

[39] C.-H. Chen and C. T. Chu, "Fusion of Face and Iris Features for Multimodal Biometrics," in *Advances in Biometrics*, D. Zhang and A. Jain, Eds., vol. 3832, Springer Berlin Heidelberg, pp. 571–580, 2005.

[40] K. Fakhar, M. Aroussi, R. Saadane, M. Wahbi, and D. Aboutajdine, "Fusion of Face and Iris Features Extraction Based on Steerable Pyramid Representation for Multimodal Biometrics," in *Proc. of the International Conference on Multimedia Computing and Systems,* pp. 1-4, 2011.

[41] H. Liau and D. Isa, "Feature Selection for Support Vector Machine-Based Face-Iris Multimodal Biometric System," *Expert Systems with Applications*, vol. 38, no. 9, pp. 11105–11111, 2011.

[42] F. Wang and J. Han, "Multimodal Biometric Authentication Based on Score Level Fusion Using Support Vector Machine," *Opto-Electronics Review*, vol. 17, no. 1, pp. 59–64, 2009.

[43] Y. Wang, T. Tan, and A. Jain, "Combining Face and Iris Biometrics for Identity Verification," in *Audio-and Video-Based Biometric Person Authentication*, J. Kittler and M. Nixon, Eds., vol. 2688, Springer Berlin Heidelberg, pp. 1060–1060, 2003.

[44] Z. Zhang, R. Wang, K. Pan, S. Li, and P. Zhang, "Fusion of Near Infrared Face and Iris Biometrics," *Advances in Biometrics*, vol. 4642, pp. 172–180, 2007.

[45] C. Lu, J. Wang, and M. Qi, "Multimodal Biometric Identification Approach Based on Face and Palmprint," in *Proc. of the 2nd International Symposium on Electronic Commerce and Security,* vol. 2, pp. 44-47, 2009.

[46] M. Ahmad, W. Woo, and S. Dlay, "Multimodal Biometric Fusion at Feature Level: Face and Palmprint," in *Proc. of 7th International Symposium on Communication Systems Networks and Digital Signal Processing,* pp. 801-805, 2010.

[47] S. Chaudhary and R. Nath, "A Multimodal Biometric Recognition System Based on Fusion of Palmprint, Fingerprint and Face," in *Proc. of the International Conference on Advances in Recent Technologies in Communication and Computing,* pp. 596-600, 2009.

[48] A. Ross and A. Jain, "Information Fusion in Biometrics," *Pattern Recognition Letters*, vol. 24, no. 13, pp. 2115–2125, 2003.

[49] F. Tsalakanidou, S. Malassiotis, and M. G. Strintzis, "A 3D Face and Hand Biometric System for Robust User-Friendly Authentication," *Pattern Recognition Letters*, vol. 28, no. 16, pp. 2238–2249, 2007.

[50] X. Wu, D. Zhang, K. Wang, and N. Qi, "Fusion of Palmprint and Iris for Personal Authentication," in *Proc. of the 3rd International conference on Advanced Data Mining and Applications,* Harbin, China, pp. 466-475 , 2007.

[51] J. Wang, Y. Li, X. Ao, C. Wang, and J. Zhou, "Multimodal Biometric Authentication Fusing Iris and Palmprint Based on GMM," in *Proc. of the 15th Workshop on Statistical Signal Processing,* pp. 349 –352, 2009.

[52] N. Covavisaruch and P. Prateepamornkul, "Personal Identification System Using Hand Geometry and Iris Pattern Fusion," in *Proc. of the IEEE International Conference on Electro/information Technology*, pp. 597 –602, 2006.

[53] A. Meraoumia, S. Chitroub, and A. Bouridane, "Multimodal Biometric Person Recognition System Based on Iris and Palmprint Using Correlation Filter Classifier," in *Proc. of the 1st International Conference on Computing and Information Technology*, pp. 782-787, 2012.

[54] A. Kumar, D. Wong, H. Shen, and A. Jain, "Personal Verification Using Palmprint and Hand Geometry Biometric," in *Audio- and Video-Based Biometric Person Authentication*, J. Kittler and M. Nixon, Eds., vol. 2688, Springer Berlin Heidelberg, pp. 1060–1060, 2003.

[55] W.-S. Chen, Y.-S. Chiang, and Y.-H. Chiu, "Biometric Verification by Fusing Hand Geometry and Palmprint," in *Proc. of the 3rd International Conference on Intelligent Information Hiding and Multimedia Signal Processing, , vol. 2, pp. 403 – 406, 2007.

[56] C.-C. Han, "A Hand-Based Personal Authentication Using a Coarse-To-Fine Strategy," *Image and Vision Computing*, vol. 22, no. 11, pp. 909–918, 2004.

[57] A. Kumar and D. Zhang, "Integrating Shape and Texture for Hand Verification," in *Proc. of the 3rd International Conference on Image and Graphics,* pp. 222–225, 2004.

[58] A. Kumar, D. Wong, H. Shen, and A. Jain, "Personal Authentication Using Hand Images," *Pattern Recognition Letters*, vol. 27, no. 13, pp. 1478–1486, 2006.

[59] F. Wang and J. Han, "Robust Multimodal Biometric Authentication Integrating Iris, Face and Palmprint," *Information Technology and Control*, vol. 37, no. 4, pp. 326–332, 2008.

[60] R. Snelick, U. Uludag, A. Mink, M. Indovina, and A. Jain, "Large-scale Evaluation of Multimodal Biometric Authentication Using State-of-the-Art Systems," *IEEE Transactions on Pattern Analysis and Machine Intelligence*, vol. 27, no. 3, pp 450-455, 2005.

[61] R. Mesiar and A. Mesiarova, "Fuzzy Integrals—What Are They?," *International Journal of Intelligent Systems*, vol. 23, no. 2, pp. 199–212, 2008.

[62] A. Jain, K. Nandakumar, and A. Ross, "Score Normalization in Multimodal Biometric Systems," *Pattern Recognition*, vol. 38, no. 12, pp. 2270-2285, 2005.

[63] M. Belahcene, A. Ouamane, and A. Ahmed, "Fusion by Combination of Scores Multi-Biometric Systems," in *Proc. of the 3rd European Workshop on Visual Information Processing*, pp. 252 –257, 2011.

[64] L. Fong and W. Seng, "A Comparison Study on Hand Recognition Approaches," *in Proc. of the International Conference of Soft Computing and Pattern Recognition*, pp. 364-368,2009.

[65] L. Masek, "Recognition of Human Iris Patterns for Biometric Identification," The University of Western Australia, 2003.

[66] Z. Hafed and M. Levine, "Face Recognition Using the Discrete Cosine Transform," *International Journal of Computer Vision*, vol. 43, no. 3, pp. 167–188, 2001.

[67] S. Khayam, "The Discrete Cosine Transform (DCT): Theory and Application." Michigan State Univeresity, 2003.

[68] J. Movellan, "Tutorial on Gabor Filters," Univ. of California, San Diego, Tech. Rep., MPLab Tutorials, 2005.

[69] D. Zhang, W.-K. Kong, J. You, and M. Wong, "Online Palmprint Identification," *IEEE Transactions on Pattern Analysis and Machine Intelligence*, vol. 25, no. 9, pp. 1041– 1050, 2003.

[70] S. Selvarajan, V. Palanisamy, and B. Mathivanan, "Human Identification and Recognition System Using more Significant Hand Attributes," in Proc of the International Conference on *Computer and Communication Engineering,* , pp. 1211 –1216, 2008.

[71] D. Nicolae, "A Survey of Biometric Technology Based on Hand Shape," *Pattern Recognition*, vol. 42, no. 11, pp. 2797–2806, 2009.

[72] http://www.cse.ust.hk/

[73] W. Silverman. (1986). Density Estimation for Statistics and Data Analysis *[Online]. Available: http://journal.mercubuana.ac.id/data/*.

[74] R. Raghavendra, B. Dorizzi, A. Rao, G. H. Kumar "Particle Swarm Optimization Based Fusion of Near Infrared and Visible Images for Improved Face Verification," *Pattern Recognition*, vol. 44, no. 2, 2011.

[75] J. Kennedy and R. Eberhart, "Particle Swarm Optimization," in *Proc. of the IEEE International Conference onNeural Networks*, vol. 4, pp. 1942-1948, 1995.

[76] D. Floreano and C. Mattiussi, *Bio-Inspired Artificial Intelligence, Theories, Methods, and Technologies*. Cambridge, MA: The MIT Press, 2008.

[77] A. Temko, D. Macho, and C. Nadeu, "Fuzzy Integral Based Information Fusion for Classification of Highly Confusable Non-Speech Sounds," *Pattern Recognition*, vol. 41, no. 5, pp. 1814–1823, May 2008.

[78] G. J. Klir and B. Yuan, Fuzzy Sets and Fuzzy Logic. Michigan: Prentice Hall, 1995.

[79] M. Ayub, "Choquet and Sugeno Integrals," Thesis for the degree Master of Science, Blekinge Institute of Technology in Mathematical Modelling and Simulation, 2009.

[80] V. Torra and Y. Narukawa, "The Interpretation of Fuzzy Integrals and Their Application to Fuzzy Systems," *International Journal of Approximate Reasoning*, vol. 41, pp. 43–58, 2006.

[81] G. M. Binmakhashen and E.-S. M. El-Alfy, "Fusion of Multiple Texture Representations for Palmprint Recognition Using Neural Networks," *Lecture Notes in Computer Science*, Springer Berlin Heidelberg, vol. 7667 LNCS (PART 5), pp. 410-417, 2012.

[82] E.-S. M. El-Alfy, "Automatic Identification Based on Hand Geometry and Probabilistic Neural Networks," in *Proc. of the 5th International Conference on New Technologies, Mobility and Security*, NTMS, 2012.

[83] E.-S. M. El-Alfy, R. E. Abdel-Aal, and Z. A. Baig, "Abductive Neural Network Modeling for Hand Recognition Using Geometric Features," *Lecture Notes in Computer Science*, Springer Berlin Heidelberg, vol. 7666 LNCS (PART 4), pp. 593-602, 2012.

[84] E.-S. M. El-Alfy and G. M. Binmakhashen, "Evaluation of Support Vector Machine with Universal Kernel for Hand-Geometry Based Identification," in *Proc. of the International Conference on Innovations in Information Technology*, IIT, 2012.

[85] T. Murofushi and M. Sugeno, "An Interpretation of Fuzzy Measures and the Choquet Integral as an Integral with Respect to a Fuzzy Measure," *Fuzzy Sets and Systems*, vol. 29, no. 2, pp. 201–227, Jan. 1989.

[86] Y. Zheng, G. Shi, Q. Wang, and L. Zhang, "Palmprint Image Quality Measures in Minutiae-based Recognition," *in Proc. of the 14th International Workshop on Systems, Signals and Image Processing and 6th EURASIP Conference focused on Speech and Image Processing, Multimedia Communications and Services,* pp. 140-143, 2007.

[87] L. Lam and C. Y. Suen, "Application of Majority Voting to Pattern Recognition: an Analysis of its Behavior and Performance," *IEEE Transactions on Systems, Man and Cybernetics, Part A: Systems and Humans*, vol. 27, no. 5, pp. 553 – 568, 1997.

[88] E.-S. M. El-Alfy and G. M. Binmakhashen, "Improved Personal Identification Using Face and Hand Geometry Fusion and Support Vector Machines," in *Networked Digital Technologies, Communications in Computer and Information Science*, R. Benlamri, Eds., Springer Berlin Heidelberg, vol. 294, pp. 253-261, 2012.

[89] R. Raghavendra, B. Dorizzi, A. Rao, G. H. Kumar, "Particle Swarm Optimization Based Fusion of Near Infrared and Visible Images for Improved Face Verification," *Pattern Recognition*, vol. 44, no. 2, 2011.

[90] http://www.cl.cam.ac.uk/research/dtg/attarchive/facedatabase.html

[91] O. M. Duarte and P. Melin, "The Fuzzy Sugeno Integral as a Decision Operator in the Recognition of Images with Modular Neural Networks," in *Hybrid Intelligent Systems*, O. Castillo, P. Melin, J. Kacprzyk, and W. Pedrycz, Eds., Springer Berlin Heidelberg, vol. 208, pp. 299–310, 2007.

[92] CASIA-IrisV1, http://biometrics.idealtest.org/

[93] M. Sugeno, "Fuzzy Measures and Fuzzy Integrals-ASurvey," in *Fuzzy Automata and Decision Processes*, M. M. Gupta, G. N. Saridis and B. R. Gaines, Eds., Amsterdam, The Netherlands: North Holland, pp. 89-102, 1977.

[94] K.-C. Kwak and W. Pedrycz, "Face recognition Using Fuzzy Integral and Wavelet Decomposition Method," *IEEE Transactions on Systems, Man and Cybernetics, Part B: Cybernetics*, vol. 26, no. 6, pp. 719–733, May 2005.

VITAE

Galal Munassar Abdullah Bin Makhashen from Yemen has been a Master student in Computer Science at King Fahd University of Petroleum and Minerals (KFUPM) since September 2009. He finished his B.Sc. in Computer Science and Engineering from Hadramout University of Science and Technology (HUST) in 2005. After finishing his Bachelor, he has been in the teaching profession in different information technology institutes. His research interests include pattern recognition, biometric authentication, artificial intelligence, computer vision, and information security. He can be reached through his e-mail: binmakhashen@gmail.com